

AD-A146 467

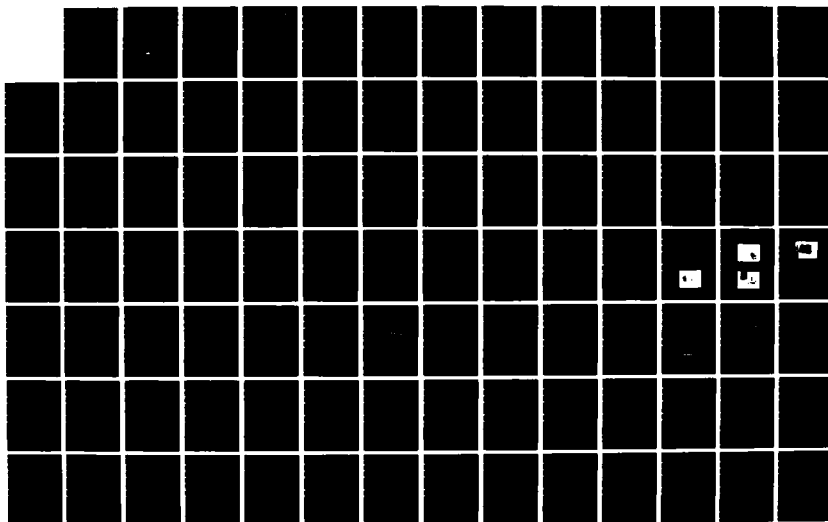
THE DESIGN AND OPERATION OF A REAL-TIME POLYNUCLEAR
AROMATIC HYDROCARBON (U) NAVAL WEAPONS CENTER CHINA
LAKE CA R T LODA AUG 84 NWC-TP-6525

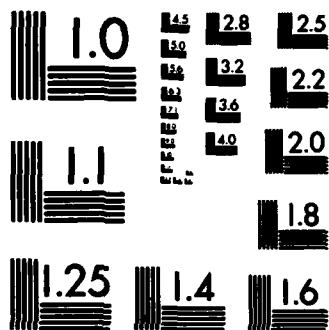
1/2

UNCLASSIFIED

F/G 13/2

NL





MICROCOPY RESOLUTION TEST CHART
NATIONAL BUREAU OF STANDARDS-1963-A

**The Design and Operation
of a Real-Time Polynuclear Aromatic
Hydrocarbon (PAH) Monitor for the Analysis
of Combustion Products Formed
in the Incineration of Navy Colored
Smoke Compositions**

by
Richard T. Loda
Research Department

AUGUST 1984

**NAVAL WEAPONS CENTER
CHINA LAKE, CA 93555-6001**



Approved for public release;
distribution is unlimited.

OCT 11 1984

A

AD-A146 467

DTIC FILE COPY

84 10 09 056

Naval Weapons Center

AN ACTIVITY OF THE NAVAL MATERIAL COMMAND

FOREWORD

Polynuclear aromatic hydrocarbons (PAHs) can be produced during the thermal destruction of unserviceable colored smoke compositions. Because some of these compounds are carcinogenic, there is a need to monitor their possible release into the environment. The design, construction, and implementation of a real-time incinerator monitor system for PAHs is the subject of this report.

The work described in this report took place between December 1982 and October 1983. The work was performed with Pollution Abatement Research funds, Program Element No. 62765N, SEATASK Task Area Number WF65559 under the sponsorship of G. Young and under Task Area 50400 under the sponsorship of J. Short.

This work has been reviewed for technical accuracy by E. D. Erickson and C. E. Dinerman.

Approved by
E. B. ROYCE, Head
Research Department
30 July 1984

Under authority of
K. A. DICKERSON
CAPT, U.S. Navy
Commander

Released for publication by
B. W. HAYS
Technical Director

NWC Technical Publication 6525

Published by	Research Department
Collation	Cover, 68 leaves
First printing	150 copies

UNCLASSIFIED

SECURITY CLASSIFICATION OF THIS PAGE (When Data Entered)

REPORT DOCUMENTATION PAGE		READ INSTRUCTIONS BEFORE COMPLETING FORM
1. REPORT NUMBER NWC TP 6525	2. GOVT ACCESSION NO. ADA146467	3. RECIPIENT'S CATALOG NUMBER
4. TITLE (and Subtitle) THE DESIGN AND OPERATION OF A REAL-TIME POLYNUCLEAR AROMATIC HYDROCARBON (PAH) MONITOR FOR THE ANALYSIS OF COMBUSTION PRODUCTS FORMED IN THE INCINERATION OF NAVY COLORED SMOKE COMPOSITIONS		5. TYPE OF REPORT & PERIOD COVERED Final Dec 1982-Oct 1983
		6. PERFORMING ORG. REPORT NUMBER
7. AUTHOR(s) Richard T. Loda		8. CONTRACT OR GRANT NUMBER(s)
9. PERFORMING ORGANIZATION NAME AND ADDRESS Naval Weapons Center China Lake, CA 93555-6001		10. PROGRAM ELEMENT, PROJECT, TASK AREA & WORK UNIT NUMBERS PE 62765N & 63721N, Task Area WF65559 & 50400, Work Unit 138567
11. CONTROLLING OFFICE NAME AND ADDRESS Naval Weapons Center China Lake, CA 93555-6001		12. REPORT DATE August 1984
14. MONITORING AGENCY NAME & ADDRESS (if different from Controlling Office)		13. NUMBER OF PAGES 134
		15. SECURITY CLASS. (of this report) UNCLASSIFIED
16. DISTRIBUTION STATEMENT (of this Report) Approved for public release; distribution is unlimited.		
17. DISTRIBUTION STATEMENT (of the abstract entered in Block 20, if different from Report)		
18. SUPPLEMENTARY NOTES		
19. KEY WORDS (Continue on reverse side if necessary and identify by block number) Colored Smoke Compositions Polynuclear Aromatic Hydrocarbons (PAHs) Combustion Products Real-time Fluorescence Spectroscopy Incineration		
20. ABSTRACT (Continue on reverse side if necessary and identify by block number) See back of form.		

DD FORM 1 JAN 73 1473

EDITION OF 1 NOV 65 IS OBSOLETE

S/N 0102- LF- 014- 6601

UNCLASSIFIED

SECURITY CLASSIFICATION OF THIS PAGE (When Data Entered)

UNCLASSIFIED

SECURITY CLASSIFICATION OF THIS PAGE (When Data Entered)

(U) *The Design and Operation of a Real-Time Polynuclear Aromatic Hydrocarbon (PAH) Monitor for the Analysis of Combustion Products Formed in the Incineration of Navy Colored Smoke Compositions* by Richard T. Loda, China Lake, Calif., Naval Weapons Center, August 1984. 134 pp. (NWC TP 6525, publication UNCLASSIFIED).

(U) This publication describes the design and construction of a fluorescence-based polynuclear aromatic hydrocarbon (PAH) monitor and calibration system. It also covers the installation and operation of this real-time monitor system during the incineration testing of Navy colored smoke compositions at the Los Alamos National Laboratory Controlled Air Incinerator facility, Los Alamos, N. Mex. During these tests, no PAHs were found to be present in the incinerator effluent gases at a concentration level > 1 ppm \rightarrow *> approx 1 ppm* (the approximate gas-phase detection limit of the monitor). Recommendations are listed for future system improvements. *Only auto assigned*

reagents include fluorescence spectroscopy, and Real Time.

A

Accession For	
NTIS GRA&I <input checked="" type="checkbox"/>	
DTIC TAB <input type="checkbox"/>	
Unannounced <input type="checkbox"/>	
Justification <input type="checkbox"/>	
By _____	
Distribution/ _____	
Availability Codes	
Dist	Avail and/or Special
A-1	



UNCLASSIFIED

SECURITY CLASSIFICATION OF THIS PAGE (When Data Entered)

CONTENTS

Disclaimer	2
Acknowledgment	2
Introduction	3
Background	5
Experimental	8
Materials	8
Laboratory Flow System	9
Laser Induced Fluorescence (LIF) System	11
LANL Incinerator Complex	14
PAH Monitor Design	17
Basic Spex Fluorimeter	17
Flow Cell Modifications	20
PAH Monitor Flow System	22
Results and Discussion	24
Diffusion Cell Evaluation	24
Theory	24
PAH Diffusion Rate Measurements	26
Laboratory Flow System Experiment Using LIF	27
Comparison of PAH Spectra (Static Cell)	30
Beckman DU-7 Absorption Spectrophotometer	30
Perkin-Elmer MFP-44B Spectrofluorimeter	31
Spex F112 Fluorimeter	34
LANL Incineration Tests	36
Preliminary Observations	37
PAH Analysis in a Static Cell	37
PAH Analysis in the Flow System	47
Real-Time Analysis of Navy Colored Smoke	51
Conclusions and Recommendations	72
Conclusions	72
Recommendations	73
List of Company Names	76
References	77

NWC TP 6525

Appendices:

A. Program AD RLTIME	83
B. Spex DATAMATE Specifications	99
C. Diffusion Rate Program	101
D. Spex Diffusion Rate Program	107
E. Spex Fluorimeter Correspondence	115

DISCLAIMER

The mention of specific equipment manufacturers, brand names, or specific contractors in this report does not imply their endorsement. Other commercially available equipment, having similar operational capabilities, or other qualified contractors, could be substituted for the equipment or contractors mentioned. Statements made in this document do not necessarily represent official Navy or DOD policies and practices; they are the best judgment of technical personnel, based on an experimental investigation of the problem, and a review of pertinent information. No statements in this document are intended to modify or replace any official safety SOPs, instructions, etc. Any prices listed were as of August 1983 and may not be the same now.

ACKNOWLEDGMENT

The author would like to thank J. Short (Naval Weapons Support Center, Crane, Indiana), and the entire Waste Management Group at Los Alamos, New Mexico, without whose help, much of the Los Alamos Scientific Laboratory work could not have been accomplished. Thanks also go to T. Griffith of this laboratory for the construction of the diffusion cells, and to P. Plassmann of this laboratory for his contributions to the HP9836A data acquisition programs and the diffusion rate measurements.

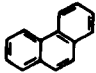
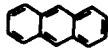
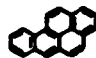


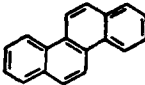
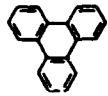
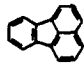

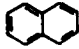
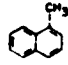
INTRODUCTION

The Navy has an inventory of obsolete and unserviceable colored smoke compositions that must be disposed of in a safe, economical, and environmentally acceptable manner. Disposal by thermal destruction (incineration) has been demonstrated to be technically feasible (Reference 1), but this process, under certain conditions, produces polynuclear aromatic hydrocarbons (PAHs) from the incomplete oxidation of organic dyes present in the smoke compositions. A listing of the materials that have been found is given in Table 1. Since some of these PAHs are carcinogenic, effective control of PAH emissions must be achieved for the incineration process to be fully acceptable.

Pilot-plant scale experimentation is necessary to obtain a "best set" of incineration conditions to ensure the maximum destruction efficiency of these smokes, and a real-time monitor is required for the detection of PAHs in the combustion product. To accomplish these tasks, the Naval Weapons Support Center (NWSC), Crane, Ind., awarded a contract to the Los Alamos National Laboratory (LANL), Los Alamos, N. Mex., to experiment with incinerating the smoke compositions in their research incinerator. In addition, both the Naval Weapons Center (NWC) and the Battelle Columbus Laboratories (BCL), Columbus, Ohio (Reference 2) were contracted to design a monitor capable of detecting mixtures of PAHs on a one part-per-million (ppm) level. Ultimately, it was the PAH monitor system design of NWC that was implemented during the incineration tests undertaken at the LANL (References 3 and 4). If these tests prove successful, the Navy will subsequently build its own incinerator facility using the knowledge gained through these experiments.

This report describes the NWC's PAH monitor and calibration device design considerations. A listing of all of the company names and their addresses is included at the back of the report. It also covers the on-line installation and operation of this real-time system during the incineration tests performed at the LANL in September 1983. During these tests, no PAHs were found to be present in the incinerator effluent gases at a concentration level ≥ 1 ppm (the approximate detection limit of the monitor). Background material, specific to the PAH problem, will be discussed first. Following this, the experimental apparatus details will be given. This section covers the actual monitor design, before some of the results influencing it are presented.

TABLE 1. PAH Materials Found in the Combustion
Product of Navy Colored Smoke Compositions.

PAH	Formula	Structure
Phenanthrene	$C_{14}H_{10}$	
Anthracene	$C_{14}H_{10}$	
Benzo(a)pyrene	$C_{20}H_{12}$	
Benzo(e)pyrene	$C_{20}H_{12}$	
Perylene	$C_{20}H_{12}$	
Chrysene	$C_{18}H_{12}$	
Triphenylene	$C_{18}H_{12}$	
Fluoranthene	$C_{16}H_{10}$	
Pyrene	$C_{16}H_{10}$	
Naphthalene	$C_{10}H_8$	
1-Methyl Naphthalene	$C_{11}H_{10}$	

^a Reference 1.

If this bothers the reader, it is suggested that the report be reviewed in the following order: the Introduction section (p. 3) through the Laser Inducted Fluorescence (LIF) System (p. 14); Results and Discussion section (p. 24) through the Comparison of PAH Spectra Static Cell section (p. 36); the LANL Incinerator Complex section (p. 14) through the PAH Monitor Design section (p. 24); and then the LANL Incinerator Tests section to the end (p. 36 through 75).

The results will essentially be presented in chronological order. Work on the flow and calibration system, with known PAH materials, will be described first. This will be followed by the evaluation of some commercially available instrumentation, and the choice of the monitor. Next, the PAH monitor system installation, and the on-line, real-time analysis will be discussed. Lastly, a series of recommendations, to improve the monitor operation for future work, will be presented.

BACKGROUND

Although PAHs are naturally present in many forms of vegetation and fossil fuel, the principal sources of ambient atmospheric PAH concentrations result from the incomplete combustion of hydrocarbons. Processes such as the combustion of coal, oil, gasoline, and diesel fuel, along with the operation of refuse burning power plants and wood burning stoves, all contribute significantly to the PAH pollutant problem.

Since many compounds of the PAH class have been shown to be mutagenic and/or carcinogenic in animals, it is no surprise that a large body of work has been devoted to the study of these materials (References 5 and 6). Most analytical methods for PAH determination have been based on the isolation of individual PAHs in collected environmental samples through a variety of chromatographic techniques. Quantitative information is then gathered after the individual components have been identified. Quite often this entire process is carried out using a combination of instruments. For example, the gas chromatography/mass spectrometry (GC/MS) technique combines the high separation efficiency of gas chromatography with the high sensitivity and identification capabilities of mass spectrometry. High performance liquid chromatography with fluorescence detection is another popular instrumental combination for PAH analysis, and many other extensions of this basic idea are possible. Unfortunately, most of these procedures require time-consuming and troublesome collection, extraction, and concentration techniques. Sample recovery and the maintenance of sample integrity during the work up prior to analysis represent serious problems, and the desired information cannot be obtained in real-time.

The inherently high sensitivity of fluorescence detection, coupled with the intense fluorescence of many PAH compounds (References 7 through 11) makes fluorescence spectroscopy a powerful tool for the detection and identification of PAHs. Fluorescence spectroscopy has been used to measure PAH concentrations below 1 ppm, and this technique has the potential for making real-time measurements.

Fluorescence is a process in which radiation is emitted by molecules that have been previously excited by the absorption of radiation. When a sample is excited at a fixed wavelength λ_{ex} , a fluorescence emission spectrum is produced by recording the emission intensity as a function of the emission wavelength λ_{em} . Alternatively, a fluorescence excitation spectrum may be obtained by scanning λ_{ex} , while recording the emission intensity at a fixed λ_{em} .^{*} These excitation and emission spectra are characteristic of the materials present in the sample. In the study of multicomponent mixtures, the ability of the analyst to select two wavelengths (excitation and emission) for the measurement of the fluorescing species leads to an enhanced selectivity for fluorescence detection over other techniques such as absorption spectrophotometry (since not all absorbing molecules fluoresce). This is especially true for the highly-fluorescing PAHs.

The problems associated with the separation and purification steps mentioned above have lead to an active effort to develop improved instrumental and mathematical curve fitting techniques for the total analysis of PAH mixtures without first isolating the individual components. The major problem area has not been sensitivity, but selectivity. The overlap of spectra from the different sample components and the inherently featureless nature of the individual spectra, especially when measured under ambient or higher temperature conditions, are the essential causes for this limitation. Nevertheless, low temperature site-selection spectroscopy (References 12 through 16), matrix isolation spectroscopy (References 12, 17 and 18), polarization measurements (Reference 19), time-resolved spectroscopy (References 20 and 21), selective excitation (Reference 22), derivative spectroscopy (References 23 through 28), selective modulation (Reference 23), synchronous excitation (Reference 29) and video fluorimetry (References 30 and 31) have all been employed to improve multicomponent analysis. A variety of numerical algorithms have also been used to deconvolute the overlapping spectra (References 32 and 33).

* A fluorescence excitation spectrum is essentially an absorption spectrum, but measured indirectly by monitoring sample emission. The key point is that the sample cannot emit unless it first absorbs.

When we consider the specific requirements for a real-time PAH mixture analysis of stack gases, a number of the approaches mentioned above have definite drawbacks. Site selection and matrix isolation would require sample collection and cryogenic sample preparation. In addition, these techniques, along with time-resolved spectroscopy, need relatively expensive laser sources for sample excitation. Cryogenic equipment and sample preparation are also required for polarization measurements, and selective modulation necessitates extensive modifications to standard spectrometers and the construction of additional electronics. In both selective modulation and synchronous excitation, the *selectivity* is enhanced, relative to simpler methods such as selective excitation, but the *sensitivity* is reduced because the data results from a convolution of the excitation and emission spectra. Derivative spectroscopy can enhance selectivity over selective excitation and is rather simple to implement, but the signal to noise (S/N) ratio is reduced by a factor of about 2 for each derivative taken (Reference 23). This reduces the potential *sensitivity* of this approach. Video fluorimetry can provide an entire excitation-emission matrix on a complex sample, in real-time, and is probably the most powerful technique of all those mentioned above. Its major drawback is that it requires the modification of a standard spectrometer and the purchase of an expensive (approximately \$50K), image intensified array detector, along with a computer controlled data acquisition system. Furthermore, even after one obtains and stores the vast amount of information contained in one, or multiple excitation-emission matrices, the subsequent analysis is by no means trivial. Sophisticated deconvolution techniques have been developed (References 32 and 33); but for complex samples, one still must know the total number of components in the mixture. This would not be easy to determine, *a priori*, for our particular problem. Therefore, one must question whether the additional instrumental cost would be justified in this case.

A real-time aromatic vapor monitor has been previously reported (References 26 and 28). It uses derivative ultraviolet (UV)-absorption spectrophotometry as its detection method and has been primarily successful in analyzing mixtures of smaller, highly-volatile aromatic compounds. Since it was expected that larger, less-volatile PAH compounds would be encountered in the smoke composition incineration process (Reference 1), and that interfering, non-fluorescent but absorbing species would also be present, it was felt that an absorption-based PAH monitor would not meet the program requirements.

As will be presented in greater detail, our PAH monitor design, which is based on the purchase and minor modification of a commercial fluorimeter, allows the capability to exploit absorption, selective excitation and emission, derivative spectroscopy, and synchronous excitation techniques. Complete excitation-emission matrices can also be acquired; not on the same time scale as video fluorimetry, but at a greatly reduced cost.

There is one final technique that has been used to detect PAHs that also deserves discussion. It is a simple spot test (References 34 and 35) that allows a person to visually detect the presence of <10 picograms of PAH in a collected sample. The sensitivity of this technique is a consequence of a process called sensitized fluorescence. Sensitized fluorescence can be thought of as an energy transfer between two materials. A donor molecule may be excited with UV radiation and transfer its excitation energy to an acceptor molecule whose excited state is lower in energy than the excited state of the donor molecule. This acceptor molecule can then fluoresce after having been indirectly excited (sensitized). The transfer of energy is most efficient when the acceptor molecule is present in a much lower concentration than the donor molecule. When a PAH is used as the acceptor in an appropriate mixture (PAH plus sensitizer), the limit of detection can be significantly lower than the non-sensitized fluorescence detection limit of the acceptor molecule (PAH) alone.

To perform this spot test on a sample extract, one makes three application spots on a filter paper with a microliter pipette. Two of the spots contain portions of the sample extract. A naphthalene sensitizing solution is applied to the third spot and one of the sample spots. After the spots have dried, they are observed under black-light (254 nm) illumination. Visual differences in intensity and color between the sample/sensitizer spot and either spot alone indicates sensitized fluorescence and the possible presence of PAHs. This spot test is very useful as a prescreen and can eliminate the need for costly analysis when no PAHs are present. Although this test cannot be used in a real-time fashion, and can only be used to detect the presence of PAHs as a class, its description has been included here because it is simple, rapid, sensitive, and quite inexpensive.

EXPERIMENTAL

MATERIALS

The PAH compounds that were used in the laboratory scale experiments and for calibration purposes during the LANL incineration tests were purchased from the Matheson Chemical Company and Eastman Chemical Company. They were used without further purification if their melting points and melting point ranges agreed with the quoted literature values. When discrepancies were found, the PAH compound in question was recrystallized from ethanol and the melting point remeasured until satisfactory results were obtained. The nitrogen gas used in the laboratory flow system experiments was generated from the boil-off of a liquid nitrogen source. The air used for the same experiments was filtered laboratory compressed air. No fluorescence background signal was seen from the air alone.

LABORATORY FLOW SYSTEM

The pyrex diffusion cell used to produce known gas phase concentrations of PAH material is shown in Figure 1. Its design is quite simple (Reference 36), and it has been used previously for the delivery of constant quantities of PAH vapor into a nitrogen gas stream (Reference 37). The solid PAH sample is introduced through a removable 1/4-inch outer diameter (OD) sample tube, which is connected to the main body of the diffusion cell with a brass Swagelok union. A Teflon ferrule is used to make the seal on the pyrex sample tube. The main body of the diffusion cell is fashioned from a 3.0 cm OD pyrex tube. The inlet and outlet ports are approximately 1 cm OD, and a 2.5 cm length of 0.1 cm inside diameter (ID) capillary tubing is used on the inlet side of the cell. The 3.0 cm diameter portion of the cell is 9 cm long, and the sample tube length is 11.5 cm. We took the average diameter of the sample tube to be 0.40 cm, including the Swagelok union. The sample tube length and diameter will be used later in the diffusion rate calculations as the average length of the diffusion path ($l = 11.5$ cm) and the cross sectional area of the diffusion tube ($A = 0.126$ cm²).

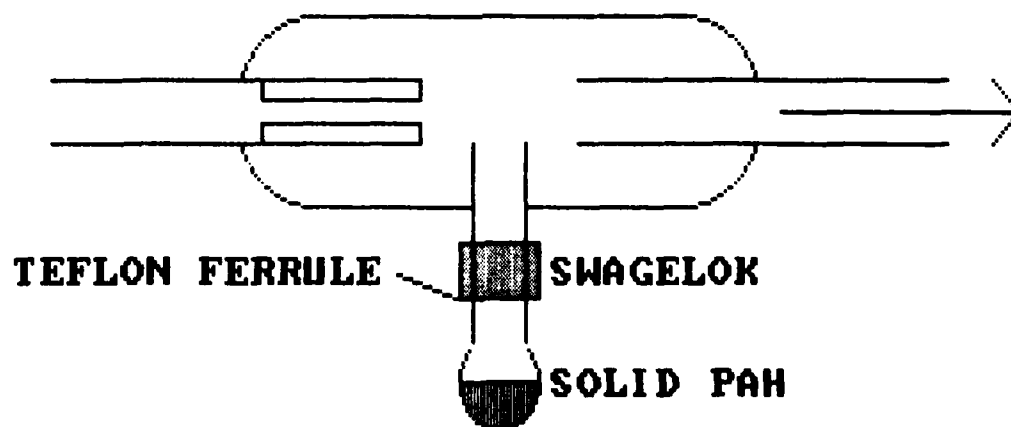


FIGURE 1. Diffusion Cell.

The diffusion cell is incorporated into the laboratory flow system as diagrammed in Figure 2. A 13-foot length of 1/4-inch OD copper tubing precedes the diffusion cell to allow the gases to achieve thermal equilibrium at the furnace temperature before picking up the PAH vapor being generated in the diffusion cell. The connection of the copper tubing to the diffusion cell is made via flexible stainless steel tubing, a Swagelok union, and a glass-to-metal transition tube on the diffusion cell. The purpose of the flexible tubing is to reduce the strain on the fragile glass components.

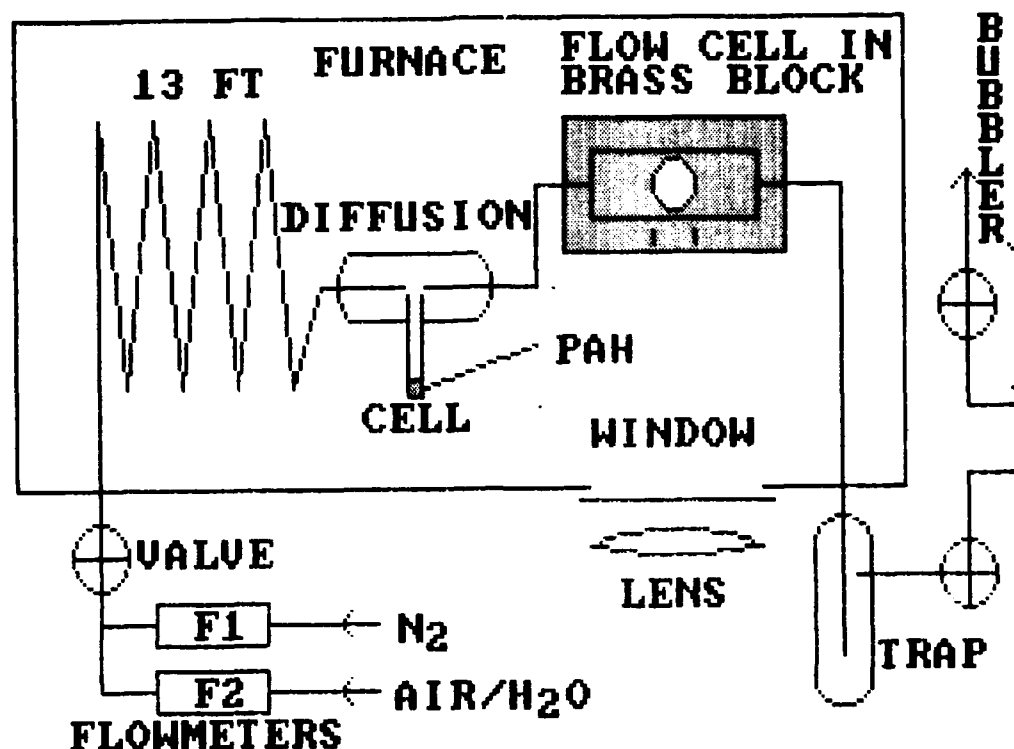


FIGURE 2. Laboratory Flow System.

After exiting the diffusion cell, the diluted PAH vapor stream then passes through a Suprasil-1 quartz fluorescence flow cell (1 x 1 x 2 cm), mounted within a brass block. Holes were made in the block so that the gas phase sample could be excited with laser radiation and the fluorescence emission could be observed at right angles to the excitation beam. A (f7 efficiency) lens collects the emitted light after it passes through a 2-inch diameter window in the insulated faceplate of the furnace. Quartz optics are used throughout to ensure high UV transmission.

The gas stream next flows out of the furnace through an ice/water trap which captures the PAH material. The connection from the fluorescence flow cell to the swagelok feed-through in the furnace faceplate is again made with flexible stainless steel tubing to reduce any strain on the fragile quartz flow cell. Finally, the gases pass through a mineral oil bubbler on the way to a chemical fume hood exhaust.

In order to set the gas flow rates and create gas mixtures, two Brooks Instruments, R-2-15-AAA flowmeters are connected in parallel. These flowmeters have metering valves at their inlet connections which are not shown in Figure 2. Before use, the calibration curves for these flowmeters were checked for accuracy with a bubble flowmeter.

The flow system was enclosed in a Forma Scientific Vacuum furnace (Cat. No. 3053). The door to the furnace was removed and replaced with an insulated faceplate containing the quartz window assembly. The vacuum gauge and valves were also removed, leaving a 1/2-inch diameter hole in the top of the furnace to be used as an access port for the laser beam. A quartz window was mounted over the hole to maintain thermal stability in the furnace. The maximum attainable temperature of the entire assembly is limited by the 232°C temperature rating of the Teflon ferrules. Higher temperatures could be achieved if these were replaced with a more heat resistant material, such as graphite.

Three chromel-alumel thermocouples are positioned in the furnace to monitor the temperature. The first is placed at the PAH sample tube, and the second on the main body of the diffusion cell. The third is placed inside the brass block. The brass block is also wrapped with a heating tape to allow some additional variac adjustment of the fluorescence flow cell temperature. The thermocouple potentials are monitored on three channels of a Hewlett-Packard model 3480A digital voltmeter, equipped with a model 3485A scanning unit, and converted to temperature readings using standard tables.

Before assembling the flow system, all the tubing was thoroughly flushed with several washings of methylene chloride. It has been our experience (Reference 38) that new copper tubing contains a significant number of PAHs, probably formed from the lubricants used during the manufacturing process. After assembly, but before use, the entire flow system was leak checked with helium using a Gow-Mac Instruments model 21-250 gas leak detector. This was done, not only to ensure system integrity, but also as an important safety check.

LASER INDUCED FLUORESCENCE (LIF) SYSTEM

The LIF system used for the laboratory scale experiments is diagramed in Figure 3. The flow system and furnace described previously are present in the upper right corner of the figure. The sample excitation is provided by a Lumonics TE 861T-3 rare gas halide excimer laser, operated on the XeCl line (308 nm). This laser can easily output 70 mJ in an 8 ns pulse at this wavelength, and it is also capable of generating a variety of other UV and vacuum-UV wavelengths when operated with other rare gas halide mixtures. The maximum pulse repetition frequency of the laser is 140 Hz.

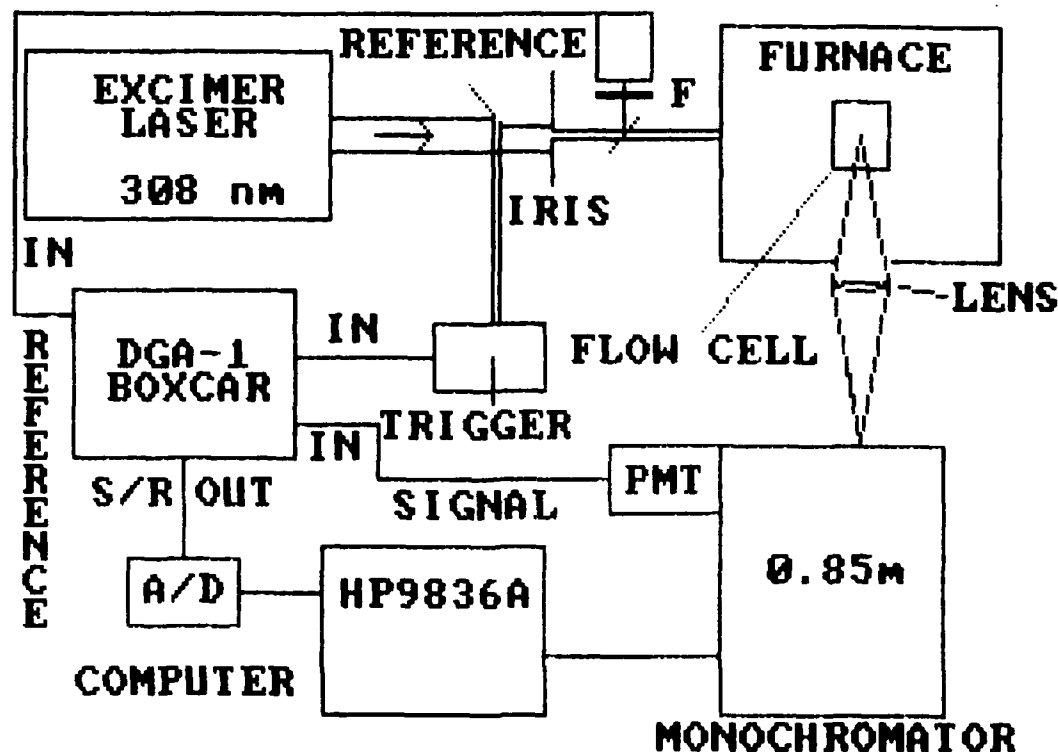


FIGURE 3. LIF System.

From the burn pattern of the excimer beam at 308 nm, its cross section is 4 x 20 mm. The excimer beam is irised to approximately 4 x 7 mm on its way to the furnace/flow cell and a small unused portion of it is reflected off of a pyrex plate to a photodiode trigger for the dual gated amplifier (boxcar). A quartz beamsplitter also picks off about 4% of the excimer beam and, after passing the beam through a 310 nm narrow bandpass filter and a Corning 7380 glass filter (F), sends the beam to a RCA 1P21 reference channel photomultiplier. The purpose of the reference channel is to correct the measured fluorescence emission signal for shot-to-shot laser intensity fluctuations and long term degradation of the laser power.

The beam is also reflected off of two mirrors which, for clarity, are not shown in Figure 3. The first is a 2-inch diameter CVI Corporation XC-2 dielectrically coated, >99% reflectivity, 308 nm mirror which is positioned before the beamsplitter and iris shown in the figure. The second is an ordinary aluminum mirror which is positioned on top of the furnace to steer the beam down through the access hole to excite

the sample in the fluorescence flow cell. Using the area factor for the iris, the maximum power to the sample would be on the order of 24 mJ/pulse. This estimate does not include beam divergence and reflectivity losses from the aluminum mirror and quartz plates. In the work described in this report, the actual power at the sample could have been as much as a factor of two lower than the value quoted above.

The emitted fluorescence is collected and focused into a Spex Instruments model 1404, 0.85 m, double monochromator equipped with 2400 g/mm holographic gratings and controlled by a CD2A Compudrive spectrometer driver. The dispersed emission then strikes the photocathode of an RCA C31034/76 photomultiplier inside a Products for Research model TE104RF thermoelectrically cooled photomultiplier housing mounted on the exit slit of the monochromator. The photomultiplier output is then sent to a Quanta Ray DGA-1 dual gated amplifier, and its ratioed output analog to digitally (A/D) converted for processing with a Hewlett-Packard model HP9836A desktop computer system. The CD2A Compudrive spectrometer driver is connected to the HP9836A computer via a RS-232 interface so that the whole experiment can be controlled from the HP9836A.

The data acquisition is handled under the software control of a program titled AD RLTIME (A/D real-time) written for these laboratory flow system experiments. The operator manually sets the monochromator to the emission wavelength to be monitored and enters information describing the PAH sample and the experimental conditions. The program then pauses, after displaying and labeling the axes for a fluorescence intensity versus real-time plot on the computer monitor screen. When all is ready, the program is continued by the operator and the data acquisition commences at time zero. The program plots the data and simultaneously displays the numeric values of the dependent and independent variables. Since each data point is the average of N samples over an operator prescribed sampling period, the standard deviation is also calculated and displayed, along with the point number, average intensity, and average time over which the samples were taken. A real-time interrupt function key can be pressed during the processing to record the point at which gas flowrates and/or concentrations are changed while the experiment is in progress. At the end of the data acquisition period the operator can then print the information on the experimental conditions and move a cursor through the plotted data to examine and print any points of particular interest (i.e., points taken near flowrate or gas mixture adjustments). Finally, the data set can be stored on disk for future use.

Under steady-state conditions, this program can also be used to generate a plot of fluorescence intensity versus wavelength by scanning the monochromator at a constant rate. As a check, the operator can use the real-time interrupt key to record at what point the monochromator

passes specific wavelength settings during the scan.* The AD RLTIME program is listed in Appendix A, along with examples of the program output, which will be discussed further in the Results and Discussion section.

LANL INCINERATOR COMPLEX

The Los Alamos Controlled Air Incinerator (CAI) used for the incineration testing of the Navy colored smoke compositions has been described in great detail elsewhere (Reference 39). For our purposes, the relationship of the PAH monitor sampling location to the rest of the system is of primary importance. A schematic of the CAI is given in Figures 4 and 5, and a block diagram is presented in Figure 6. The

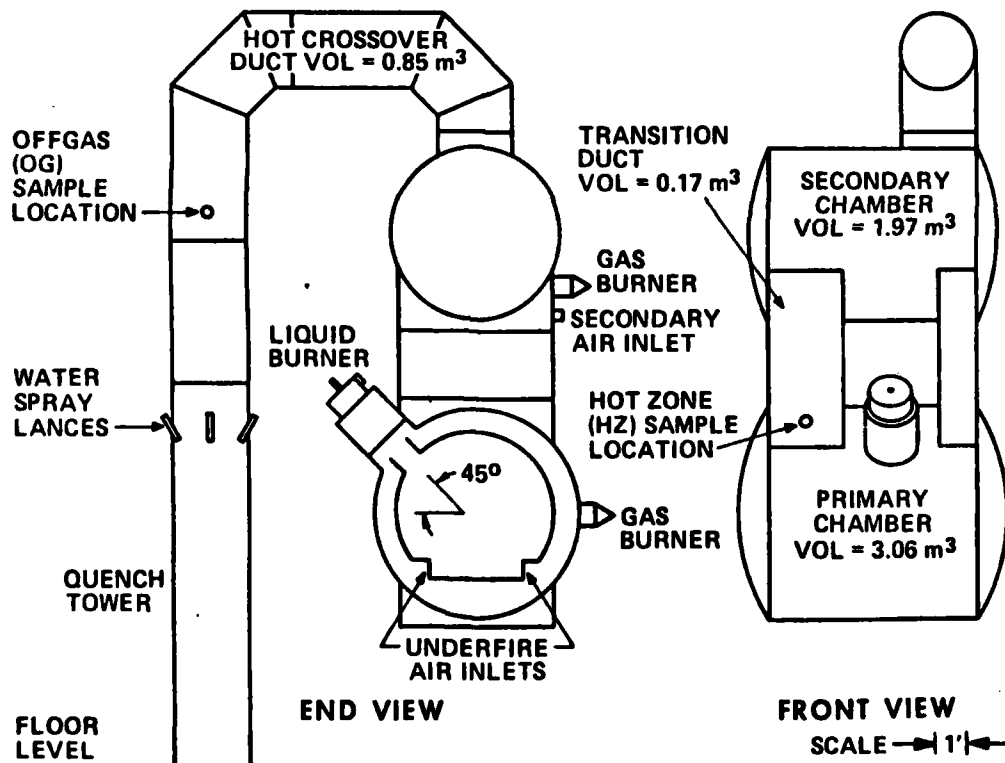


FIGURE 4. Schematic of LANL Controlled Air Incinerator.

*We also have developed other, more elegant data acquisition programs that allow the HP9836A to have complete control of the monochromator scanning.

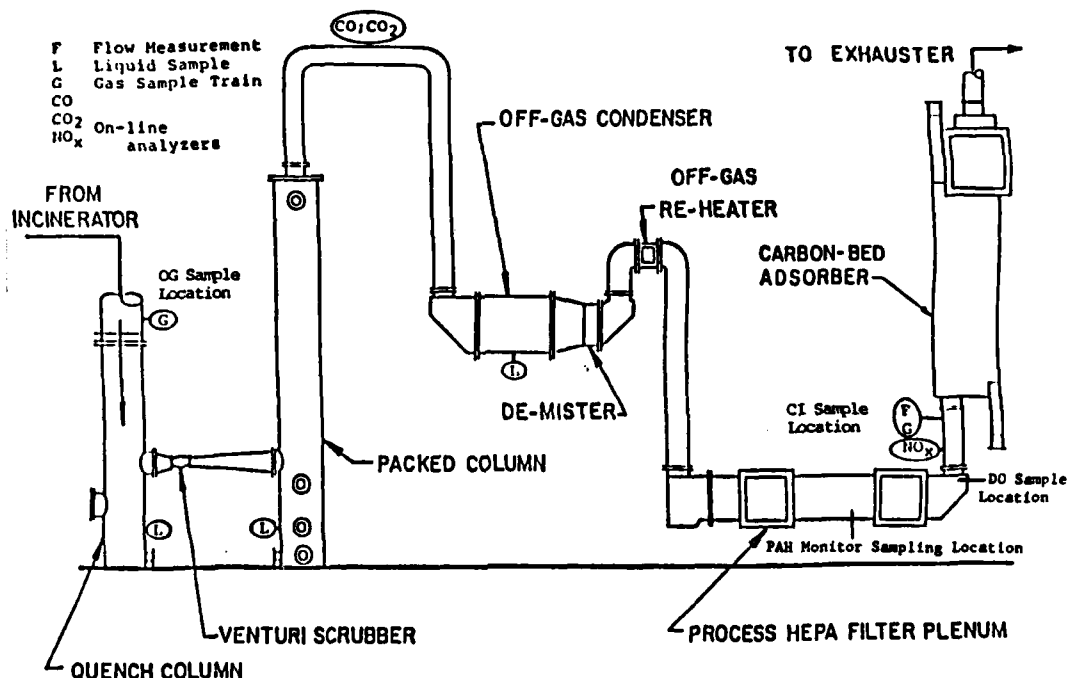


FIGURE 5. CAI Offgas System Sampling and Monitoring Locations.

HZ (hot zone, $T = 982^{\circ}\text{C}$) sampling location is between the primary and secondary incineration chambers. The OG (offgas, $T = 1093\text{--}1204^{\circ}\text{C}$) sampling location is just upstream of the spray quench column, and the DO (demister outlet, $T < 93.3^{\circ}\text{C}$) sampling location is downstream of the offgas demister unit, just after the two High Efficiency Particulate Air (HEPA) filters. The PAH monitor sampling location ($T < 93.3^{\circ}\text{C}$) is in between the HEPA filter assemblies, just before the DO sampling location.

Entropy Environmentalists, Inc., were contracted to perform offgas sampling at the HZ, OG, and DO locations during all phases of the incineration tests. They also recovered and prepared the samples for subsequent analysis by independent laboratories. For the details of the gas sampling equipment, procedures, reporting, and scheduling one should refer to their offgas sampling work plan (Reference 40).

The feed liquid for the incineration tests is a mixture of Navy smoke composition, fuel oil, water, and a wetting agent. It is injected into the incinerator after being dispersed with an atomization nozzle. Several different smoke compositions were fed into the CAI

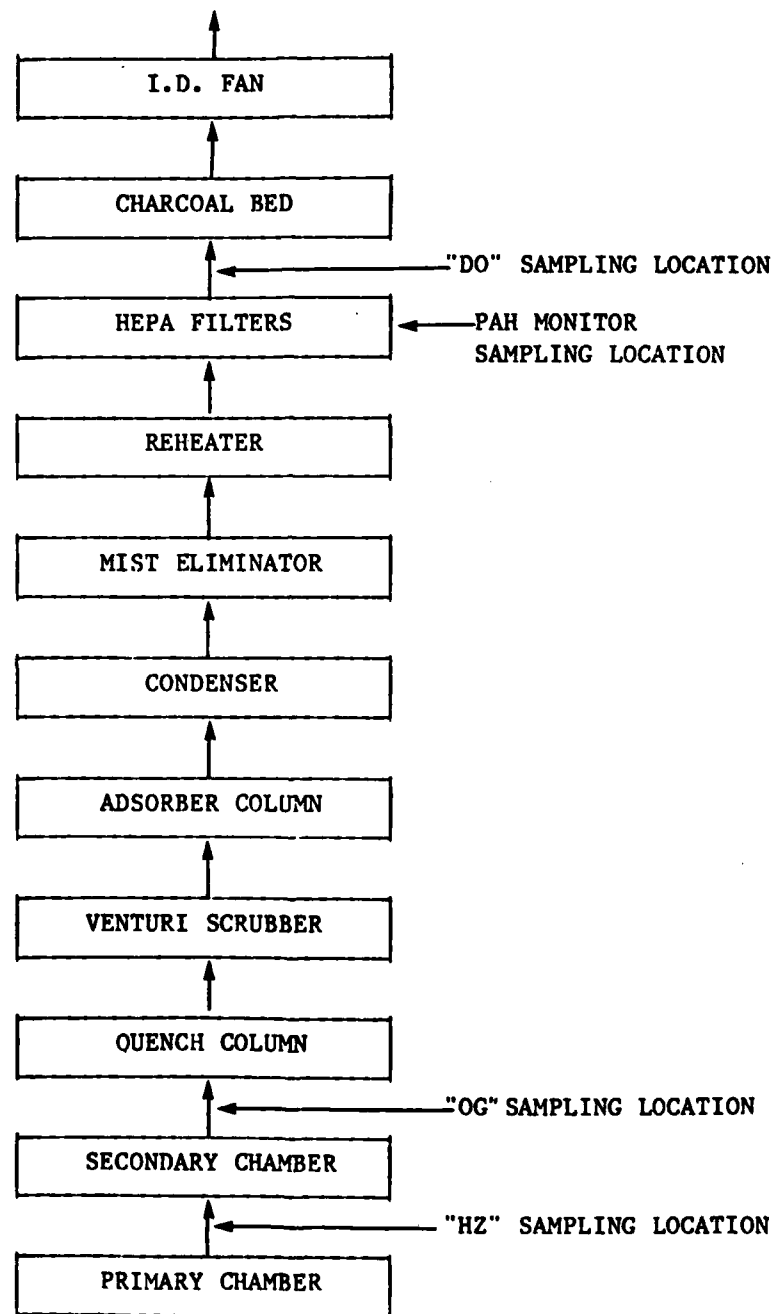


FIGURE 6. Incinerator Air Flow Schematic Showing Sampling Locations.

over 11 phases of operation. The feed schedules and operating conditions are all detailed in the Los Alamos test plan (Reference 41). Chemical compositions of the Navy colored smokes investigated have been reported elsewhere (Reference 1).

Comparative analysis of the real-time results obtained with the PAH monitor system and the collected samples will be made when data from the collected samples become available. At that time, the PAH monitor results will be compared with the data collected at the DO sampling location since these data sets were obtained under nearly equivalent sampling conditions.

PAH MONITOR DESIGN

Basic Spex Fluorimeter

The Spex Instruments, Inc., FLUOROLOG 2 series of fluorimeters are modular in their design. This allows one to choose among a variety of excitation sources, spectrometers, sample compartments, detectors, and accessories to assemble an instrument for a particular application. An optical schematic of a model F112 version of this instrument is presented in Figure 7. This figure is a composite drawing, pieces of which were taken from the Spex advertising literature (Reference 42). The F112 designation defines the spectrometer and sample compartment make-up of the instrument. As can be seen from the figure, there is a single (F1_) excitation spectrometer which disperses the light emitting from a xenon lamp source. The spectrometer grating and slits determine the wavelength and bandpass of light used to excite the sample, which is located in the single-beam (F_1_) sample module. The emitted fluorescence is then collected in either a right angle (90 degrees) or front face (22.5 degrees) geometry (user selectable), and dispersed in a double (F_2_) emission spectrometer before striking the photocathode of a photomultiplier tube mounted on the exit slit of that spectrometer. If desired, other versions of the instrument (e.g., F122, F212, and F222, etc.,) can be configured or the existing system upgraded.

The Spex DATAMATE is a microprocessor (Motorola 6800) based spectrometer controller and data processor for the FLUOROLOG 2 series. A listing of its rather extensive capabilities is given in Appendix B. It is important to note that one can easily accomplish selective excitation and emission, synchronous excitation, derivative spectroscopy, and acquire complete excitation-emission matrices with the standard fluorimeter.* DATAMATE software programs can also be written for fully automatic operation of the instrument.

*Refer to the Background section for the relevance of these methods to the problem of PAH analysis.

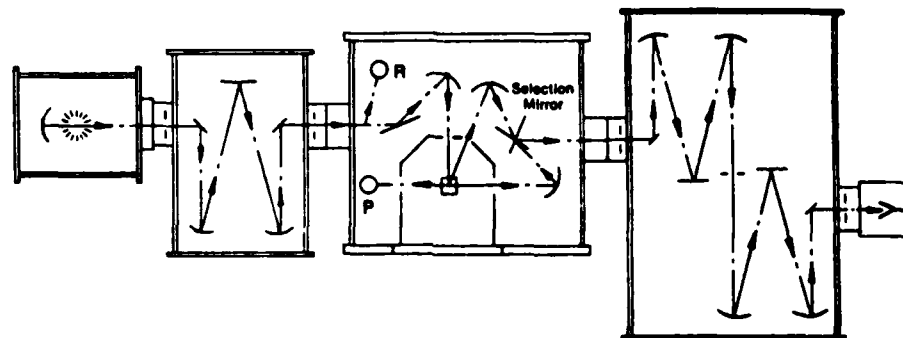


FIGURE 7. Optical Schematic for the Spex Industries, Inc. FLUOROLOG 2 Version F112.

The specific components which comprise the model F112 fluorimeter purchased for this project are given in Table 2. Comments regarding the individual components in relation to the overall PAH monitor design considerations are given below, in order of the item numbers in the table:

1. A single excitation monochromator was chosen, rather than a double, in order to maximize the throughput of the lamp. Since fluorescence intensity depends directly upon the excitation intensity, greater throughput of the lamp should translate to a greater sensitivity of the PAH monitor.
2. A double emission monochromator was chosen because of its superior stray light rejection as compared to a single monochromator. It was felt that scattered light might be a problem if particulates were encountered in the work.
3. We chose the cheaper fixed slit sets over the more expensive micrometer adjustable ones realizing that there would probably be little need for adjustments because of the broad nature of the PAH fluorescence.
4. The excitation grating was blazed at 250 nm to maximize the lamp throughput for wavelengths known to excite the PAHs of primary interest.
5. The two emission gratings were blazed at 300 nm to maximize the fluorescence throughput for those wavelengths over which the PAHs emit.

TABLE 2. FLUOROLOG 2 Model F112.^a

Item	Qty	Cat. no.	Description
1	1	1681B	Single excitation monochromator, 0.227 m f/4
2	1	1680B	Double emission monochromator, 0.227 m f/4
3	4	1679	Sets of fixed slits
4	3	16016	Gratings, 1200 g/mm, in kinematic mounts. Excitation blaze = 250 nm, emission blaze = 300 nm
5	1	1691	Single-beam sample module
6	1	1909	Xenon lamp housing
7	1	1907	Xenon lamp, 450 watt (W)
8	1	1907P	Power supply for 1907
9	1	1914G	Cooled R928 photomultiplier assembly
10	1	1910	Quantum counter reference assembly
11	1	DM1A	DATAMATE, with DM101 and DM104
12	1	DM101	Input channel (additional)
13	1	DM102	Photon counting (PC) acquisition module
14	1	DM103	Direct current (DC) acquisition module
15	1	DM104	High voltage (HV) power supply (additional)
16	1	DM105	Data and programming package
17	1	DM111	Dual disk drive
18	1	DM112	Digital plotter
19	1	1931A	Brass sample heater/cooler block

^aThe total cost, including installation and General Services Administration (GSA) discount, was \$36K.

7. A 450-watt xenon lamp was chosen rather than the standard 150-watt lamp to again maximize the excitation (and therefore emission) intensity.

9. The cooled photomultiplier housing was chosen in order to reduce the dark count (thermal noise) of the photomultiplier. The relatively inexpensive R928 photomultiplier was chosen because its spectral response, over the wavelength range germane to the PAH problem, is actually better than some more expensive tubes.

10. This assembly enables one to ratio the lamp intensity to the fluorescence emission intensity. Thus, one can correct the fluorescence excitation spectra for the fact that the lamp intensity is a function of wavelength. It also corrects for errors caused by lamp intensity fluctuations during a scan.

12. Needed for 10.

13. PC is much more sensitive than DC measurement for weak fluorescent signals.

14. The DC module is for the reference channel. The more expensive PC module is not needed here because plenty of light gets to the reference channel (R in Figure 7).

15. Needed for 10.

17. Needed for program and data storage.

18. Needed for hard copy output.

19. Needed to house and heat the fluorescence flow cell.

Flow Cell Modifications

In order to perform the real-time fluorescence analysis of the incinerator effluents or calibration cell samples with this fluorimeter a minor modification of the standard F112 sample chamber is required. The fluorescence flow cell assembly constructed for this purpose is diagramed in Figure 8. An NSG Precision Cells type 501 FL UV flow cell (\$185.00) is mounted within the Spex 1931A brass sample heater/cooler block. The hose connectors on the 1931A were drilled out to allow for the insertion of two, 100-watt Chromalox cartridge heaters (CIR-1012). The heaters are controlled with a Chromalox model 3912 digital indicating on-off temperature controller, and the feedback is provided by a type J thermocouple (iron/constantan). Initially, with the thermocouple positioned in a hole at the top of the brass block, a range of 7.2°C was measured during the on-off cycle of the controller. By positioning the thermocouple in a hole in the brass block at the center of one of the cartridge heaters and wiring the heaters in series with a resistor, we were able to reduce the temperature fluctuations to an acceptable $\pm 1.4^\circ\text{C}$ at a set point of 65.6°C.

The connection from the flexible stainless steel tubing to the quartz flow cell was made with a short length of 1/4-inch OD Teflon tubing. This size fits nicely over the 5 mm OD flow cell ports and can be softened with a heat gun to stretch over the stainless steel tubing.

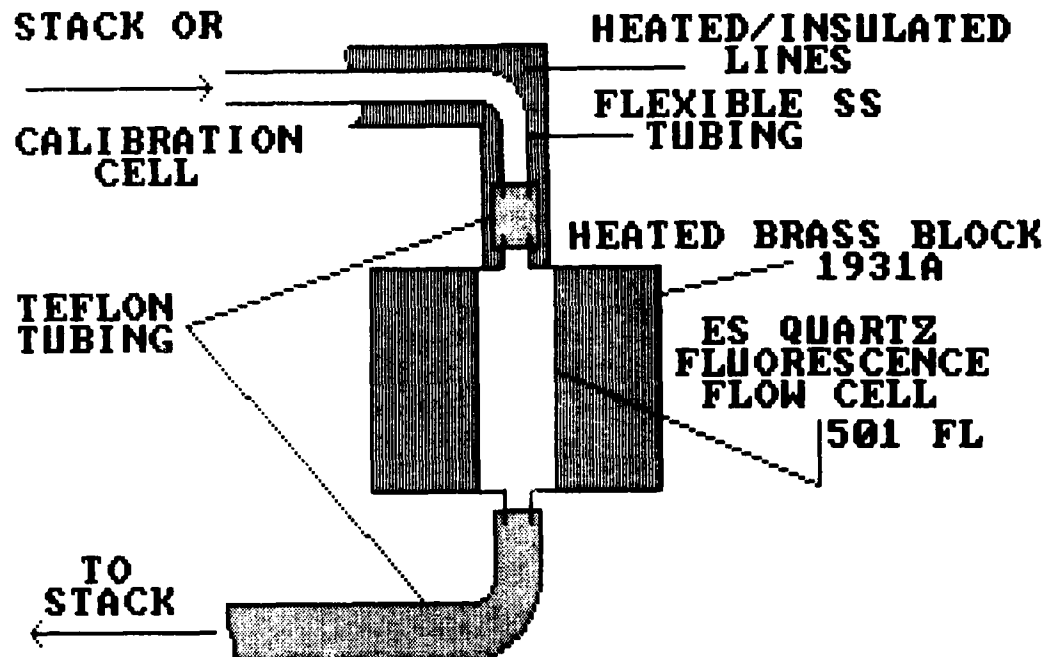


FIGURE 8. Fluorescence Flow Cell.

The 232°C rating of the Teflon limits the maximum temperature of the assembly, but given the temperature range of the stack gases at the PAH monitor sampling location (<93.3°C), the Teflon range is more than adequate. The flexible Teflon tubing is also used on the exit side of the flow cell, and this part of the line is unheated. Variac controlled heating tapes maintain the temperature of the incoming line, which is also wrapped with insulating tape. The temperature of the line is monitored with a type J thermocouple (see next section for more details).

The incoming and exiting lines, along with the cartridge heater wires and thermocouple, all fit through holes which are already in the Spex 1691 sample module. The 1931A brass block is made to mount into the sample module such that the flow cell is optically aligned with the rest of the instrument. No additional adjustments are necessary. This means that the flow system can be very easily dismantled at the Teflon joints for cleaning, repair, etc. Also, since the brass block will hold standard 1 cm cuvettes, the system can be easily reconfigured for the fluorescence analysis of liquid (or solid) samples. To do this, one need only cool down the block and flow lines, stop the flow, dismantle and remove the flow cell, and replace it with the sample of interest contained in a standard 1 cm cuvette. This could be done to analyze for PAHs in collected and extracted samples from other parts of the incinerator system.

PAH Monitor Flow System

The overall PAH monitor flow system incorporating the fluorescence flow cell assembly of Figure 8 is given in Figure 9. The stack gases from the PAH monitor sampling location (refer to Figures 5 and 6) pass through 11 feet of heated and insulated tubing (lines 1 and 2) before entering the fluorescence flow cell, mounted in the Spex instrument. A calibration cell (line 3) is teed into line 2 so that the instrument response to a known PAH concentration can also be measured. The length of lines 3 and 2, from the exit of the furnace to the entrance of the fluorescence flow cell, is 8 feet. All the heated and insulated lines are made from 1/4-inch diameter stainless steel tubing which was cleaned with acetone before use. Variac controlled heating tapes maintain the temperatures in the heated lines, and type J thermocouples are positioned at the points labeled 1-4 in the figure. An Omega Engineering model DSS-650 type J thermocouple thermometer monitors the temperatures at those locations.

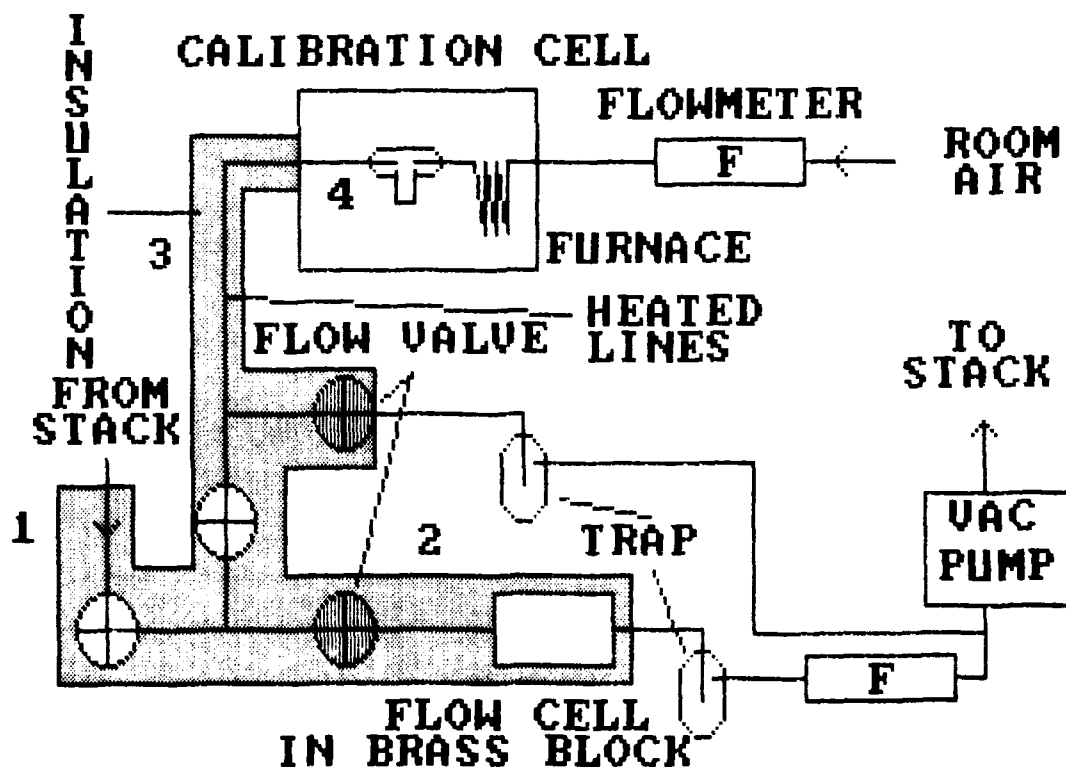


FIGURE 9. PAH Monitor Flow System.

The line running parallel to line 2 (and teed into it just before the vacuum pump) permits the calibration cell to continue functioning normally when the incinerator gases are being analyzed. If it were not there, PAH materials in the heated furnace would continue to diffuse and eventually plate-out on line 3 and the line going to the calibration cell flowmeter. This would defeat the purpose of the calibration cell and could expose workers to PAH vapors coming from the flowmeter inlet.

The unheated lines are made of either Teflon or polyethylene tubing, and an ice-water mixture is used to cool the traps. The flowmeters are Gilmont Instruments Cat. No. F1100 size #1 (maximum flowrate 270 ml/min, standard air at one atmosphere and 70°F). They are connected in series (for line 2) so that one can check for leaks in the monitor system by observing the relative flowrates on the two flowmeters. A modest vacuum pump is needed to generate the flow because the Los Alamos CAI operates at a negative pressure (50 inches of water less than atmospheric at the site). At negative pressures, any leaks in the incinerator system would cause materials to leak in, not out. This is done as a safety precaution, which also permits the processing of radioactive waste materials on other contracts.

To check the instrument response to a known PAH concentration, the system is operated with the on/off valve from the incinerator stack in the off position. The on/off valve from the calibration cell is in the on position, and the flow valve for the line parallel to line 2 is closed. In this configuration, ambient room air from the area near the furnace is drawn through the flowmeter under the action of the vacuum pump. The flowrate is set by the flow valve just before the fluorescence flow cell. The 10-foot coil of tubing inside the Fisher model 556 laboratory furnace allows the air to equilibrate at the furnace temperature before entering the diffusion cell (refer to Figure 1).^{*} The air stream dilutes the PAH vapor being generated in the diffusion cell, and the mixture flows through the heated lines to the fluorescence flow cell for analysis. After exiting the flow cell, the PAH material is collected in the trap, and the air stream passes through the second flowmeter. Following its passage through the pump, the air is returned to the incinerator stack well beyond the DO sampling location (refer to Figure 5).

To analyze the incinerator stack gases, one simply opens the on/off valve from the stack, closes the on/off valve from the calibration cell, and opens the flow valve in the line parallel to line 2. This

^{*}An Ultratorr fitting with a Viton O-ring was used at the LANL, rather than a Swagelok fitting with a Teflon ferrule, as shown in Figure 1.

keeps the calibration cell functioning while the stack gas analysis proceeds. The flowrate in the parallel line need only be enough to keep the PAH material in the calibration cell from plating out in the lines. The flowrates in both lines are set by their respective flow valves. If, at any time, the operator wishes to recheck the calibration, the valves are simply reconfigured as described in the last paragraph.

RESULTS AND DISCUSSION

DIFFUSION CELL EVALUATION

Theory

The diffusion coefficient for two perfect gases, designated 1 and 2, can be calculated using the following expression (References 43 and 45):

$$D = \frac{3}{8(2\pi)^{1/2} N_o} \times \frac{(RT)^{3/2}}{P} \times \frac{\left(\frac{M_1 + M_2}{M_1 M_2} \right)^{1/2}}{d_{12}^2} \quad (1)$$

where

D = diffusion coefficient in $\text{cm}^2/(\text{sec-molecule})$

N_o = Avagadro's number = 6.023×10^{23} molecules/mole

R = ideal gas constant = 8.31448×10^7 (dyne-cm)/(mole-°K)

T = temperature in °K

P = total pressure in dynes/ cm^2 (1.01325×10^6 at 760 torr)

M_1 = molecular weight 1 in g/mole. (N_2 , air, etc.)

M_2 = molecular weight 2 in g/mole. (PAH)

$d_{12} = 1/2(d_1 + d_2)$ in cm

d_1 = molecular hard sphere diameter for vapor 1 in cm

d_2 = molecular hard sphere diameter for vapor 2 in cm

One can make an estimate of the hard sphere collision diameter from data on the bond lengths and angles of the molecules involved. Using values of 1.4 and 1.1 Å for the aromatic C=C and C-H bond lengths, 1.1 Å for the N₂ bond length, and the cosine of 30 degrees, $d_{12} = 5.14$ Å can be easily computed for the anthracene-N₂ combination. A geometry where the long axes of the molecules were placed end to end was assumed in the calculation.

The vapor concentration delivered by the diffusion cell is determined by the ratio of the rate of diffusion of vapor from the diffusion tube and the diluent gas flow rate. The diffusion rate can either be measured from the change in weight of the sample tube, or calculated from the diffusion equation (Reference 36):

$$r = \frac{DAM_2P}{RTl} \times \ln \left(\frac{P}{P-p} \right) \quad (2)$$

where

r = molecular diffusion rate in mg/(sec-molecule)

D = molecular diffusion coefficient in cm²/(sec-molecule) (from equation 1 above)

A = cross sectional area of diffusion tube in cm²

M_2 = molecular weight of vaporizing species in g/mole

R = gas constant = 0.08205 (l-atm)/(mole-°K)

T = temperature in °K

l = average length of diffusion path in cm

P = total gas pressure in diffusion cell in atm

p = partial pressure of vapor at temperature T

Equations 1 and 2 are incorporated in a BASIC program called DIFF RATE (Diffusion-Rate), listed in Appendix C along with sample output (which should be rounded to 3 significant figures). The program contains the parameters specific for the flow system experiments done at the NWC, i.e., $P = 700$ torr, $l = 11.5$ cm, and $A = 0.126$ cm². Two other versions of this program are parametrized for sea-level, and the LANL.

They are called DIFF SEA and DIFF LASL, respectively, and sample output is also included in Appendix C for comparison purposes. A program equivalent to DIFF LASL, but written in the Spex Datamate programming language, is presented in Appendix D. All these programs permit the calculation of the PAH vapor concentration delivered by the diffusion cell under a variety of conditions.

PAH Diffusion Rate Measurements

In order to determine the accuracy of the simple calculations outlined previously, experimental measurements of PAH diffusion rates were undertaken, using the laboratory flow system of Figure 2. To do this, the cleaned diffusion cell sample tube was first loaded with approximately 10 mg of solid PAH. Next, this tube was weighed on a Mettler HL52 microbalance, and replaced in the flow system. At this point, the time was recorded and the furnace was heated to the desired operating temperature. A N₂ diluent gas flow was also initiated to keep the diffusing PAH vapor from condensing in the flow lines (nominally 40 ml/min). The system was maintained at a steady state for such a time as to ensure a measurable weight loss in the sample tube. After the prescribed time period had elapsed, the furnace was turned off and the total time recorded. When room temperature was achieved, the N₂ flow was stopped, and the sample tube reweighed. The mass loss, divided by the total time, gives a measure of the appropriate PAH diffusion rate for that set of experimental conditions. This value can then be compared to that calculated using equations 1 and 2.

To minimize the error caused by the finite time required to achieve steady state operating conditions, the start and stop times were defined as the times when power to the furnace was started and stopped. In this way, the "lack" of material diffused while the furnace was heating up was partially corrected for by the "extra" material diffused as the furnace was cooling down. Also, each experiment was run over a total time period of several days. Therefore, the approach of the diffusion cell to the steady state (a few hours) represented a small error.

The results presented in Table 3 show that the simple calculation can reasonably predict the measured diffusion rate for a number of PAHs over a range of conditions. In the case of the largest discrepancy between measured and calculated values (pyrene), it is quite likely that the biggest problem was in the accuracy of the pyrene

TABLE 3. PAH Diffusion Rate Measurement.^a

PAH	Anthracene	Phenanthrene	Naphthalene	Pyrene
T (°C)	159.0	133.5	25.0	128.0
p (torr) (Reference 46-48)	2.25	2.03	0.087	0.105
d ₁₂ (A)	5.14	5.15	3.9	5.15
M ₂ (g/mole)	178.0	178.0	128.0	202.0
Weight loss (mg)	7.73	5.73	0.20	0.51
Time x 10 ⁻⁵ (sec)	3.723	2.628	1.980	4.968
r x 10 ⁵ (mg/sec) measured	2.08	2.18	0.101	0.103
r x 10 ⁵ (mg/sec) calc. (DIFF_RATE)	2.28	1.98	0.0935	0.115

^aN₂ diluent gas (M₁ = 28 g/mole) at P = 700 torr (NWC).

vapor pressure parameter. The value used had to be extrapolated* from literature data measured over a 69 to 85°C range (Reference 48). In addition, some laboratory temperature fluctuation could also have occurred during the naphthalene experiment, thereby affecting its accuracy. The largest difference between measured and calculated values encountered was approximately a factor of two, and this "worst case" measurement was purposefully made using impure phenanthrene.

LABORATORY FLOW SYSTEM EXPERIMENT USING LIF

When we were ready to begin our flow system experiments, the research group at Battelle Laboratories had already measured the LIF emission spectra of a number of the PAHs listed in Table 1. These observations were made with the PAHs at elevated temperatures in a

*The literature data was fit to an equation of the form $\log_{10}P = -a/T + b$ to determine values for a and b. With these values, P could then be calculated at another T. For accuracy, the T value, for which the new calculation of P is required, should be close to the measured data range.

static nitrogen atmosphere. The question of fluorescence quenching by oxygen and other atmospheric gas components (water, carbon dioxide, etc.) had not yet been addressed. Quenching would significantly reduce the measurable fluorescence intensity for a given PAH concentration, which in turn, would raise minimum detection limits of the fluorescence technique. Since this information was critical to the monitor design considerations, flow system experiments were conducted with the apparatus shown in Figures 2 and 3. The intent was to complement the LIF work already begun at Battelle.

The first molecular combination studied in the flow system was anthracene-N₂. The RUN #1 output, given in Appendix A, shows the LIF emission spectrum of anthracene taken at 164°C (fluorescence cell temperature). This spectrum was taken under steady state conditions while scanning the wavelength drive of the monochromator at a constant rate. Therefore, the time axis is also the wavelength axis. From the DIFF RATE sample calculation, given in Appendix C, the anthracene concentration was calculated to be 7.47 ppm at the 40 mL/min N₂ flowrate. Using the data in Table 3, the calculated value should be adjusted by a factor of $2.08/2.28 = 0.912$, which gives a measured value of 6.81 ppm. This LIF emission spectrum, obtained with a flow system, agrees quite well with the static cell measurement given in Figure 3 of the Battelle report (Reference 2), although their results were obtained at much higher concentrations (210 - 500 ppm). The excimer laser at 308 nm does not excite into the absorption maximum for anthracene at 344 nm. Using the excimer pumped dye laser at this wavelength could increase the LIF intensity by about a factor of 7. In addition, the broad emission spectrum does not require the 0.23 nm resolution used. The throughput (and therefore sensitivity) could be increased by increasing the bandpass of the monochromator. The use of a smaller, higher throughput (and cheaper) monochromator could increase the sensitivity even further, if desired.

The output of RUN #2, given in Appendix A, shows the results of flow changes on the anthracene-N₂ LIF intensity at fixed excitation and emission wavelengths. The calculated anthracene concentration can be obtained from the DIFF RATE output in Appendix C. The intensity versus time plot shows that the intensity response is directly proportional to concentration, i.e., a change of a factor of two in flow rate (concentration) produces a change of a factor of two in the LIF intensity. Also, after each change in flow rate, the steady state is reached in a time period given approximately by $l^2/2D$ (Reference 36). These results demonstrate, quite nicely, how easily known concentrations of PAH material can be generated with the flow system/diffusion cell combination.

The effect of laboratory air on the anthracene LIF intensity is presented in RUN #3 of Appendix A (with appropriate calculations in

Appendix C). Air was found to quench the LIF intensity by about a factor of 5.5. The comments regarding the problems in setting the flow rate in the AD RLTIME output listing meant that one needed to keep an eye on the flowmeter and make minor adjustments with time, not that there were major deviations of the flow. When the change was made from N₂ to laboratory air at the same flow rate, the response time for the LIF intensity change reflected the time required for the new diluent gas to travel through the volume of tubing before reaching the fluorescence flow cell. Flow rate changes, on the other hand, were reflected in immediate intensity changes, as with the previous experiments. Our air quenching results were consistent with those on other PAHs studied by Battelle (Reference 2), and an order of magnitude was found to be a reasonable quenching estimate for the PAHs as a class. The largest value observed was for naphthalene (times 20, taken from Figures 21 and 22, Reference 2). This makes intuitive sense in that naphthalene has a relatively long fluorescence lifetime and would therefore undergo a larger number of collisions in the excited state before emitting a photon. This would increase the probability of its fluorescence being quenched relative to a molecule like anthracene, whose fluorescence lifetime is shorter. It was not felt that the magnitude of the air induced fluorescence quenching of the PAHs was large enough to warrant any basic PAH monitor design changes.

In examining the standard deviation data for all three runs, and comparing it to the graphic plots, the magnitude of the "noise" in the data was initially perplexing. The approximately 0.5 volt intensity fluctuations in the LIF, versus the ≤ 0.1 volt standard deviations (over the 20 data reads per second), were traced to the mineral oil bubbler in Figure 2. The bubbling action of the gas was causing pressure (and therefore concentration) fluctuations in the fluorescence cell. This phenomenon was not discovered early in the testing because no fluctuations were seen on the flowmeters, where one would expect to observe them. The 13 feet of tubing in the flow line acted as a ballast on the inlet side of the system, which damped them out. Also, the capillary tubing on the inlet side of the diffusion cell (Figure 1) would prevent the pressure backup to the flowmeters. Taking the data in the plots as an estimate, concentration fluctuations on the order of 500 parts-per-billion (ppb) were being observed in these experiments. The mineral oil was subsequently removed from the bubbler.

A program update meeting was held at LANL in April 1983. The reason for holding the meeting there was to familiarize all those concerned with the CAI site, where the incineration testing of the Navy colored smokes would be conducted. One of the outcomes of this meeting was the decision to move away from the laboratory LIF oriented experiments and towards the construction of a PAH monitor utilizing fluorescence detection. Our work shifted to the evaluation of commercially available equipment for this purpose. This topic will be discussed in the next section.

COMPARISON OF PAH SPECTRA (STATIC CELL)

Beckman DU-7 Absorption Spectrophotometer

In the process of developing a suitable test for the ability of commercial instrumentation to detect gas phase PAH concentrations, it was decided to measure the absorption spectrum of some possible candidate materials. One such spectrum of a mixture of naphthalene and phenanthrene is given in Figure 10. A small crystal of each material was carefully placed in the bottom of a cuvette (the special care was taken to make sure none of the solid material stuck to the cuvette windows). The cuvette was capped, placed inside a Beckman DU-7 absorption spectrophotometer, and the UV/VIS spectrum was obtained. The concentration of the gas phase material was determined by the partial pressure of each component. The spectrum of Figure 10 is essentially that of naphthalene alone since it is identical to a similar spectrum obtained with no phenanthrene in the cuvette. The instrument is incapable of detecting phenanthrene under these conditions.

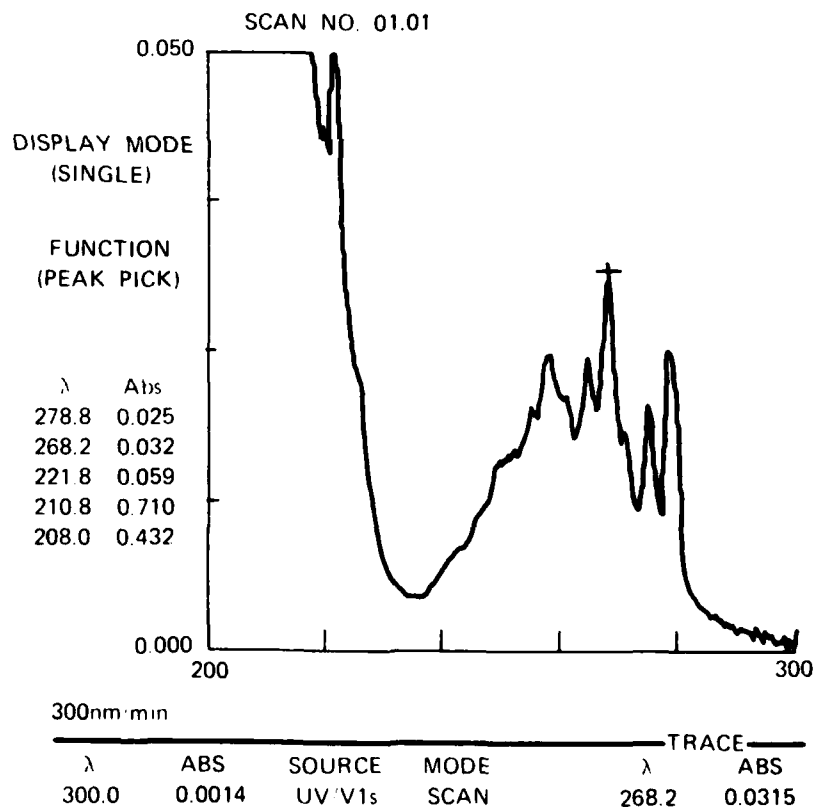


FIGURE 10. Absorption Spectrum of a Naphthalene/Phenanthrene Mixture, Taken in Air, at 23°C. Pathlength = 1.0 cm.

From the absorbance, pathlength, and the molar extinction coefficient, the naphthalene concentration can be calculated. Using an approximate value of 6×10^3 L/(mole-cm) for the extinction coefficient of naphthalene near 286 nm (Reference 49), a value of 5.25×10^{-6} molar can be calculated for the concentration, given the absorbance value from the figure. Multiplying by the molecular weight, and using the conversion factors in Appendix D, this translates into approximately 138 ppm. "Approximately" is used here because the extinction coefficient value was taken from a solution spectrum and because the background and absorption spectra were not taken in matched cells. Nonetheless, it is a reasonable estimate and an independent check on what follows below.

The concentration can also be calculated with the following expression:

$$\text{ppm} = (p/P) \times 10^6 \quad (3)$$

where

ppm = parts-per-million

p = partial pressure of vapor

P = total gas pressure

At 23°C, the vapor pressure of naphthalene is 0.0712 torr (Reference 46). At a total pressure of 700 torr (NWC), equation 3 gives a value of 102 ppm. Given the considerations mentioned above, there is reasonable agreement with the absorbance-derived result. For phenanthrene, with a vapor pressure of 1.39×10^{-4} torr (Reference 48), the concentration would be 0.2 ppm. It is not surprising that it went undetected.

In all fairness to the absorption technique, it should be mentioned that a long pathlength cell (e.g., 10 m) can be added to an absorption instrument, greatly increasing its sensitivity. Unfortunately, this still does not solve the selectivity problems discussed in the Background section. Also, alignment of a 10 m cell requires a certain amount of patience, and it can be difficult to clean, if contaminated.

Perkin-Elmer MFP-44B Spectrofluorimeter

Figure 11 shows the fluorescence excitation and emission spectra of the same naphthalene/phenanthrene sample studied above. Again, the 0.2 ppm phenanthrene component was not detected, but the signal to

noise ratios for the naphthalene spectra were somewhat better than those in Figure 10. The emission spectra compare quite favorably to the LIF results of Battelle (Reference 2), and we now have a selective excitation capability. Because this sample was studied in air, the fluorescence quenching factor is also included in the measurement. Extrapolation of these data would indicate that one could detect naphthalene down to about a 10 ppm level.

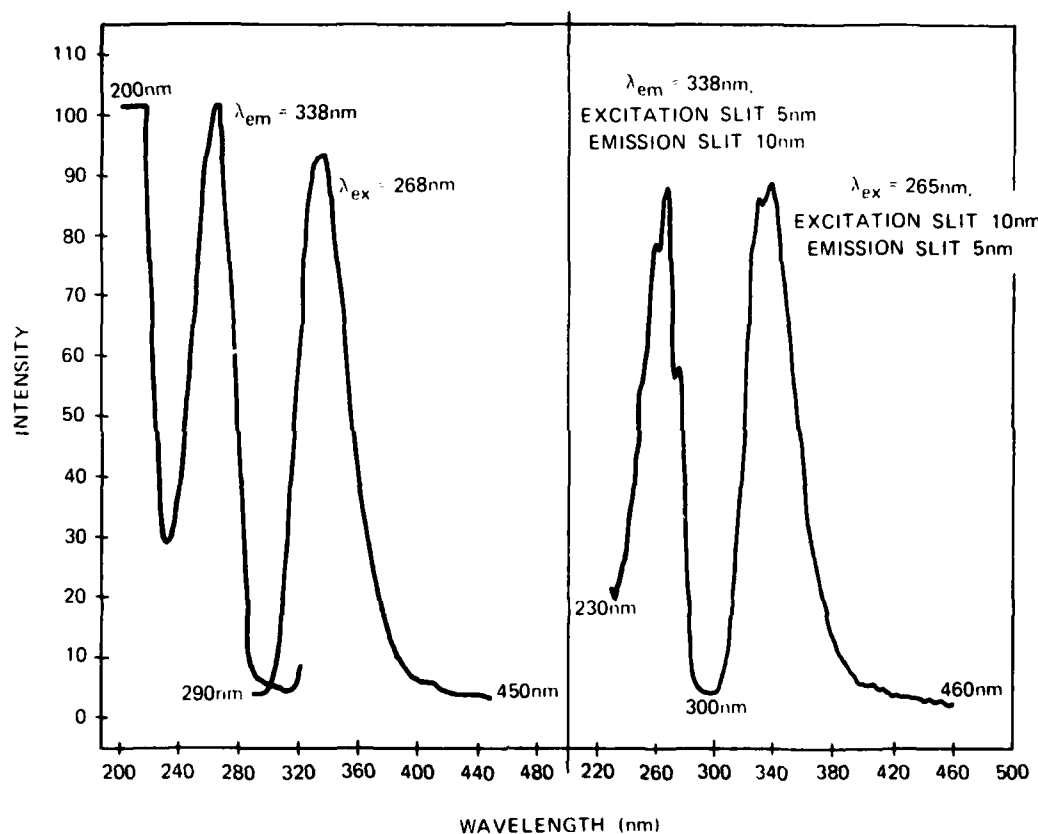


FIGURE 11. Fluorescence Excitation and Emission Spectra of a Naphthalene/Phenanthrene Mixture, Taken in Air, at 23°C. Pathlength = 1.0 cm.

As a further test of the instrument, a cuvette containing phenanthrene was mounted in a brass block which fits inside the Perkin-Elmer instrument. Heated water, flowing through the block can bring the cell temperature to as high as 80°C. Figure 12 shows the phenanthrene excitation and emission spectra taken in air, at 80°C. The concentration

was about 53 ppm, and the spectra are consistent with other measurements (References 2, 7, 8 and 11). The excitation intensity, below approximately 237 nm, should be regarded with suspicion. The xenon lamp intensity falls off dramatically in this wavelength region and there may well be other instrumental artifacts. The feature near 480 nm in the emission spectrum is the second order scatter from the excitation wavelength used (237 nm). Again, it would appear that a 10 ppm level would be the approximate detection limit.

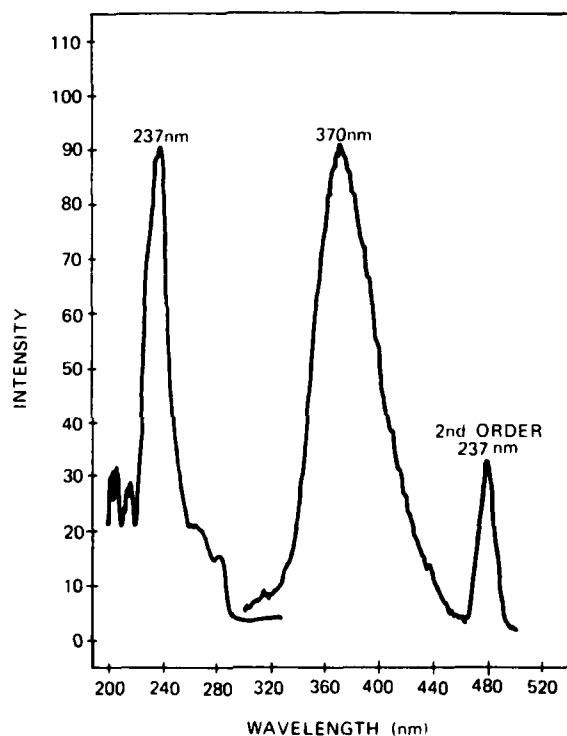


FIGURE 12. Fluorescence Excitation and Emission Spectra of Phenanthrene, Taken in Air, at 80°C.

The fluorescence spectra of pyrene in air, at 80°C, are given in Figure 13. The vapor pressure of pyrene is 2.42×10^{-3} at 80°C (Reference 48), which gives a concentration of 3.5 ppm. The greater sensitivity for this PAH follows from the fact that the quantum yield of pyrene is larger than that of both naphthalene and phenanthrene (by a factor of 1.4 and 2.5, respectively, in solution) (Reference 49). The increase in the emission intensity beyond 460 nm is second order scattering from the excitation used (239 nm). By extrapolation, sub-ppm detection levels would be possible with this material.

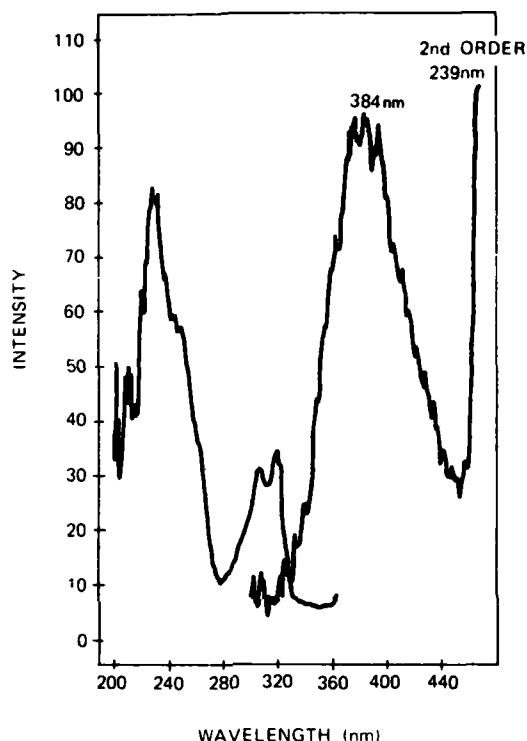


FIGURE 13. Fluorescence Excitation and Emission Spectra of Pyrene, Taken in Air, at 80°C.

The Perkin-Elmer instrument, on which the preceding work was done, is equipped with a 150 W xenon lamp, and its detection electronics work in either a direct current (DC) or an alternating current (AC) mode. Its response was such that it would not quite meet the 1 ppm PAH detection requirements of the program, and it was felt that further searching was necessary for an appropriate PAH monitor instrument. Photon counting is known to be a more sensitive method of detection than DC or AC amplification. An instrument with photon counting electronics and a greater lamp flux was next considered.

Spex F112 Fluorimeter

After we contacted Spex Industries about their FLUOROLOG 2 series of instruments, they agreed to perform some static cell, gas phase

fluorescence experiments, similar to the ones described in the previous section. The F112 version of their fluorimeter used for these tests had photon counting detection electronics, a 250 nm blazed excitation monochromator grating, and two 500 nm blazed emission monochromator gratings. The correspondence regarding the instrument, tests, and the actual PAH fluorescence spectra are given in Appendix E (Figures A through N).

The gas phase PAH spectra were all measured in air. A cuvette, containing a crystal of the PAH material, was mounted in a water heated brass block to maintain the elevated temperatures. The phenanthrene vapor pressures (Reference 48) at 60, 50, and 30°C are 6.46×10^{-3} , 2.49×10^{-3} , and 3.08×10^{-4} torr, respectively. At sea level ($P = 760$ torr) this corresponds to 8.50, 3.28, and 0.405 ppm. For pyrene, the corresponding pressures (Reference 48) are 3.64×10^{-4} , 1.29×10^{-4} , and 1.33×10^{-5} torr, which translates into 0.479 and 0.170 ppm, and 17.5 parts per billion (ppb).

The 60°C fluorescence excitation spectrum of pyrene is given in Figure A (Appendix E). The features at 308 and 321 nm compare favorably with Figure 13, but there are some additional features near 265 and 284 nm. The region below 230 nm should again be regarded with suspicion, since instrumental artifacts may be present here, as with the Perkin-Elmer instrument.

The corresponding fluorescence emission spectrum of pyrene is given in Figure B. The sharp feature near 384 nm is due to pyrene (refer to Figure 13), but the broad emission, present from about 410 nm and extending beyond 480 nm, must be an impurity. Nonetheless, the instrument has the capability to detect pyrene at a concentration of 0.479 ppm.

Figures C and D show the fluorescence excitation and emission spectra of phenanthrene at 60°C. They compare quite favorably with Figure 12. Note that phenanthrene shows no absorption (excitation) feature at 321 nm, whereas both phenanthrene and pyrene absorb in the 241 nm region (with phenanthrene dominating). This fact will form the basis for the selective excitation study of a mixture of these two materials (although at least three will be present, given the observation of the impurity in the pyrene sample).

Figures E and F present the fluorescence emission spectra of a pyrene/phenanthrene mixture excited at two different wavelengths. With 241 nm excitation, both molecules absorb, and the phenanthrene emission predominates. With 321 nm excitation, the pyrene (and impurity) emission is selected. These spectra nicely show the advantages of selective excitation for the analysis of multicomponent mixtures.

Figures G and H are a repeat of the spectra of Figures E and F, but the spectra were collected at 50°C. It is important to note that one can still discern the pyrene feature near 384 nm. This is at a concentration of 0.170 ppm. Figures I and J depict the same kind of experiment but at 30°C. The phenanthrene emission can still be seen in Figure I at 0.405 ppm, but only the impurity emission can be seen in Figure J. This is not surprising since the pyrene concentration would be 17 ppb at this temperature.

After discussing these spectra with Spex Industries personnel, particularly concerning the pyrene impurity, they agreed to repeat the pyrene experiments with a fresh sample. The results are given in Figures K through N. Of particular note is the lack of the strong 470 nm impurity emission in Figure K. Both Figures K and N agree reasonably well with Figure 13, ignoring the bluest region of Figure N (especially since this is an uncorrected excitation spectrum).

Comparing Figures F and H, it can be seen that the 384 nm pyrene emission intensity scales well with the concentration change calculated from the vapor pressures. The agreement is not as good in the case of phenanthrene (refer to Figures E, G, and I). Since we have confidence in the vapor pressure values (they were extrapolated from experimental measurements (Reference 48) over the temperature range of 36.70 to 49.65°C), it may have been that the sample was not allowed to reach equilibrium temperature before the fluorescence measurement was made. Since the pyrene measurements were made following the phenanthrene ones, the sample would have had more time to reach equilibrium. Hence, the better agreement for pyrene. Despite this discrepancy, the Spex F112 fluorimeter is capable of detecting sub-ppm levels of gas phase pyrene and phenanthrene in air. With regard to other PAHs, it should be noted that a number of them have quantum yields greater than these two molecules. For example, benzo(a)pyrene (BaP) has a quantum yield that is about two times greater than pyrene (References 5 and 49). Therefore, one might expect a detection limit for BaP that is about two times lower than for pyrene.

The decision was made to purchase a Spex F112 fluorimeter as the heart of the PAH monitor system, and make the minor flow cell modifications described in the Experimental section.

LANL INCINERATION TESTS

Since we had no previous "hands-on" experience with the Spex fluorimeter prior to our arrival at the LANL, it was decided that it would be best to proceed in stages to get the PAH monitor into operation. Static cell, gas phase experiments were performed first, followed by the flow and calibration modifications to the system. This preliminary work eventually led to the real-time, on-line stack gas sampling

analysis during the Navy colored smoke incineration tests. Because of the time frames involved (the basic instrument was being installed during the incinerator warm-up), some of the minor problems encountered were not dealt with in the most elegant manner, but solved "on the fly" so as to get the instrument on-line during the test schedule. Further system improvements are certainly possible, and a number of suggestions are listed in the Conclusions and Recommendations section.

All the fluorescence spectra were taken with an approximate 5 nm resolution for both the excitation and emission. The wavelengths were scanned in a burst mode at 0.5 nm/step with an integration time of 1 second. A 100 nm spectrum could be obtained in 3.3 minutes at this scan rate. The intensity versus time plots, at fixed excitation and emission wavelengths, were taken with an integration time of 1 second.

In the case of the static cell and calibration flow system measurements, the concentration calculations (equation 3) were done with a value of 585 torr for the atmospheric pressure. The pressure inside the CAI is 492 torr, and this value should be used for all the on-line monitoring situations.

Preliminary Observations

PAH Analysis in a Static Cell. Following the initial installation of the basic Spex F112 fluorimeter, the first experiments were performed with naphthalene in a static cell. The capped sample cuvette (1.0 cm pathlength) was mounted in the Spex model 1931A heater/cooler block. The block had been modified for temperature control, as described in the Experimental section. Figures 14 and 15 show the naphthalene fluorescence emission and excitation spectra, taken in a front face (FF) emission collection geometry. These spectra agree well with Figure 11, but there was concern about the large background signal level. Unwanted scattering is usually more pronounced in a FF type experiment. To reduce this contribution, and to ensure that only gas phase emission was contributing to the spectra, the emission collection geometry was switched to right angle (RA). The resulting emission spectrum is presented in Figure 16. Note the dramatically reduced baseline, as compared to that in the previous spectra. Based on these results, it was decided to maintain a RA emission collection geometry for all successive spectra.

Next, the solid naphthalene was dumped from the sample cell, and the cell was washed, dried, and replaced in the instrument after a crystal of anthracene was added to it. Upon reexamination, it was found that there was still a small amount of naphthalene in the cell, despite our cleaning efforts. Figure 17 shows the naphthalene emission in the naphthalene/anthracene mixture at 30 and 50°C. The

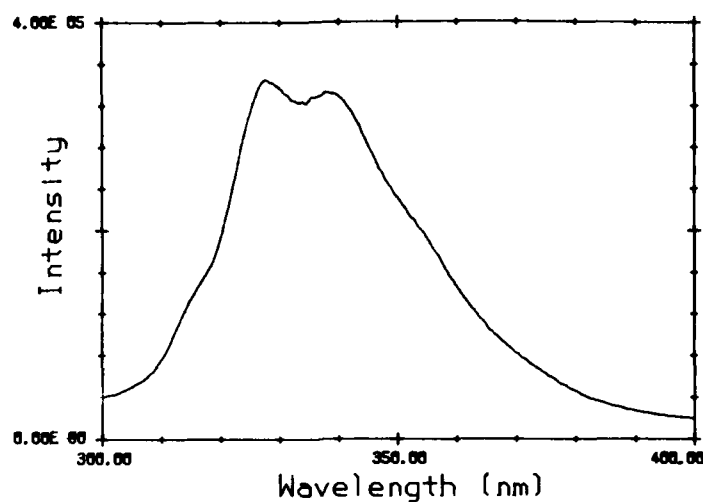


FIGURE 14. Fluorescence Emission Spectrum of Naphthalene in a Static Cell. The temperature was 30°C and the concentration was 239 ppm. A front face emission collection geometry was used. $\lambda_{ex} = 268$ nm.

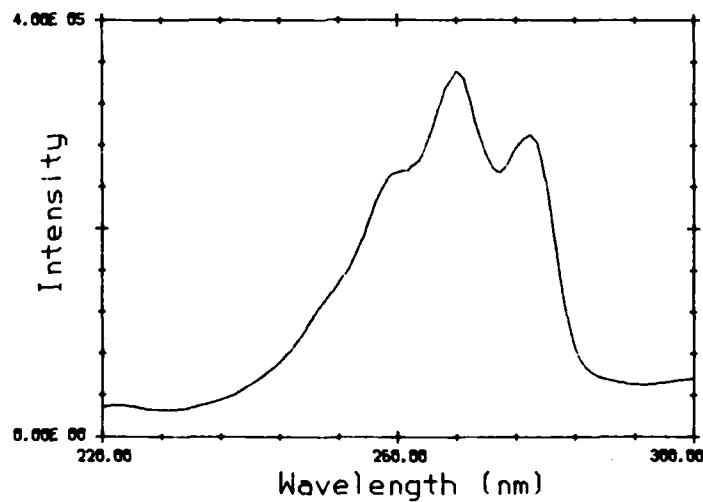


FIGURE 15. Fluorescence Emission Spectrum of Naphthalene in a Static Cell. The temperature was 30°C and the concentration was 239 ppm. A front face emission collection geometry was used. $\lambda_{ex} = 328.5$ nm.

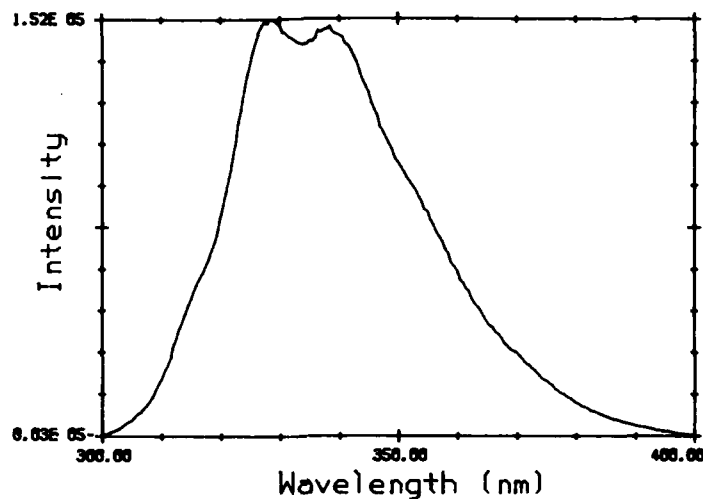


FIGURE 16. Fluorescence Emission Spectrum of Naphthalene in a Static Cell. The temperature was 30°C and the concentration was 239 ppm. A front face emission collection geometry was used. $\lambda_{\text{ex}} = 268 \text{ nm}$.

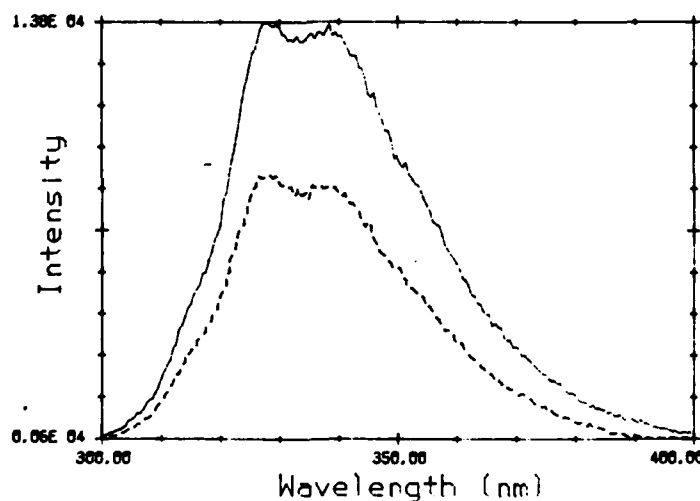


FIGURE 17. Fluorescence Emission Spectrum of a Naphthalene-Anthracene Mixture in a Static Cell. $\lambda_{\text{ex}} = 268 \text{ nm}$. Comparison at 30°C (---) and 50°C (—).

naphthalene vapor pressure changes by approximately a factor of 8 over this temperature range, but the fluorescence intensity only changed by 1.6. This is because there was not enough naphthalene in the cell to maintain the vapor pressure. A rough calculation, using the ideal gas law, shows that 20 μg would be needed to attain the required 0.809 torr in the 4 ml cell. Although this is enough material to see with the naked eye, we did not see any during the visual inspection of the cell.

The fluorescence excitation and emission spectra of the anthracene in the mixture are presented in Figures 18 and 19. At 50°C, the vapor pressure is 2.13×10^{-3} , which corresponds to 3.6 ppm. Figure 19 compares quite well with the results in Appendix A, and other work (References 2, 7, 8 and 11). Figures 17 through 19 clearly show the advantage of selective excitation in a multicomponent mixture analysis. The spectra can be completely separated for the two materials!

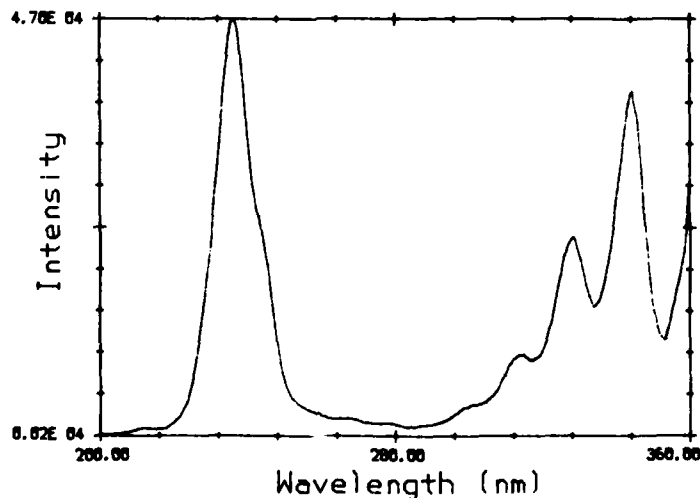


FIGURE 18. Fluorescence Excitation Spectrum of a Naphthalene-Anthracene Mixture in a Static Cell. $\lambda_{em} = 384.5 \text{ nm}$. The temperature was 50°C and the concentration of anthracene was 3.6 ppm.

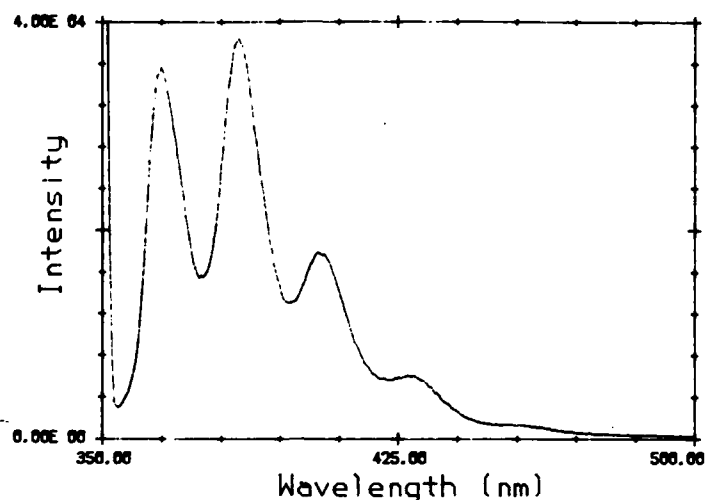


FIGURE 19. Fluorescence Emission Spectrum of a Naphthalene-Anthracene Mixture in a Static Cell. $\lambda_{ex} = 344$ nm. The temperature was 50°C and the concentration of anthracene was 3.6 ppm.

To prove that the fluorescence emission was not coming from solid anthracene that might have been plated-out on the cell windows, the emission spectrum of anthracene crystals is given in Figure 20. It was obtained under 365 nm mercury lamp excitation, which is a wavelength where the gas phase anthracene happens to emit. Comparing Figures 19 and 20, note that there is a completely different structure and wavelength dependence for the emission of the gas and solid phase material. Similar arguments should also hold for the other PAH compounds.

Figures 21 and 22 show the effects of selective excitation on the naphthalene/anthracene mixture for the excitation region near 250 nm. In this case, relatively small excitation wavelength changes can produce either an anthracene, or naphthalene, dominated emission spectrum. The vibronic structure in the anthracene emission (compare Figures 19 and 21) appears washed out when deep UV excitation is used. We are not sure of the reason for this, but an energy transfer process involving the naphthalene may be occurring (References 2, 34 and 25).

To carry the mixture analysis one step further, phenanthrene was added to the cell containing the naphthalene/anthracene. The fluorescence excitation spectrum of this mixture is given in Figure 23. The concentrations for anthracene and phenanthrene were 3.6 and 4.3 ppm. The concentration of naphthalene was probably <30 ppm. This spectrum

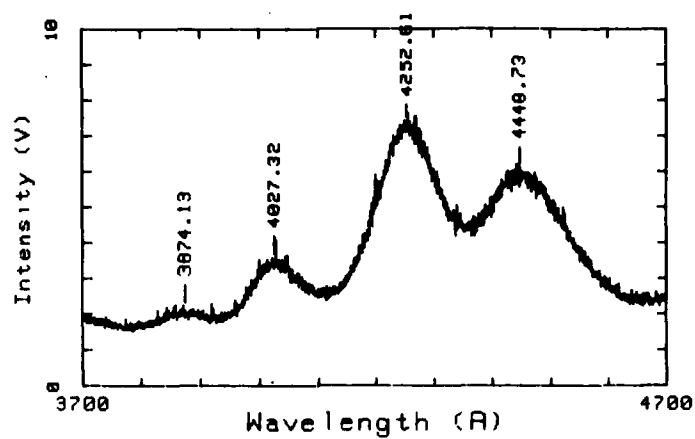


FIGURE 20. Fluorescence Emission Spectrum of Anthracene Crystals. $\lambda_{\text{ex}} = 365 \text{ nm}$.

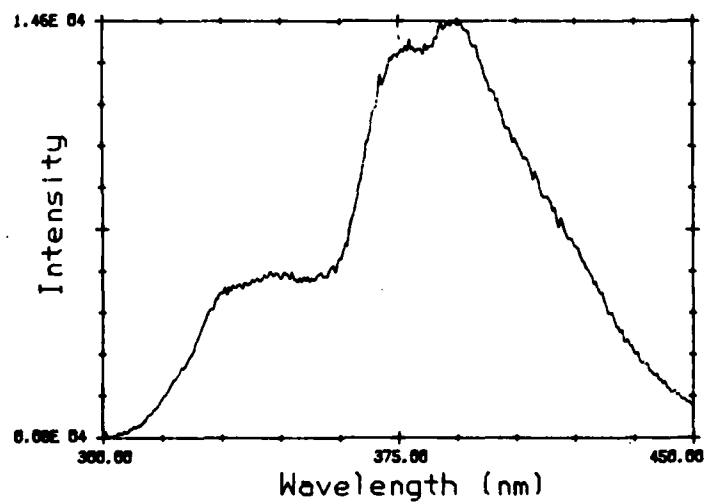


FIGURE 21. Fluorescence Emission Spectrum of a Naphthalene-Anthracene Mixture in a Static Cell. $\lambda_{\text{ex}} = 247 \text{ nm}$. The temperature was 50°C .

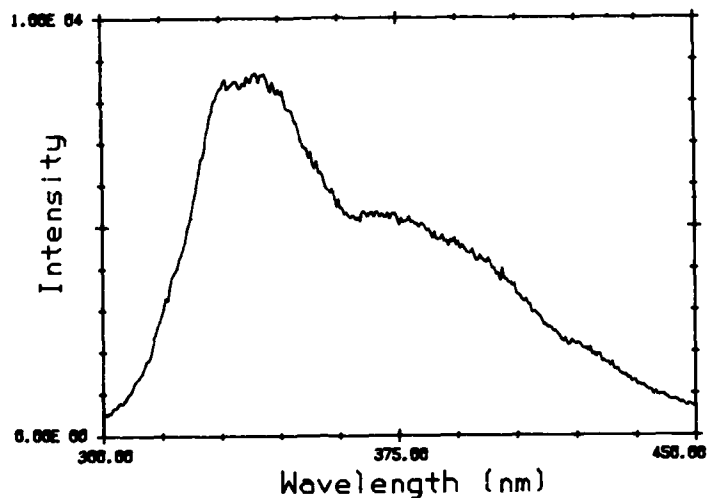


FIGURE 22. Fluorescence Emission Spectrum of a Naphthalene-Anthracene Mixture in a Static Cell. $\lambda_{ex} = 251$ nm. The temperature was 50°C.

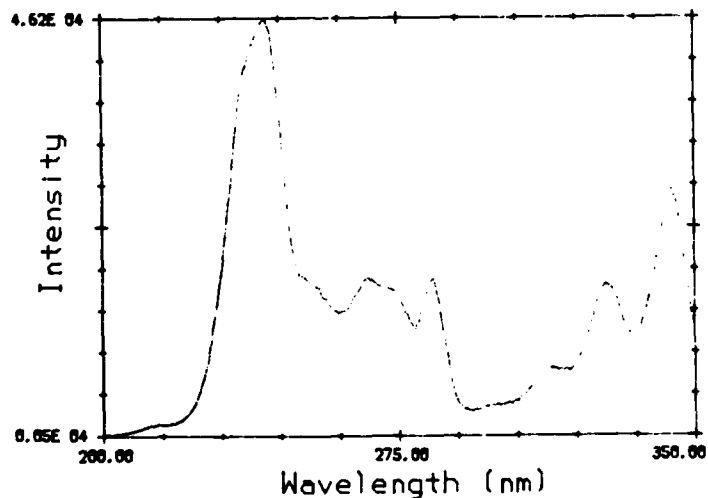


FIGURE 23. Fluorescence Excitation Spectrum of a Naphthalene-Anthracene-Phenanthrene Mixture in a Static Cell. $\lambda_{em} = 367.5$ nm. The temperature was 50°C and the concentrations of anthracene and phenanthrene were 3.6 and 4.3 ppm, respectively.

should be compared to the excitation spectra for anthracene (Figure 18) and phenanthrene (Figure D in Appendix E). In fact, it is approximately the addition of the two separate spectra, plus a small contribution from the naphthalene, near 268 nm. When the fluorescence emission is monitored at 367.5 nm, anthracene and phenanthrene contribute strongly (refer to Figure 19 and Figure C of Appendix E). The naphthalene emission contribution at this wavelength is somewhat weaker (see Figure 16). The emission spectrum of this mixture, taken with 250 nm excitation, is presented in Figure 24. This excitation wavelength discriminates against anthracene. The strong 370 nm emission is characteristic of phenanthrene (refer to Figure C of Appendix E), and the naphthalene contribution can be seen as a shoulder near 330 nm. There is also an additional feature at 415 nm which must be from an impurity in the phenanthrene.* This impurity contribution to the total (now at least 4-component) emission can be selected with 290 nm excitation, as depicted in Figure 25. This excitation wavelength discriminates against the phenanthrene, anthracene, and naphthalene in the sample. Figures 26 and 27 show the emission spectra of the mixture, irradiated with 284 and 344 nm excitation. The latter is primarily an anthracene emission spectrum.

Using a program provided with the instrument (Spex Tech. Note #62), the computer controlled acquisition of an excitation-emission matrix was performed on the naphthalene/anthracene/phenanthrene/impurity mixture. The result is plotted in Figure 28. It is a series of emission spectra, taken at a series of excitation wavelengths. The vertical axis is intensity. The largest peak corresponds to phenanthrene and anthracene, and one can just make out the naphthalene contribution in the emission scans which were taken with the excitation wavelength at 255 and 260 nm. It took approximately an hour to generate the plot, but it should be emphasized that routine work would not need to be done with such a fine grid of points, and could be accomplished much faster. The graph is presented here, mainly to show the type of result that can be obtained quite easily with the Spex instrument.

In a final prelude to the conversion of the system to flow cell operation, the 33.3°C fluorescence excitation and emission spectra of benzene (another environmentally hazardous material, in its own right) was measured using another applications program (Spex Tech. Note #60). The results are presented in Figure 29. As can be seen from the figure, this program automatically plots the excitation and emission

*From the data in Table 3, the measured diffusion rate is approximately 10% higher than the calculated value. The impurity in the phenanthrene could well be a contributing factor to this discrepancy.

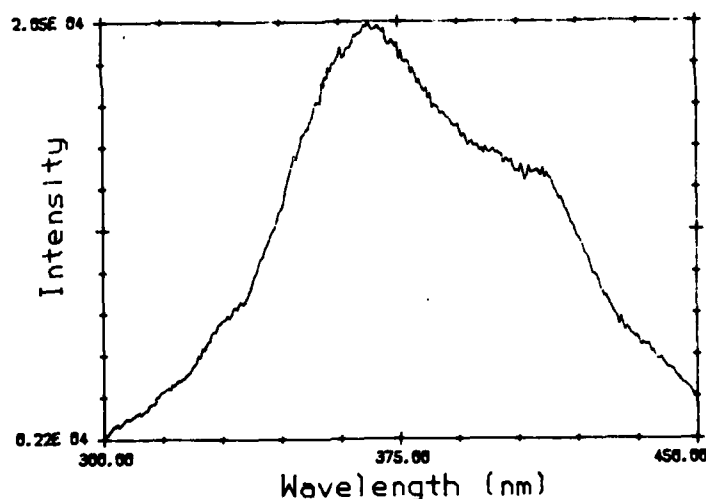


FIGURE 24. Fluorescence Emission Spectrum of a Naphthalene-Anthracene-Phenanthrene Mixture in a Static Cell. $\lambda_{ex} = 250$ nm. The temperature was 50°C.

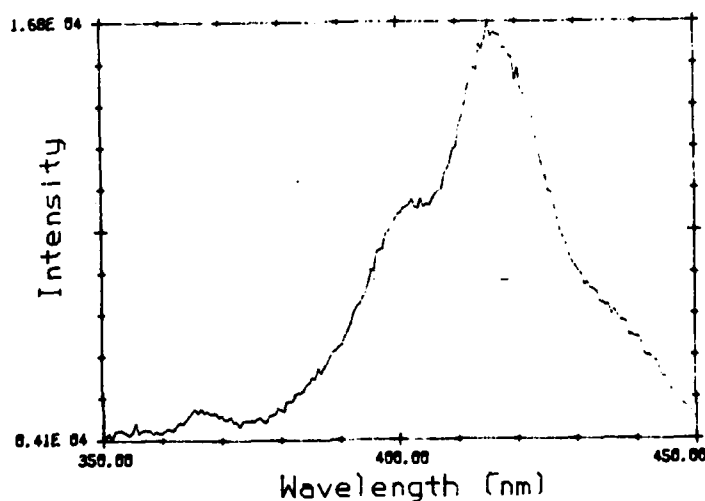


FIGURE 25. Fluorescence Emission Spectrum of a Naphthalene-Anthracene-Phenanthrene Mixture in a Static Cell. Impurity emission selected with $\lambda_{ex} = 290$ nm. The temperature was 50°C.

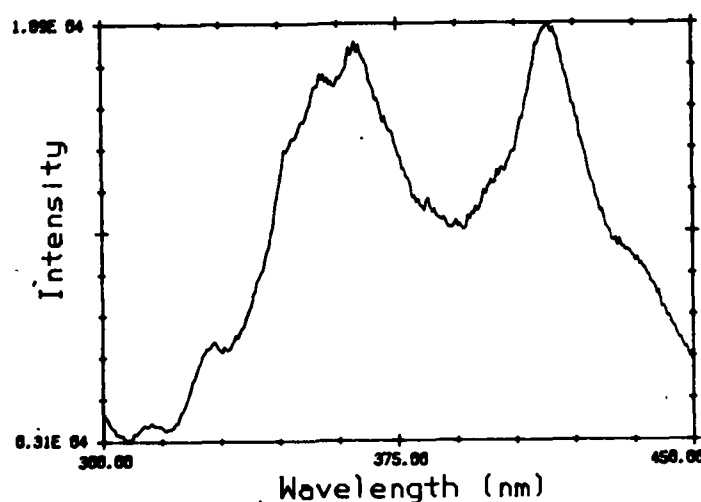


FIGURE 26. Fluorescence Emission Spectrum of a Naphthalene-Anthracene-Phenanthrene-Impurity Mixture in a Static Cell. $\lambda_{ex} = 284$ nm. The temperature was 50°C.

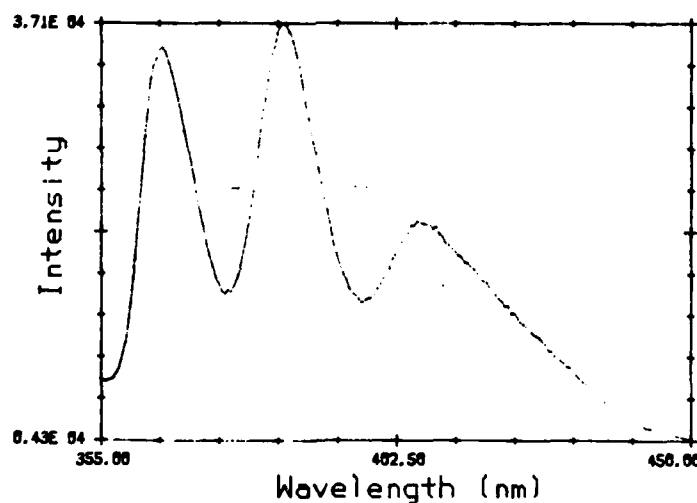


FIGURE 27. Fluorescence Emission Spectrum of a Naphthalene-Anthracene-Phenanthrene-Impurity Mixture in a Static Cell. Selectively excited for anthracene with $\lambda_{ex} = 344$ nm. The temperature was 50°C.

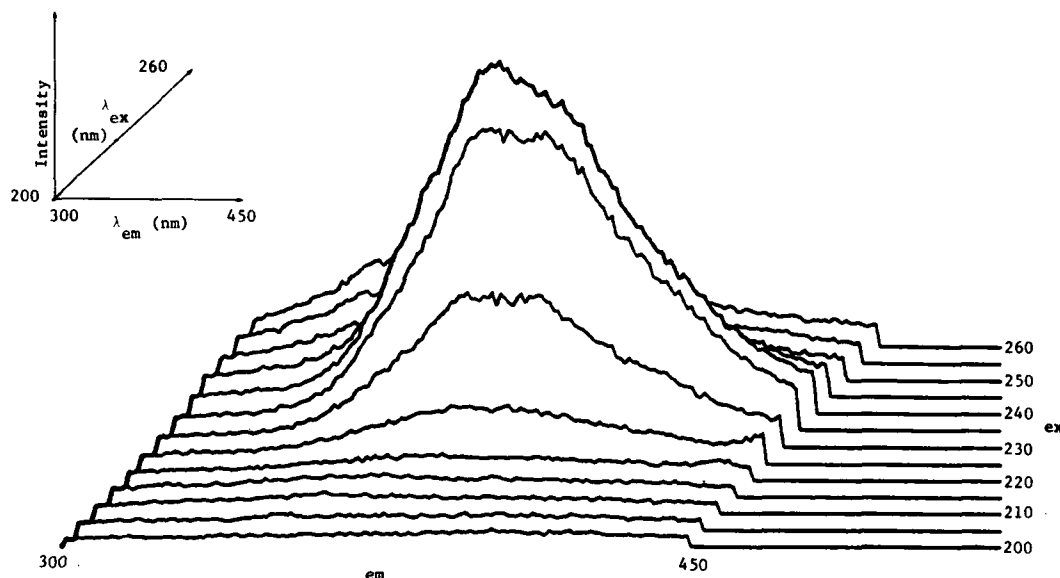


FIGURE 28. Excitation-Emission Matrix Generated from the Naphthalene-Anthracene-Phenanthrene-Impurity Mixture in a Static Cell. The temperature was 50°C. The λ_{ex} values were incremented in 5 nm steps from 200-260 nm. The emission was scanned from 300-450 nm in 1 nm steps. The program was from Spex Technical Note #62.

spectra on the same graph. The gas phase concentration of benzene in the static cell was very high for our purposes (about 200K ppm), but the relevant wavelengths will be useful for the next stage of the work.

PAH Analysis in the Flow System. The instrument was next configured to the PAH monitor flow system of Figures 8 and 9 (described in the Experimental section). Photographs of the actual instrument, at the site, are given in Figures 30 through 32. The diffusion cell, inside the furnace, is shown in Figure 33. The initial flow system experiments were done with benzene. Because of its high vapor pressure (>100 torr at 33.3°C), the operation of the flow system could be checked out with benzene before being heated. Figure 34 shows the instrumental background, taken with the excitation source at the wavelength maximum for benzene (also blue enough to excite other unwanted materials that might be present). At this point, laboratory air from the general instrument location was flowing through the cell. Benzene was next added to the diffusion cell and the fluorescence excitation

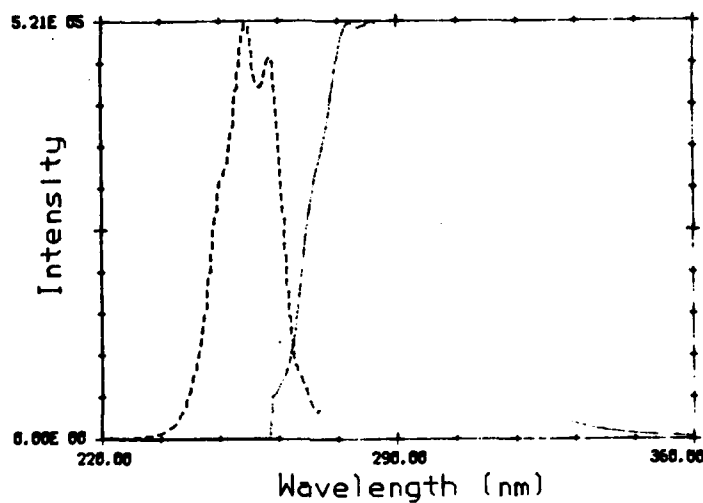


FIGURE 29. Excitation (---) and Emission (—) Spectra of Benzene Vapor in a Static Cell. The temperature was 33.3°C and the concentration was > 200K ppm. The program used to generate the plot was from Spex Technical Note #60.



FIGURE 30. PAH Monitor and Flow System Showing Sampling Line to Incinerator.



FIGURE 31. PAH Monitor and Flow System Showing DATAMATE Computer and Operator.



FIGURE 32. PAH Monitor and Flow System.



FIGURE 33. Calibration Cell and Furnace Assembly.

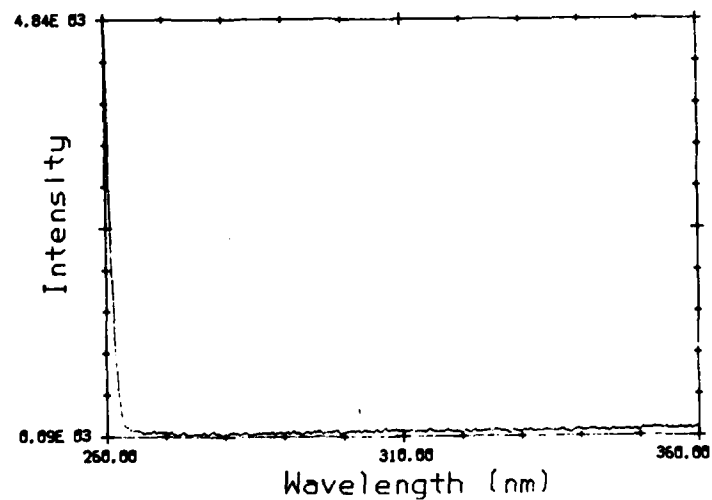


FIGURE 34. Flow Cell Background Spectrum. Excitation and emission parameters selected to detect benzene.

and emission spectra were obtained at several flow rates. Figures 35 through 38 show the excellent agreement between the flow rates (concentrations)* and the observed intensities. The benzene concentrations were high (a few hundred ppm, even at the highest flow rate), and this lack of sensitivity for benzene can be quite easily explained. First, the extinction coefficient for benzene (Reference 49) is 200 L/(mole-cm) near 254 nm, compared to naphthalene's 6,000 L/(mole-cm) at 268 nm. The quantum yield for benzene is also 3.3 times smaller than the yield of naphthalene (Reference 49). This accounts for a two order of magnitude difference in emission intensity between these two materials, not even taking into consideration the fact that the benzene fluorescence may be more highly quenched by air.

The next day, the cell background was remeasured to be sure that all of the benzene was out of the system. It is shown in Figure 39. Naphthalene was then added to the diffusion cell, and the system was heated to 65.5°C. The transfer lines were normally kept 5 to 10°C higher than the diffusion cell furnace and fluorescence flow cell in order to keep material from condensing in the lines. The fluorescence emission and excitation spectra of naphthalene in the flow system are given in Figures 40 through 43. The DIFF_RATE calculations for the 3.9 and 2.3 ppm concentration values are given in Appendix C. It should be noted that the observed intensities again scale quite well with the flow rates (concentrations). The 2.3 ppm plots have been mathematically smoothed. This is part of the standard Spex DATAMATE processing (see Appendix B).

The above experiments indicated that the PAH monitor flow system was in working order, and that the monitor was responding to PAH concentrations on the order of 1 ppm. At this point, the final stage of the work, on-line testing, was begun.

Real-Time Analysis of Navy Colored Smoke

The stack gas temperature at the PAH monitor sampling location (refer to Figures 5 and 6) was 65.5°C during all the incineration tests. The fluorescence cell was also maintained at that set point. The sampling lines were kept 5 to 10°C higher than the sampling location temperature in order to prevent the possibility of condensation in the lines. Because of the low sampling temperature, the PAH monitoring wavelengths were chosen to detect the smaller, higher vapor pressure materials. The larger materials, if present, would most likely be

* Although the flowmeter curves were calibrated for air at 760 torr and 70°F, the calculated correction factors for the LANL altitude and temperature were found to be generally less than 10%. In what follows, no correction was used.

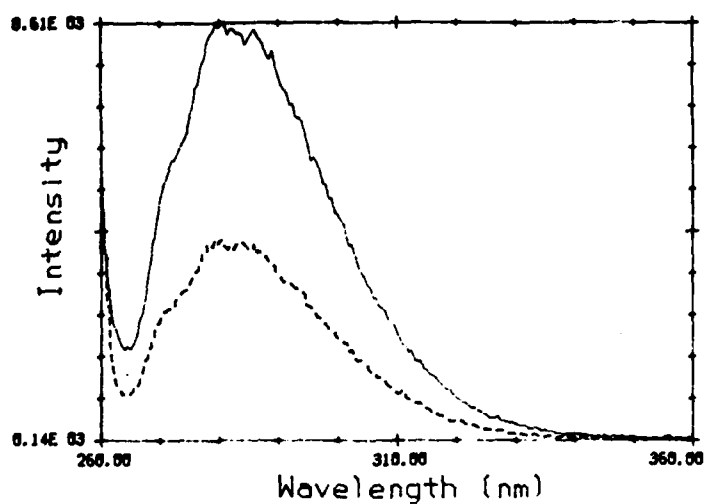


FIGURE 35. Fluorescence Emission Spectrum for Benzene Vapor in the Flow System. $\lambda_{ex} = 254$ nm. The temperature was 33.3°C and the flow rates were 22 mL/min (—) and 44 mL/min (---).

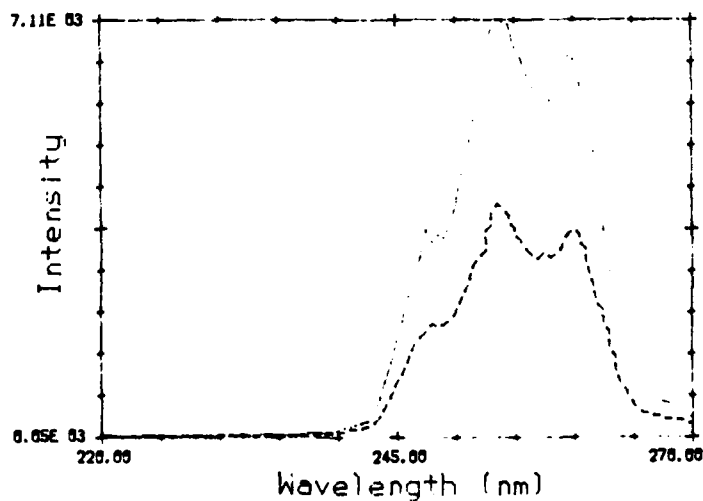


FIGURE 36. Fluorescence Excitation Spectrum for Benzene Vapor in the Flow System. $\lambda_{em} = 285$ nm. The temperature was 33.3°C and the flow rates were 22 mL/min (—) and 44 mL/min (---).

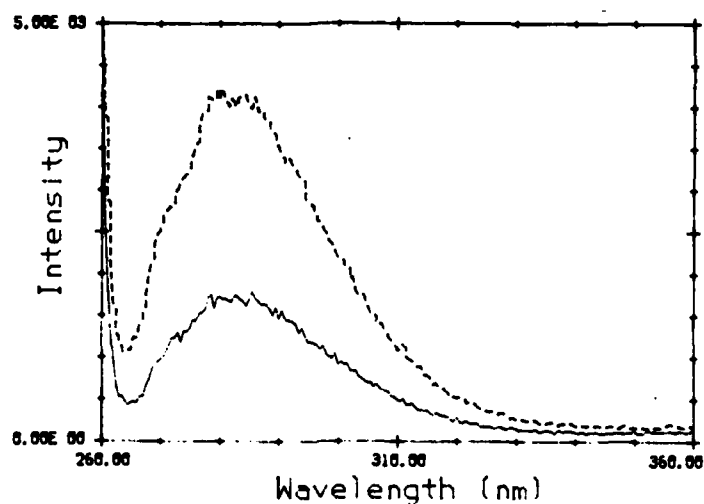


FIGURE 37. Fluorescence Emission Spectrum for Benzene Vapor in the Flow System. $\lambda_{ex} = 254$ nm. The temperature was 33.3°C and the flow rates were 110 mL/min (—) and 44 mL/min (---).

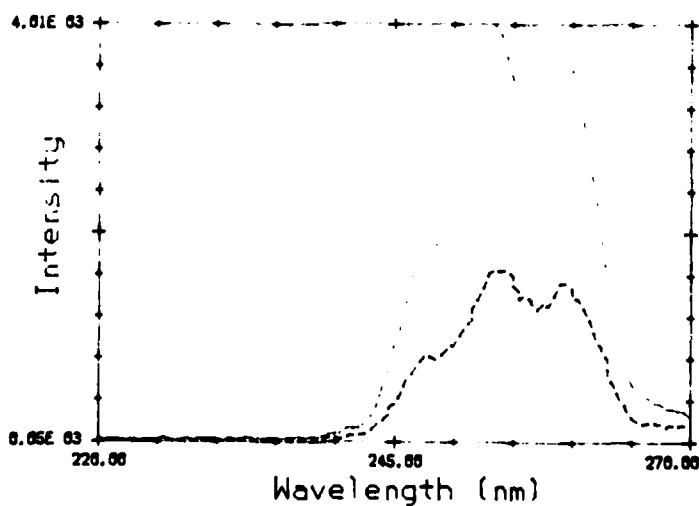


FIGURE 38. Fluorescence Excitation Spectrum for Benzene Vapor in the Flow System. $\lambda_{em} = 285$ nm. The temperature was 33.3°C and the flow rates were 44 mL/min (—) and 110 mL/min (---).

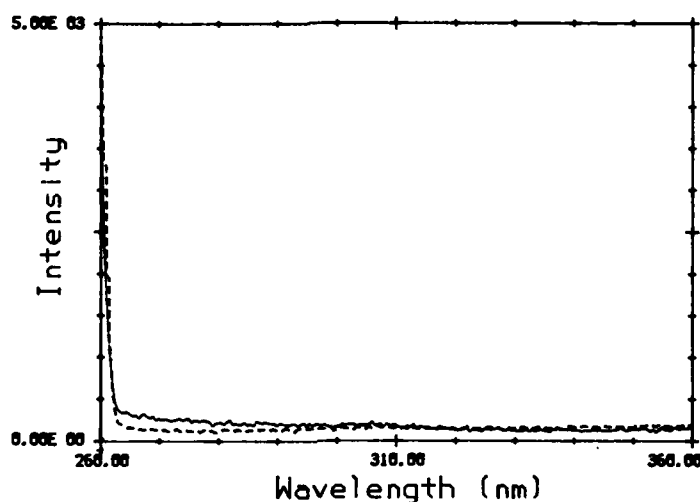


FIGURE 39. Comparison of the Flow Cell Background Spectrum for Two Separate Days. Figure 34 is the second spectrum (---). Excitation and emission parameters were selected to detect benzene.

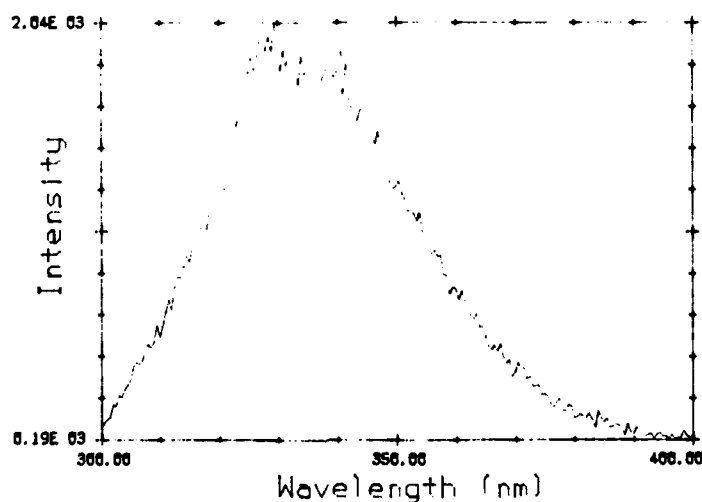


FIGURE 40. Fluorescence Emission Spectrum for Naphthalene in the Flow System. $\lambda_{ex} = 269$ nm. The temperature was 65.5°C and the flow rate was 160 mL/min. The concentration of naphthalene was 3.9 ppm.

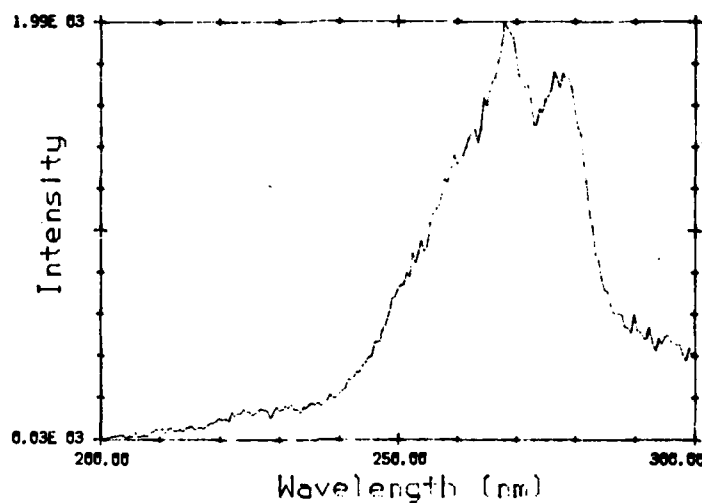


FIGURE 41. Fluorescence Excitation Spectrum for Naphthalene in the Flow System. $\lambda_{em} = 328$ nm. The temperature was 65.5°C and the flow rate was 160 mL/min. The concentration of naphthalene was 3.9 ppm.

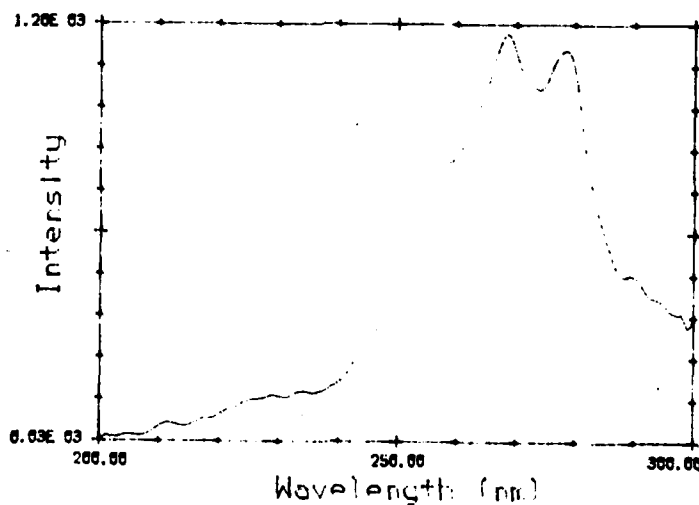


FIGURE 42. Fluorescence Excitation Spectrum for Naphthalene in the Flow System. $\lambda_{em} = 328$ nm. The temperature was 65.5°C and the flow rate was >270 mL/min. The concentration of naphthalene was 2.3 ppm.

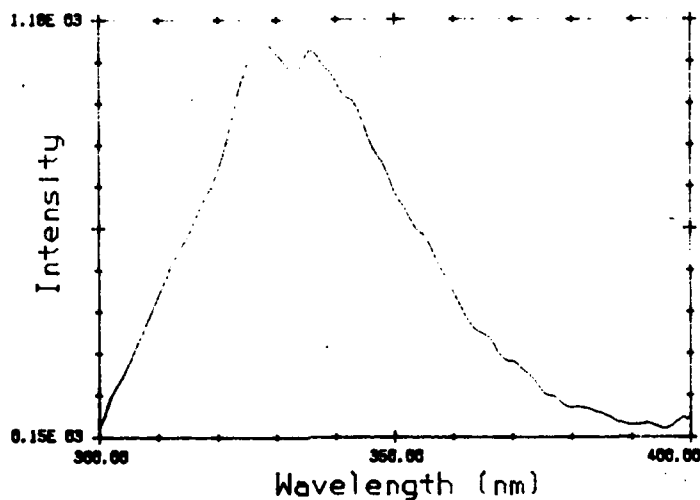


FIGURE 43. Fluorescence Emission Spectrum for Naphthalene in the Flow System. $\lambda_{ex} = 269$ nm. The temperature was 65.5°C and the flow rate was >270 mL/min. The concentration of naphthalene was 2.3 ppm.

condensed on particulates. For example, BaP has a vapor pressure of 5.49×10^{-9} torr at 25°C (Reference 2). Even allowing for a factor of 20 increase at 65.5°C , the ambient concentration would be approximately 0.2 ppb. This is well below the detection capabilities of the monitor as configured and operated here. If, for some reason larger PAHs were present, they would be excited by the UV wavelengths used for the smaller compounds, and would contribute to the emission at redder wavelengths. Therefore, their possible presence was not entirely ignored in the work. The actual chemical composition of the Navy colored smokes have been defined previously (Reference 1), and the CAI feed schedules and operating conditions are given in the LANL experimental test plan (Reference 41).

The results from the first attempt to put the PAH monitor system on-line are given in Figure 44. The Mk 13 colored smoke composition was being incinerated at the time. Unfortunately, the incineration test was aborted a few minutes after the monitoring began, because the incinerator was running at the wrong temperature for the Mk 13, phase 4, period 1 test. The gas sampling was initiated at $t = 116$ seconds on the plot, and the excitation and emission wavelengths of the instrument were set for the naphthalene maxima. The important thing to

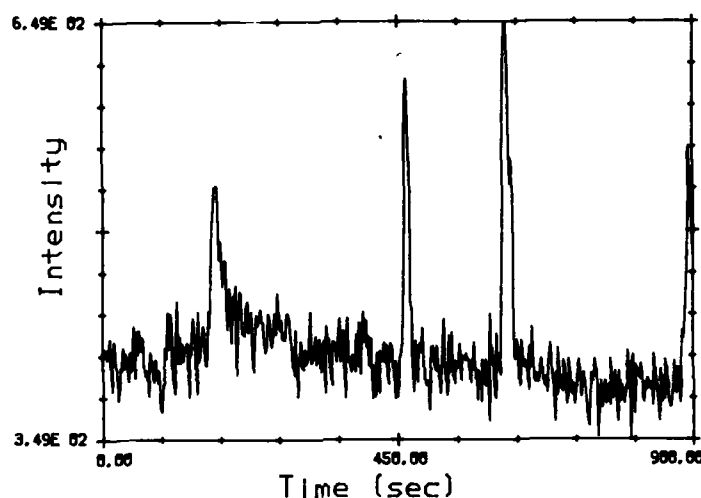


FIGURE 44. On-Line Temporal Scan Started at 1204 Hours on 11 September 1983. Mk 13 smoke composition. $\lambda_{ex} = 269 \text{ nm}$, $\lambda_{em} = 328 \text{ nm}$. Wavelength parameters for naphthalene detection.

note is that after a momentary response at the switching point no significant change occurred in the background level. There also were a few additional intensity spikes in the 450 to 900 second region. At this time, their origin is uncertain. It is tempting to speculate that these spikes may have been caused by the instrument response to PAHs deposited on particulate matter, but given that the sampling location was situated between two HEPA filters, this is unlikely.

While the CAI conditions were being reset for the next incineration test, the PAH monitor was switched back to the calibration cell (containing naphthalene). The time response of the system was next examined by monitoring the fluorescence intensity as the diffusion cell sample tube was replaced with a clean, empty plug. Figure 45 shows the decay of the naphthalene signal after the insertion of the empty plug (at $t = 80$ seconds). A steady state is reached in a few minutes.

The monitor system was next switched back on-line for the Mk 13, phase 4, period 1 test as shown in Figure 46. Again, the naphthalene excitation and emission wavelengths were used for detection. Of particular significance is the fact that the signal intensity actually

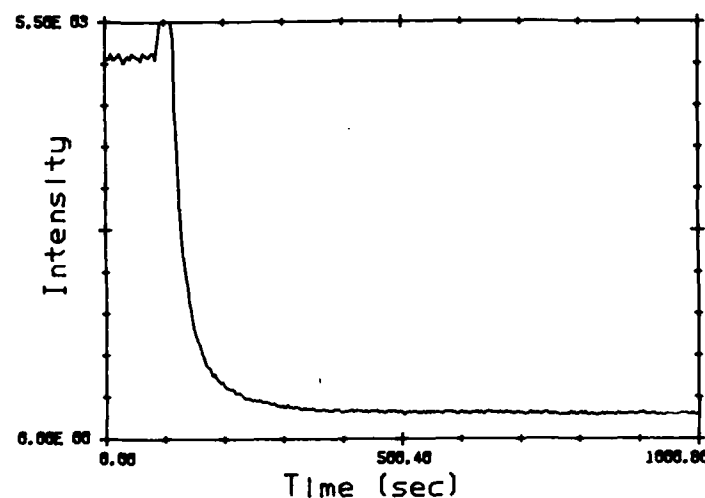


FIGURE 45. Temporal Scan During the Removal of a Naphthalene Calibration Sample and the Insertion of an Empty Plug. $\lambda_{ex} = 269$ nm, $\lambda_{em} = 328$ nm. Wavelength parameters for naphthalene detection.

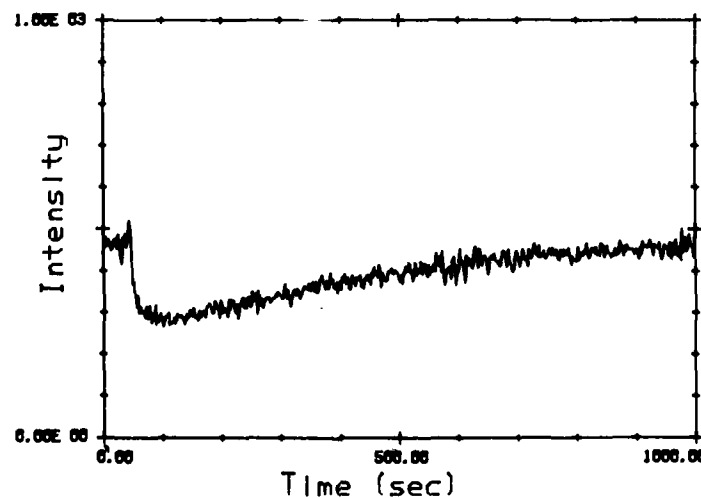


FIGURE 46. On-Line Temporal Scan Started at 1445 Hours on 11 September 1983. Mk 13, phase 4, period 1. $\lambda_{ex} = 269$ nm, $\lambda_{em} = 328$ nm. Wavelength parameters for naphthalene detection.

decreased when the instrument was put on-line (it was switched over from the empty diffusion cell configuration). This may mean that the incinerator gases at the sampling point were actually cleaner than the laboratory air flowing through the empty diffusion cell. There was, in fact, a distinct fuel-oil odor in the room at this time. The lower pressure (492 torr) inside the incinerator system, relative to the ambient atmospheric pressure (585 torr) may be a contributor to the signal decrease. Figures 47 through 52 are a series of spectra taken during the Mk 13, phase 4, period 1 incineration test. The acquisition times are given on the graph labels in 24-hour clock notation. In all cases, the signals were not caused by the presence of PAHs on a ppm level, but caused by either a background from the flow system, or scattered light contributions.* Figure 53 was generated during the switch from off-line, to the empty diffusion cell configuration (at $t = 320$ seconds).

Figures 54 through 60 were all taken during the Mk 13, phase 4, period 2 test. The CAI burner went out during the scan of Figure 56 (at $t = 1925$ hours), and Figure 57 was acquired, on-line, but with the burner down. The system was switched to the empty calibration cell for Figure 58, which shows the system background, and Figures 59 and 60 were generated with the burner functioning again. No PAHs were detected on a ppm level for this entire test.

Similar negative results (no PAHs) are shown in Figures 61 through 64, measured during the Mk 21, phase 6, period 1 incineration test. Again, the signal level decreased when the system was put on line.

Figure 65 shows the negative results for the Mk 89, phase 7, period 1 test, and Figure 66 is an excitation-emission matrix, generated while on-line. It took approximately 25 minutes to generate. Again, routine analysis would not need to be done with such a fine grid of data points, and the task in survey fashion could easily be accomplished more rapidly.

A final negative test result is shown in Figure 67. After this run, the system was switched back to the empty diffusion cell sampling configuration. Naphthalene was then put into the diffusion cell sample tube, and the time response of the system was measured. As can be seen from Figures 68 and 69, it took about an hour to reach the steady

* It was noticed that there was scattered light coming from the insulating tape used on the inlet flow line to the fluorescence cell. Baffling material was inserted into the sample compartment to temporarily improve the situation, but this problem should be more permanently addressed in future work.

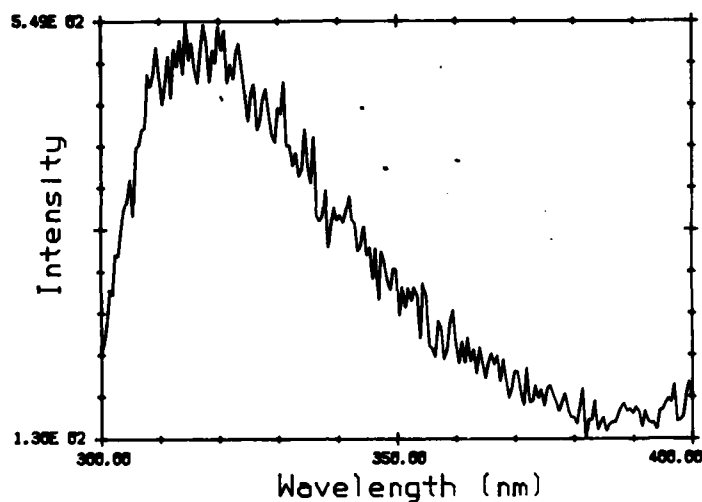


FIGURE 47. On-Line Emission Scan Started at 1500 Hours on 11 September 1983. Mk 13, phase 4, period 1. $\lambda_{ex} = 269$ nm. Wavelength parameters for naphthalene detection.

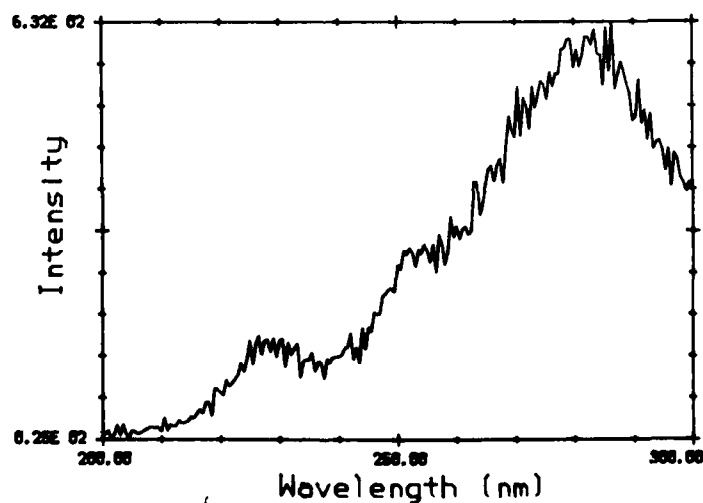


FIGURE 48. On-Line Excitation Scan Started at 1510 Hours on 11 September 1983. Mk 13, phase 4, period 1. $\lambda_{em} = 328$ nm. Wavelength parameters for naphthalene detection.

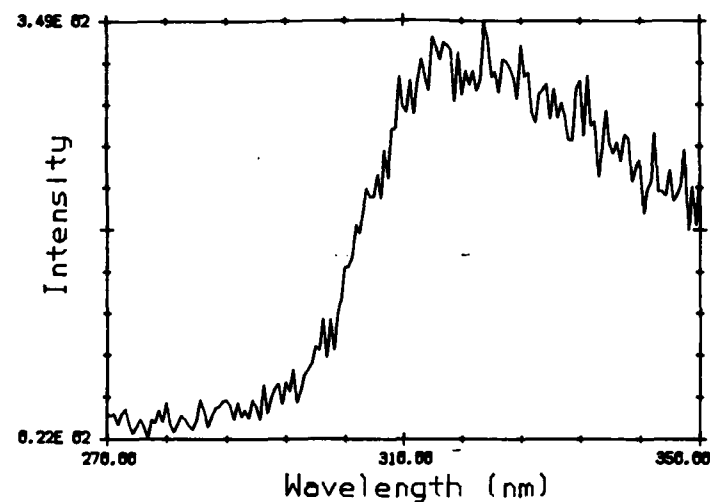


FIGURE 49. On-Line Emission Scan Started at 1517 Hours on 11 September 1983. Mk 13, phase 4, period 1. $\lambda_{ex} = 254$ nm. Wavelength parameters for benzene detection.

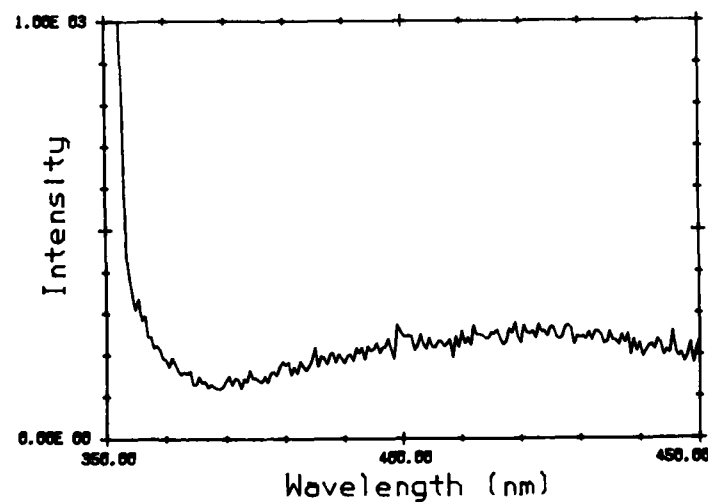


FIGURE 50. On-Line Emission Scan Started at 1530 Hours on 11 September 1983. Mk 13, phase 4, period 1. $\lambda_{ex} = 344$ nm. Wavelength parameters for anthracene detection.

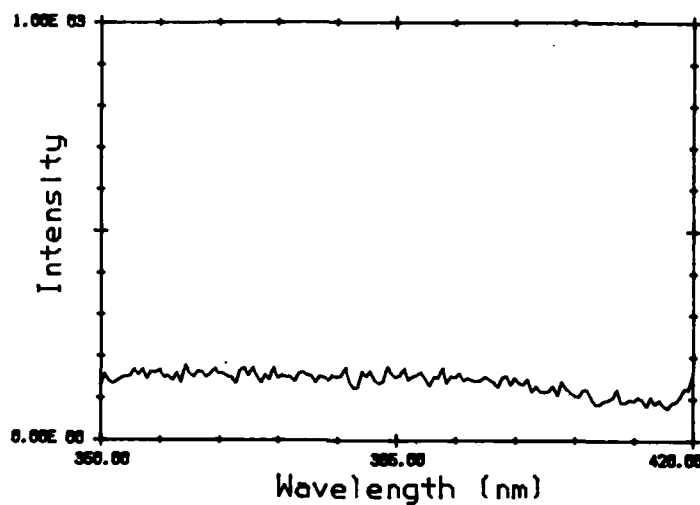


FIGURE 51. On-Line Excitation Scan Started at 1642 Hours on 11 September 1983. Mk 13, phase 4, period 1. $\lambda_{em} = 440$ nm.

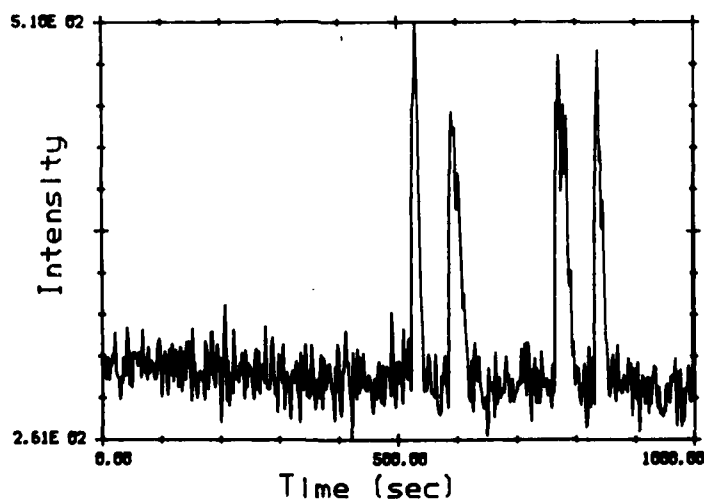


FIGURE 52. Temporal Scan Started at 1652 Hours on 11 September 1983. Just at the end of the Mk 13, phase 4, period 1 run. $\lambda_{ex} = 269$ nm, $\lambda_{em} = 328$ nm. Wavelength parameters for naphthalene detection.

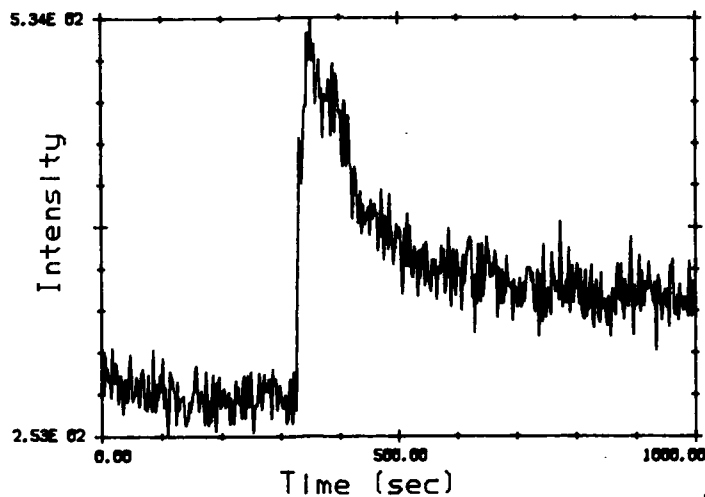


FIGURE 53. Temporal Scan Started at 1715 Hours on 11 September 1983. Switched from on-line to empty diffusion cell (room air) at $t = 320$ seconds. $\lambda_{ex} = 269$ nm, $\lambda_{em} = 328$ nm. Wavelength parameters for naphthalene detection.

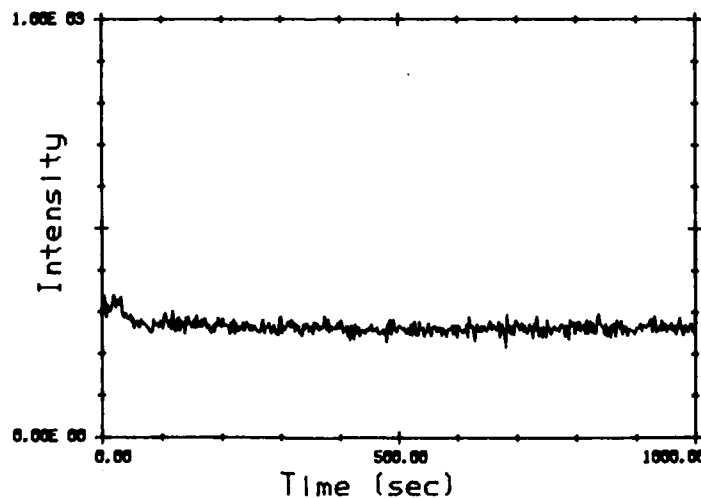


FIGURE 54. Temporal Scan Started at 1843 Hours on 11 September 1983. Switched from empty diffusion cell (room air) to on-line at $t = 40$ seconds. $\lambda_{ex} = 269$ nm, $\lambda_{em} = 328$ nm. Wavelength parameters for naphthalene detection. Just at start of Mk 13, phase 4, period 2.

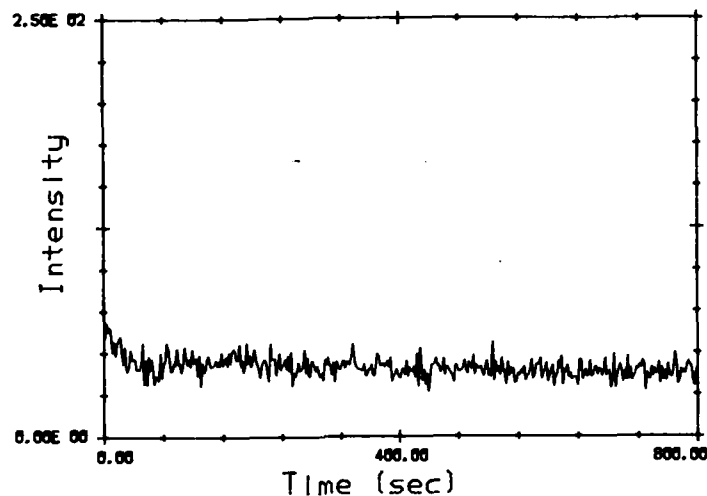


FIGURE 55. On-Line Temporal Scan Started at 1906 Hours on 11 September 1983. Mk 13, phase 4, period 2. $\lambda_{ex} = 254$ nm, $\lambda_{em} = 285$ nm. Wavelength parameters for benzene detection.

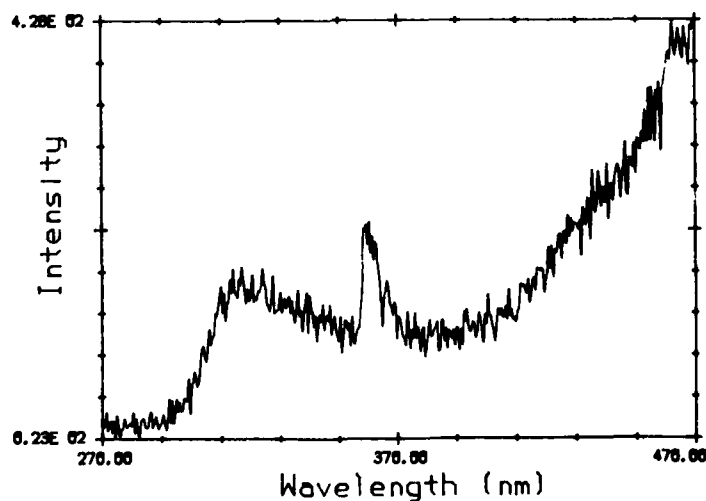


FIGURE 56. On-Line Emission Scan Started at 1924 Hours on 11 September 1983. Mk 13, phase 4, period 2. $\lambda_{ex} = 254$ nm. Wavelength parameters for benzene detection.

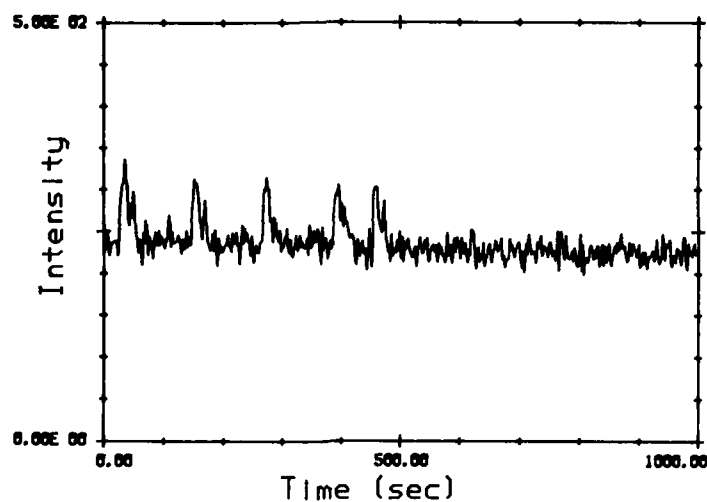


FIGURE 57. On-Line Temporal Scan Started at 1939 Hours on 11 September 1983. Mk 13, phase 4, period 2. $\lambda_{ex} = 254$ nm, $\lambda_{em} = 328$ nm. The CAI burner went out during this scan.

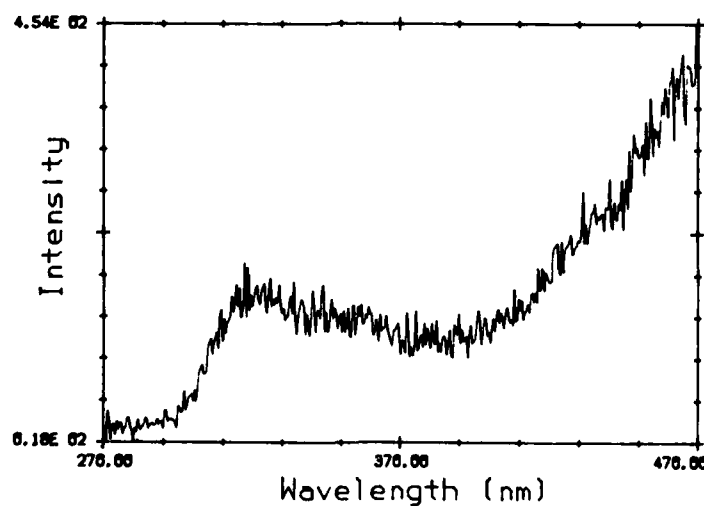


FIGURE 58. Empty Diffusion Cell (Room Air) Background Emission Scan Started at 2015 Hours on 11 September 1983. $\lambda_{ex} = 254$ nm. Wavelength parameters for benzene detection.

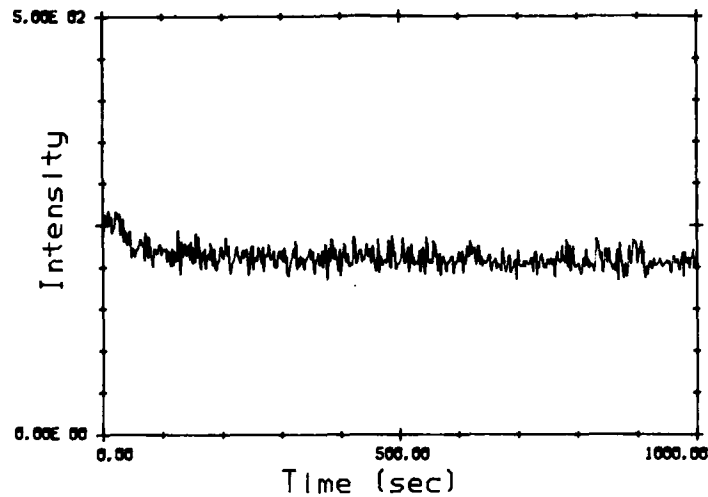


FIGURE 59. On-Line Temporal Scan Started at 2052 Hours on 11 September 1983. Mk 13, phase 4, period 2. $\lambda_{ex} = 269 \text{ nm}$, $\lambda_{em} = 328 \text{ nm}$. Wavelength parameters for naphthalene detection. The CAI burner was functioning during this scan.

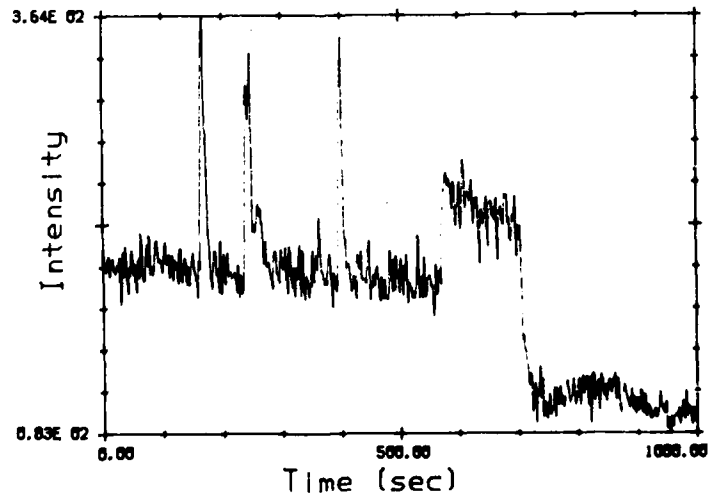


FIGURE 60. Temporal Scan Started at 2110 Hours on 11 September 1983. Just at the end of the Mk 13, phase 4, period 2 run. $\lambda_{ex} = 269 \text{ nm}$, $\lambda_{em} = 328 \text{ nm}$. Wavelength parameters for naphthalene detection.

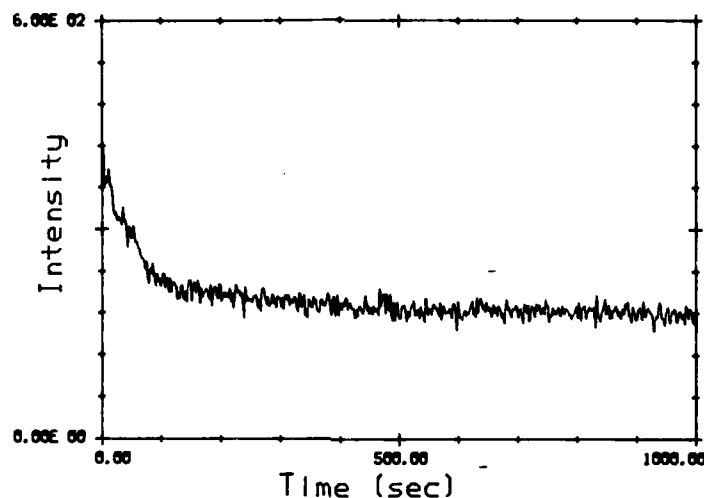


FIGURE 61. On-Line Temporal Scan Started at 1150 Hours on 12 September 1983. Mk 21, phase 6, period 1. $\lambda_{ex} = 269 \text{ nm}$, $\lambda_{em} = 328 \text{ nm}$. Wavelength parameters for naphthalene detection.

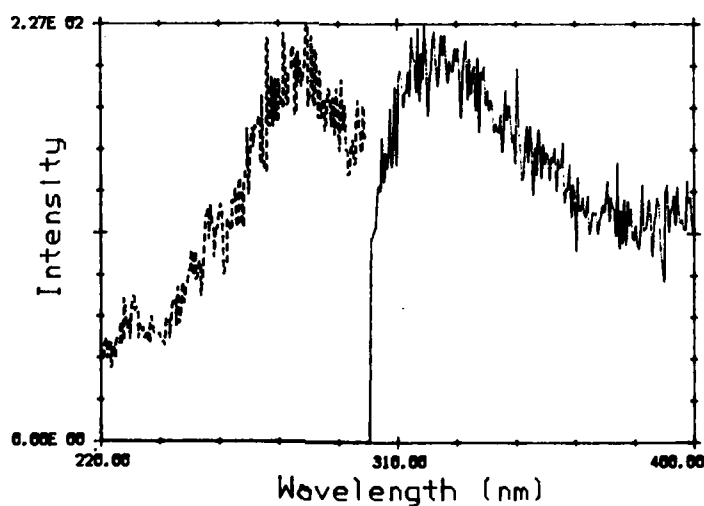


FIGURE 62. On-Line Excitation (---) and Emission Spectra Taken at 1230 Hours on 12 September 1983. Mk 21, phase 6, period 1. The program used to generate the plot was from Spex Technical Note #60.

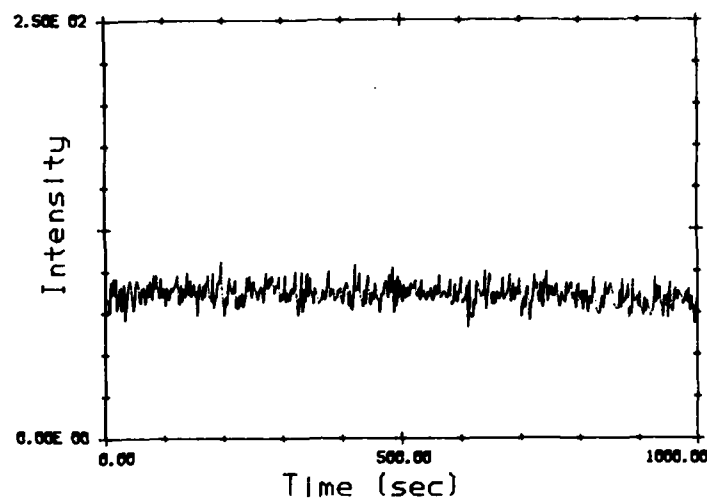


FIGURE 63. On-Line Temporal Scan Started at 1252 Hours on 12 September 1983. Mk 21, phase 6, period 1. $\lambda_{ex} = 240$ nm, $\lambda_{em} = 385$ nm.

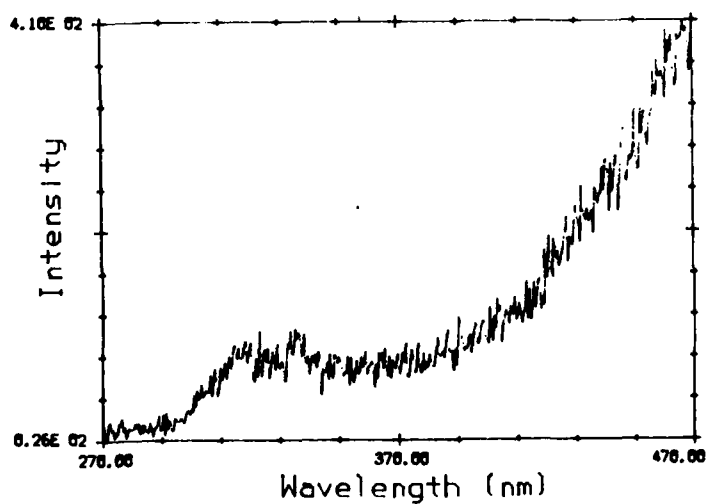


FIGURE 64. Fluorescence Emission Scan Started at 1319 Hours on 12 September 1983. Just at the end of the Mk 21, phase 6, period 1 run. $\lambda_{ex} = 254$ nm.

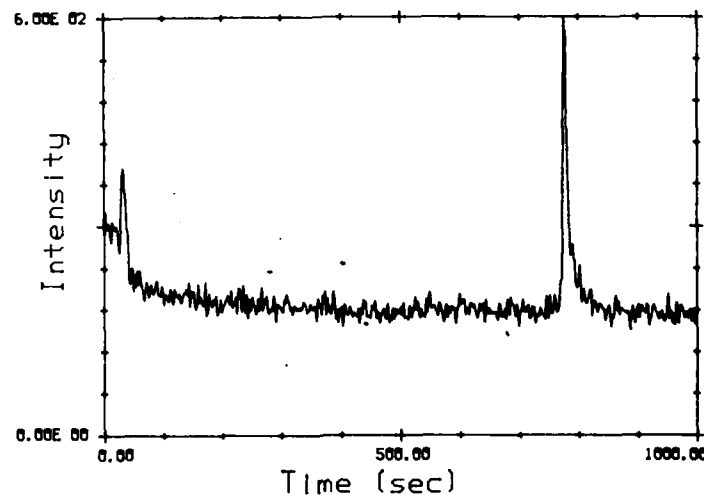


FIGURE 65. On-Line Temporal Scan Started at 0833 Hours on 13 September 1983. Mk 89, phase 7, period 1. $\lambda_{ex} = 269$, $\lambda_{em} = 328$ nm. Wavelength parameters for naphthalene detection.

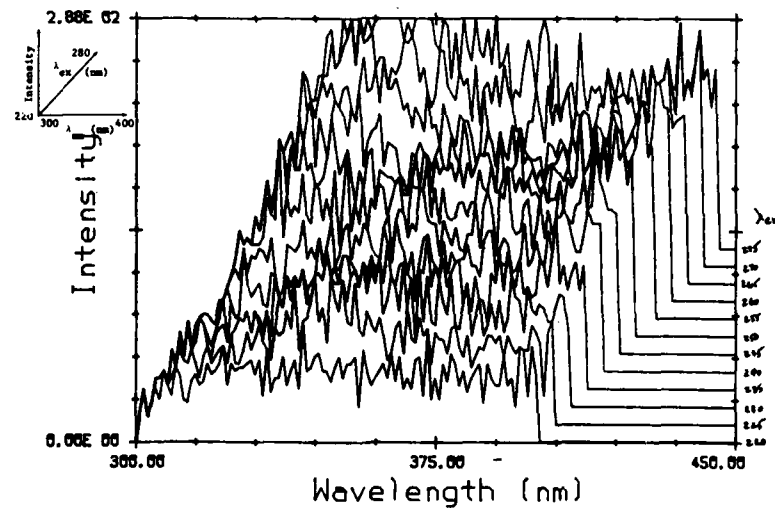


FIGURE 66. On-Line Excitation-Emission Matrix Generated at 0900 Hours on 13 September 1983. Mk 89, phase 7, period 1. The λ_{ex} values were incremented in 5 nm steps from 220-275 nm. The emission was scanned from 300-400 nm in 1 nm steps. The program was from Spex Technical Note #62.

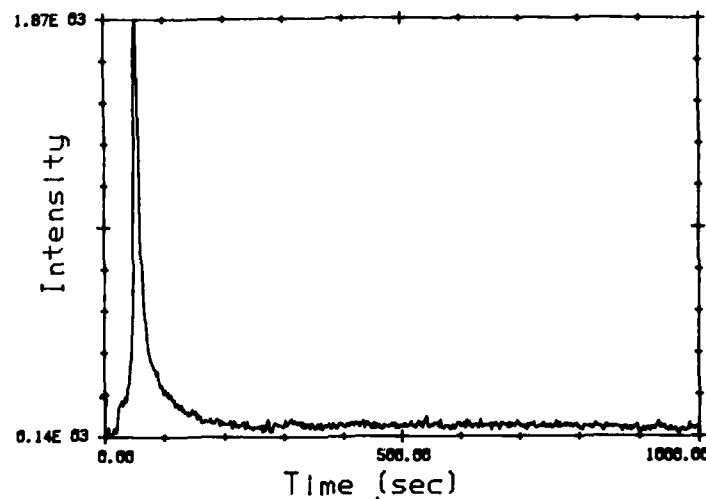


FIGURE 67. Temporal Scan Started at 1814 Hours on 14 September 1983. Taken after the Mk 23, phase 10, period 1 run. $\lambda_{ex} = 269$ nm, $\lambda_{em} = 328$ nm. Wavelength parameters for naphthalene detection.

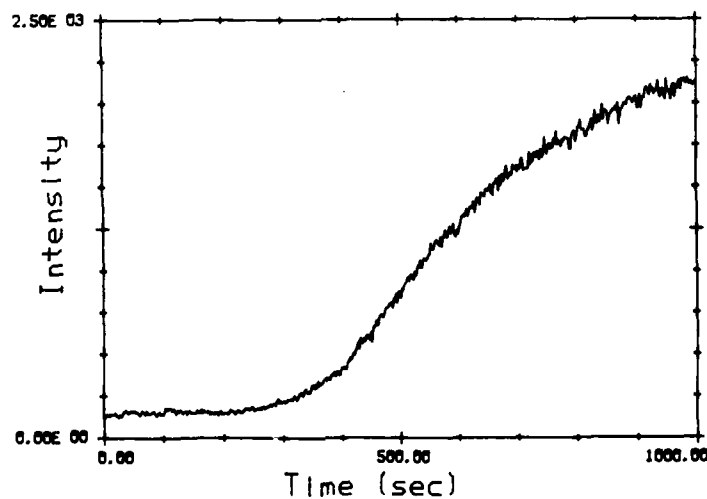


FIGURE 68. Temporal Scan Taken During the Insertion of Naphthalene into the Calibration Cell. The temperature was 65.5°C and the flow rate was 80 mL/min. $\lambda_{ex} = 269$ nm, $\lambda_{em} = 328$ nm. Wavelength parameters for naphthalene detection. Upon reaching steady state, the naphthalene concentration would be 7.8 ppm.

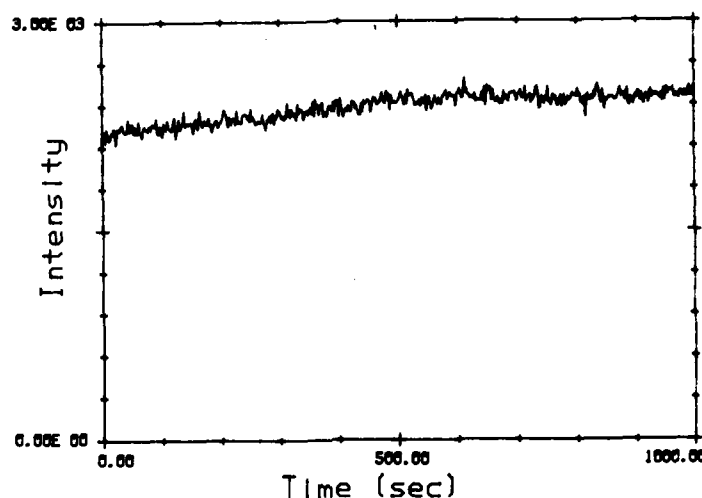


FIGURE 69. Continuation of Temporal Scan of Figure 68.

state. This is quite different from the result given in Figure 45, or the time to steady state (Reference 36) calculations that are given in Appendix C. The causes for this include the fact that the furnace cools down when the door is opened for the insertion of the naphthalene sample and that the room temperature naphthalene is held in an insulating glass sample tube. This time lag is important only when the sample is initially placed in the furnace. The times required for equilibration during flow rate changes occur on a scale more in line with the calculated time to steady state values.

Finally, an excitation-emission matrix was generated for the naphthalene sample. It is given in Figure 70, and should be compared with the on-line test data of Figure 66. The difference between the two situations is quite clear from the figures.

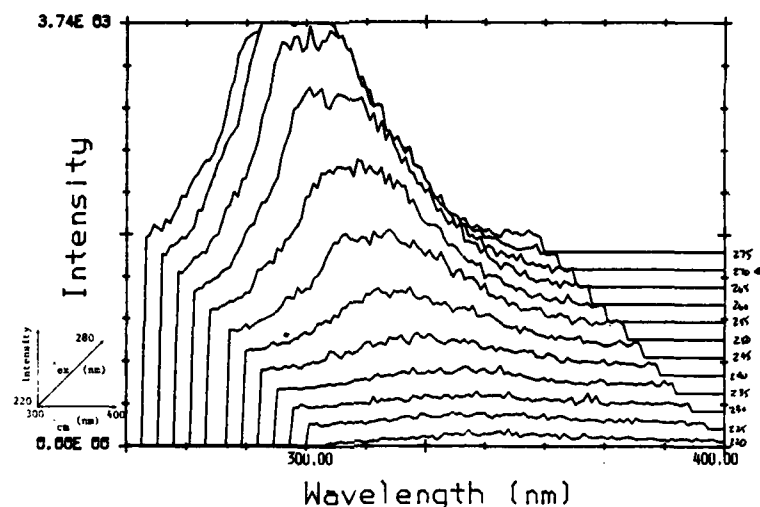


FIGURE 70. Excitation-Emission Matrix Generated from 7.8 ppm Naphthalene. The λ_{ex} values were incremented in 5 nm steps from 220-275 nm. The emission was scanned from 300-400 nm in 1 nm steps. The program was from Spex Technical Note #62.

CONCLUSIONS AND RECOMMENDATIONS

CONCLUSIONS

A number of Navy colored smoke compositions were incineration tested at the LANL CAI facility. A gas monitor analyzed the incinerator effluent for environmentally hazardous PAH materials during the tests. At the sampling location, no PAHs were detected (on a ≥ 1 ppm level) during the incineration of any of the smoke compositions studied. This was true for all the incinerator conditions used over approximately 7 days of testing.

The real-time PAH monitor system, the design, construction, and operation of which is the main focus of this report, is based on the minor modification of a commercially available, computer controlled spectrofluorimeter. The instrument is modular in design, can be upgraded, and has the advantage of being an off-the-shelf item. It performed admirably during the incineration tests, especially when one

considers the rather hostile environment in which it was placed. The monitor operated, despite the noise, vibration, dust, and >98°F temperatures at its location in the CAI facility.* It also survived three major power failures during the tests, and while being installed, had some red dye (probably from Mk 13) settle-out on it.

The computer system for spectrometer control, data manipulation, and spectral storage is user-friendly, and powerful data acquisition programs can be easily written. A number of these are supplied with the basic instrument.

The diffusion-based calibration cell was constructed and installed in the flow system to the PAH monitor. Laboratory testing demonstrated that this device was capable of producing defined concentrations of PAH compounds. This provided a method to check the monitor response to the PAHs. The known concentrations that were generated with the diffusion cell can also be calculated to within 10% accuracy, given the diffusion cell geometry, the vapor pressures of the PAHs used, and the gas flow rates as parameters.

A standard operating procedure (SOP) for the maintenance and automatic operation of the PAH monitor system will ultimately be prepared. The SOP will most likely be based on the excitation-emission matrix idea (References 30 through 33) but with a lower density of points than that obtained with video fluorimetry (References 30 and 31). Finally, the real-time results, presented here, will be compared with the analytical results from the collected samples when those data become available.

RECOMMENDATIONS

Listed below are a number of recommendations meant to improve the PAH monitor system, or its operation, for future work:

1. The temperature controller for the cartridge heaters in the fluorescence flow cell block is of the on/off type. This leads to some degree of overshoot in temperature when the controller comes on. A proportional heater/controller would give a more constant temperature set point.

2. Spex Industries sells a set of four-fused silica windows that would thermally isolate the sample compartment from the rest of the

* Spex Industries claims that the disk drives on the Datamate are prone to read/write errors at >125°F, and that the keyboard keys soften at >160°F.

instrument (about \$160.00 for the set of 4). These would keep the spectrometers in better calibration, especially if higher operating temperatures were used.

3. A line needs to be run from the diffusion cell inlet flowmeter to the outside of the building so that "clean" air can be used for calibration purposes. Laboratory air from near the furnace was being used during these tests.

4. The spectral data should have been gathered in a corrected, ratioed mode. This is especially true for the excitation spectra, since the lamp intensity is a strong function of wavelength in the deep UV. The spectra reported in this document were not corrected, or ratioed. Therefore, some error was possible due to long term lamp intensity drift. The excitation spectra are also distorted below 240 nm, but since they were all run consistently (i.e., all uncorrected), the results are still valid.

5. Permanent baffling should be installed in the sample chamber of the instrument to reduce the unwanted scattering contributions from the insulating tape on the flow cell inlet line. A darker insulating material should also be used.

6. Appropriate bandpass glass filters should be used on the emission (and excitation) beam paths so as to further reduce the level of unwanted scattered light.

7. If condensation onto the fluorescence cell windows ever becomes a problem, as part of normal operating procedure, the cell temperature could be periodically raised to bake-out the unwanted condensate. (Note that with the simple design of the flow system connections, the flow cell can also be easily removed for cleaning.)

8. All the spectra reported here were obtained at 5 nm resolution. Because of the broadband nature of these gas phase spectra, the bandpass of the spectrometers could be increased to 10 nm. This would produce an added factor of $2(2^2) = 8$, in throughput, reducing the detection limits by this same factor.

9. Although the flow system, as used in this work, performed reasonably, it should be noted that the switch-over from the calibration cell to the on-line sampling configuration was always done with the diffusion cell empty. This allowed an on-line measurement to be directly compared to the (presumably) null background. If naphthalene were in the diffusion cell at the time, one would be measuring the decay of the naphthalene signal while on-line. This would interfere with the measurement. An additional air line could be added to the system for null measurements, but this would complicate the flow design and the operation of the monitor. For the LANL tests (65.5°C),

removal and insertion of the diffusion cell sample tube represents only a minor annoyance, but for higher temperature operation, this problem would have to be addressed. The question of how often one needs to check the calibration of the instrument should also be asked. If this needs to be done only as often as does the cleaning of the fluorescence flow cell, a simpler configuration of the monitor system might involve the complete removal of the diffusion cell. In this case, a calibration check of the instrument could be done with a static cell, while the flow cell was removed for cleaning.

A few additional operational scenarios that may prove useful in future work are as follows:

1. A triangular, quartz flow cuvette (costing a few hundred dollars) would allow this same instrument to be used as an absorption spectrophotometer, if desired. The triangular cuvette would be inserted into the heated brass block such that the excitation beam enters the cell at normal incidence and passes into the sample. The beam then reflects (4 to 8%) off the hypotenuse of the triangle and passes out of the cell, into the emission monochromator. To generate a spectrum, both spectrometers (excitation and emission) would be scanned synchronously.

2. The fluorimeter can also be used for routine analysis of collected samples. One need only let the system come to room temperature and remove the flow cell. For example, it may be that as part of the SOP for the Navy incinerator system, an operator must periodically swab samples from the incinerator lines to check for the buildup of dye, or PAH material. These samples can then be extracted and put in a standard cuvette. A fluorescent analysis could be done with no modification of the instrument. Another important point is that the density of a solution sample is approximately one thousand times greater than that of air. The fluorescence quenching would also be less of a factor in solution. This all means that one could approach the advertised 0.1 parts-per-trillion (ppt) detection limit for these samples. Solid filter materials could also be examined, and the use of sensitized-fluorescence techniques (among others) would be possible (References 34, 35 and 50).

3. With some loss in the real-time feature, one can insert a trap in the sampling line and concentrate possible PAHs there before analysis. Presumably, one would warm the trap up (with slower flowrate conditions) and subsequently make fluorescence measurements. Another variant of this idea is to insert a gas chromatographic column into the line to aid in the separation of multicomponent mixtures.

LIST OF COMPANY NAMES

Battelle Memorial Institute
Columbus, OH 43201

Omega Engineering, Inc.
Stamford, CT 06907

Beckman Instruments, Inc.
Fullerton, CA 92634

Products for Research, Inc.
Danvers, MA 01923

CVI Laser Corp.
Albuquerque, NM 87112

Quanta Ray, Inc.
Mountain View, CA 94040

Eastman Chemical Products, Inc.
Kingsport, TN 37662

RCA Solid State Division
Lancaster, PA 17604

Entropy Environmentalists, Inc.
Research Triangle Park, NC

Spex Industries, Inc.
Edison, NJ 08817

Fisher Scientific Co.
Pittsburgh, PA 15219

Gilmont Instruments
Great Neck, NY 11021

Gow-Mac Instrument Co.
Bound Brook, NJ 08805

Hewlett-Packard Co.
Westlake Village, CA 91360

Lumonics Inc.
Kanata (Ottawa), Ontario
Canada K2K1Y3

Matheson Div.
Searle Medical Products USA, Inc.
E. Rutherford, NJ 07073

Mettler Instrument Corporation
Hightstown, NJ 08520

NSG Presicion Cells, Inc.
Hicksville, NY 11802

REFERENCES

1. Naval Weapons Support Center. *Controlled Incineration of Navy Colored Smoke Compositions*, by Applied Sciences Department. Crane, Ind., NSWC, July 1978, 81 pp. (NWSC/CR/RDTR-86, publication UNCLASSIFIED.)
2. Battelle Columbus Laboratories. *Development of a Polycyclic Aromatic Hydrocarbon (PAH) Measurement Method and Design of Incineration System*, by R. H. Barnes and others. Columbus, Ohio, BCL, August 1983. (Contract No. N00197-82-C-0184, publication UNCLASSIFIED.)
3. Naval Weapons Center. *Pollution Abatement Research and Development April-June 1983*, by Research Department. China Lake, Calif., NWC, October 1983, 66 pp. (NWC TP 6477, pg. 53, publication UNCLASSIFIED.)
4. ----- *Pollution Abatement Research and Development July-September 1983*, by Research Department. China Lake, Calif., NWC, December 1983, 46 pp. (NWC TP 6496 pg. 33, publication UNCLASSIFIED.)
5. *Polynuclear Aromatic Hydrocarbons: Chemistry and Biological Effects*, ed. by A. Bjorseth and A. J. Dennis. Ohio, Battelle Press, 1980, 1097 pp, and references therein.
6. *Chemical Analysis and Biological Fate: Polynuclear Aromatic Hydrocarbons*, ed. by M. Cooke and A. J. Dennis. Ohio, Battelle Press, 1981, 800 pp, and references therein.
7. H. P. Burchfield, R. J. Wheeler, and J. B. Bernos. "Fluorescence Detector for Analysis of Polynuclear Arenes by Gas Chromatography." *Anal. Chem.*, Vol. 43, No. 14 (December 1971), pp. 1976-1981.
8. D. F. Freed and L. R. Faulkner. "Characterization of Gas Chromatographic Effluents via Scanning Fluorescence Spectrometry." *Anal. Chem.*, Vol. 44, No. 7 (June 1972), pp. 1194-1198.

9. J. W. Robinson and J. P. Goodbread. "A Selective Gas Chromatographic Detector for Polynuclear Aromatics Based on Ultraviolet Fluorescence." *Anal. Chim. Acta.*, Vol. 66, (1973), pp. 239-244.
10. Mulik and others. "A Gas Liquid Chromatographic Fluorescent Procedure for the Analysis of Benzo(a)pyrene in 24 Hour Atmospheric Particulate Samples." *Anal. Lett.*, Vol. 8, No. 8 (1975), pp. 511-524.
11. R. P. Cooney and J. D. Winefordner. "Instrumental Effects on Limits of Detection in Gas Phase Fluorescence Detection of Gas Chromatographic Effluents." *Anal. Chem.*, Vol. 49, No. 7 (June 1977), pp. 1057-1060.
12. E. L. Wehry and G. Mamantov. "Low-Temperature Fluorometric Techniques and their Application to Analytical Chemistry," in *Modern Fluorescence Spectroscopy*, ed. by E. L. Wehry. New York, Plenum Press, 1981. Vol. 4, Chapt. 6, pp. 193-250. Also see references therein.
13. J. C. Brown, M. C. Edelson, and G. J. Small. "Fluorescence Line Narrowing Spectrometry in Organic Glasses Containing Parts-Per-Billion Levels of Polycyclic Aromatic Hydrocarbons." *Anal. Chem.*, Vol. 50, No. 9 (August 1978), pp. 1394-1397.
14. Y. Yang and others. "Direct Determination of Polynuclear Aromatic Hydrocarbons in Coal Liquids and Shale Oil by Laser Excited Shpol'skii Spectrometry." *Anal. Chem.*, Vol. 52, No. 8 (July 1980), pp. 1350-1351.
15. A. L. Colmsjo and C. E. Ostman. "Selectivity Properties in Shpol'skii Fluorescence of Polynuclear Aromatic Hydrocarbons." *Anal. Chem.*, Vol. 52, No. 13 (November 1980), pp. 2093-2095.
16. Y. Yang, A. P. D'Silva and V. A. Fassel. "Laser-Excited Shpol'skii Spectroscopy for the Selective Excitation and Determination of Polynuclear Aromatic Hydrocarbons." *Anal. Chem.*, Vol. 53, No. 6 (May 1981), pp. 894-899.
17. J. R. Maple, E. L. Wehry and G. Mamantov. "Laser-Induced Fluorescence Spectrometry of Polycyclic Aromatic Hydrocarbons Isolated in Vapor-Deposited n-Alkane Matrices." *Anal. Chem.*, Vol. 52, No. 6 (May 1980), pp. 920-924.
18. D. M. Hembree and others. "Matrix Isolation Fourier Transform Infrared Spectrometric Detection in the Open Tubular Column Gas Chromatography of Polycyclic Aromatic Hydrocarbons." *Anal. Chem.*, Vol. 53, No. 12 (October 1981), pp. 1783-1788.

19. J. R. Maple and E. L. Wehry. "Fluorescence Photoselection of Matrix Isolated Polycyclic Aromatic Hydrocarbons." *Anal. Chem.*, Vol. 53, No. 8 (July 1981), pp. 1244-1249.
20. L. J. Cline Love and L. M. Upton. "Analysis of Multicomponent Fluorescent Mixtures through Temporal Resolution." *Anal. Chem.*, Vol. 52, No. 3 (March 1980), pp. 496-499.
21. R. B. Dickinson and E. L. Wehry. "Time-Resolved Matrix-Isolation Fluorescence Spectrometry of Mixtures of Polycyclic Aromatic Hydrocarbons." *Anal. Chem.*, Vol. 51, No. 6 (May 1979), pp. 778-780.
22. N. Ishibashi and others. "Laser Fluorimetry of Fluorescein and Riboflavin." *Anal. Chem.*, Vol. 51, No. 13 (November 1979), pp. 2096-2099.
23. T. C. O'Haver. "Modulation and Derivative Techniques in Luminescence Spectroscopy: Approaches to Increased Analytical Sensitivity," in *Modern Fluorescence Spectroscopy*, ed. by E. L. Wehry. New York, Plenum Press, 1976. Vol. 1, Chapt. 3, pp. 65-81.
24. G. L. Green and T. C. O'Haver. "Derivative Luminescence Spectrometry." *Anal. Chem.*, Vol. 46 (1974), pp. 2191-2196.
25. A. R. Hawthorne and J. H. Thorngate. "Improving Analysis from Second-Derivative UV-Absorption Spectrometry." *Appl. Opt.*, Vol. 17, No. 5 (March 1978), pp. 724-729.
26. A. R. Hawthorne and others. "Development of a Prototype Instrument for Field Monitoring of PAH Vapors," in *Polynuclear Aromatic Hydrocarbons*, ed. by P. W. Jones and P. Leber. Ann Arbor, Ann Arbor Science Publishers, Inc., 1979, pp. 299-311.
27. A. R. Hawthorne and J. H. Thorngate. "Application of Second-Derivative UV-Absorption Spectrometry to Polynuclear Aromatic Compound Analysis." *Appl. Spect.*, Vol. 33, No. 3 (1979), pp. 301-305.
28. A. R. Hawthorne. "DUVAS: A Real-Time Aromatic Vapor Monitor for Coal Conversion Facilities." *J. Am. Ind. Hyg. Assoc.*, Vol. 41, No. 12 (December 1980), pp. 915-921.
29. T. Vo-Dinh. "Synchronous Excitation Spectroscopy," in *Modern Fluorescence Spectroscopy*, ed. by E. L. Wehry. New York, Plenum Press, 1981. Vol. 4, Chapt. 5, pp. 167-192. Also see references therein.

30. G. D. Christian, J. B. Callis, and E. R. Davidson. "Array Detectors and Excitation-Emission Matrices in Multicomponent Analysis," in *Modern Fluorescence Spectroscopy*, ed. by E. L. Wehry. New York, Plenum Press, 1981. Vol. 4, Chapt. 4, pp. 111-165.
31. I. M. Warner and L. B. McGowan. "Recent Advances in Multicomponent Fluorescence Analysis," in *CRC Critical Reviews in Analytical Chemistry*, (February 1982), pp. 115-222.
32. M. P. Fogarty and I. M. Warner. "Ratio Method for Fluorescence Spectral Deconvolution." *Anal. Chem.*, Vol. 53, No. 2 (February 1981), pp. 259-265.
33. M. P. Fogarty, C. -N. Ho, and I. M. Warner. "Data Handling in Fluorescence Spectrometry," in *Optical Radiation Measurements*, ed. by K. D. Mielenz. Vol. 3, New York, Academic Press, 1982, pp. 249-314.
34. E. M. Smith and P. L. Levins. "Sensitized Fluorescence Detection of PAH," in *Polynuclear Aromatic Hydrocarbons: Chemistry and Biological Effects*, ed. by A. Bjorseth and A. J. Dennis. Ohio, Battelle Press, 1980, pp. 973-982.
35. L. D. Johnson, R. E. Luce, and R. G. Merrill. "A Spot Test for Polycyclic Aromatic Hydrocarbons," in *Chemical Analysis and Biological Fate: Polynuclear Aromatic Hydrocarbons*, ed. by M. Cooke and A. J. Dennis. Ohio, Battelle Press, 1981, pp. 119-131.
36. A. H. Miguel and D. F. S. Natusch. "Diffusion Cell for the Preparation of Dilute Vapor Concentrations." *Anal. Chem.*, Vol. 47, No. 9 (August 1975), pp. 1705-1707.
37. A. H. Miguel and others. "Apparatus for Vapor-Phase Adsorption of Polycyclic Organic Matter onto Particulate Surfaces." *Envir. Sci. and Tech.*, Vol. 13, No. 10 (October 1979), pp. 1229-1232.
38. Naval Weapons Center. *Polycyclic Aromatic Hydrocarbons on the Inner Surfaces of Copper Tubing*, by E. D. Erickson, J. H. Johnson, and S. R. Smith. China Lake, Calif., NWC, May 1984, 28 pp. (NWC TP 6532, publication UNCLASSIFIED.)
39. Los Alamos National Laboratory. *The Los Alamos Controlled Air Incinerator for Radioactive Waste*, by R. A. Kronig and others. Los Alamos, N. Mex., LANL, October 1982. (Waste Management, Group H-7 Report No. LA-9427 Vols. I and II, publication UNCLASSIFIED.)

40. Entropy Environmentalists, Inc. *The Los Alamos Controlled Air Incinerator Navy Colored Smoke Incineration Test Run Offgas Sampling Work Plan*. Research Triangle Park, NC., September 1983.
41. Los Alamos National Laboratory. *Experimental Test Plan for CAI Test #16-CS-1*. Los Alamos, N. Mex., LANL, September 1983. (Waste Management, Group H-7, publication UNCLASSIFIED.)
42. R. Kaminski, R. Obenauf and F. Purcell. "Focus on Fluorescence." *The Spex Speaker*, Vol. 27, No. 1 (March 1982), pp. 1-9.
43. D. P. Shoemaker and C. W. Garland. "Transport Properties of Gases," in *Experiments in Physical Chemistry*. New York, McGraw-Hill Book Company, Inc., 1962. Chapt. 4, pp 68-106. See pg. 75.
44. E. H. Kennard. *Kinetic Theory of Gases*. New York, McGraw-Hill, 1938.
45. W. J. Moore. *Kinetic Theory of Gases*. New York, McGraw-Hill, 1958.
46. *CRC Handbook of Chemistry and Physics*, ed. by R. C. Weast and M. J. Astle. Florida, CRC Press, 1981-1982.
47. T. E. Jordan. *Vapor Pressure of Organic Compounds*. New York, Interscience, 1954. Also see references therein.
48. J. Timmermans. *Physico-Chemical Constants of Pure Organic Compounds*. New York, Elsevier, 1965. Volume 2.
49. I. B. Berlman. *Handbook of Fluorescence Spectra of Aromatic Molecules*. New York, Academic Press, 1971.
50. P. G. Seybold, D. A. Hinckley and T. A. Heinrichs. "Surface-Sensitized Luminescence." *Anal. Chem.*, Vol. 55, No. 12 (October 1983), pp. 1994-1996.

NWC TP 6525

Appendix A

PROGRAM AD_RLTIME

PROGRAM AD_RLTIME AS OF 7/22/83

```

10  !
20  !
30  !PROGRAM "AD_RLTIME" TO TAKE A/D READINGS IN REAL-TIME, PLOT DATA
40  ! AND CALCULATE STANDARD DEVIATION. ALSO OPTION TO STORE DATA
50  ! ON DISC
60  !
70  ! USE WITH "DSC_RDTM" PROGRAM
80  !
90  !R. LODA 3/17/83
100 ! CURSER INSERTED. P. PLASSMANN 7/20/83
110 !
120 ! USE READ/DATA STATEMENTS FOR SELDOM CHANGING VARIABLES-SEE BELOW
130 OPTION BASE 1 !ARRAYS START AT 1 NOT 0 INDEX
140 DIM Seconds(7200), Rav(7200), Std_dev(7200), Ts(8), R(1000)
150 DIM Opr$(18), Date$(8), Comment$(40), Pmt$(10), File_name$(10), Dsc_lbl$(6)
160 REAL T_ov, T_dc, T_fc, Flow_f, Flow_g, Tm_cnst, Lam_ex, Bndwth, Power, Re_rate, Lam_e
170 m, Band, Slits, Hvs, Hvr, Gate_time, Ap_dly, fcs, Tcr, Sens_s, Sens_r
180 INTEGER Run_num, N, Test_length, Tm_test
190 GOSUB Clear_screen
200 DUMP DEVICE IS 9
210 !OUTPUT 9 USING 2100
220 IMAGE /, 30X, "START OF EXPERIMENT"
230 PRINTER IS 1
240 PRINT TABXY(5,9), "<EXECUTE> SET TIME FTIME('hh:mm:ss'). THEN CONTINUE"
250 PRINT TABXY(5,10), "IF NECESSARY, OTHERWISE JUST CONTINUE."
260 PAUSE
270 GOSUB Clear_screen
280 TS=FNTIME$(TIMEDATE)
290 !INPUT "ENTER OPERATOR NAME(10CHS), DATE(8CHS)", Opr$, Date$
300 !INPUT "ENTER SAMPLE NAME(18CHS), RUN NUMBER", Sample$, Run_num
310 !INPUT "ENTER TEMPERATURES-OVEN, DIFFUSION CELL, FLUORESCENCE CELL", T_ov, T_dc,
320 c, T_fc
330 !INPUT "ENTER GAS NAMES FOR FLOWMETERS F,G(18CHS)", Gas_fs, Gas_gs
340 !INPUT "ENTER STARTING FLOWRATES-F,G IN CM", Flow_f, Flow_g
350 !
360 !
370 READ Opr$, Date$, Sample$, Run_num, T_ov, T_dc, T_fc, Gas_fs, Gas_gs, Flow_f, Flow_g
380 DATA LODA/PLASSMANN, 7/22/83, PHENANTHRENE N2, 1, 113, 118, 119, NITROGEN, LAB AIF
390 !
400 !
410 !
420 !
430 !INPUT "ENTER N SAMPLES AVERAGED(1000MAX), TIME CONSTANT OF AVERAGE(2<N<=
440 100*TM_CNST)", N, Tm_cnst ! BASED ON .01 SEC READ-TIME
450 IF 2>N THEN GOTO 480
460 IF N<=100*Tm_cnst THEN
470 GOTO 510
480 ELSE
490 BEEP
500 GOTO 430
510 END IF
520 !INPUT "ENTER TEST LENGTH-SECONDS(7200 MAX), NUMBER OF X TICS ", Test_length,
530 .Xticno
540 IF Test_length>7200 THEN 510
550 IF (Test_length/Tm_cnst<=7200) THEN

```

NWC TP 6525

```

540 GOTO 720
550 ELSE
560 Test_length=7200*Tm_cnst
570 BEEP
580 END IF
590 DISP "MAX TEST LENGTH IS ":Test_length:" FOR A ":Tm_cnst:" TIME CONSTANT."
600 WAIT 10
610 BEEP
620 INPUT "ENTER 0 TO CONTINUE WITH THIS TEST LENGTH, ANY KEY TO REENTER TIME C
ONSTANT", Jnk
630 IF Jnk=0 THEN
640 GOTO 680
650 ELSE
660 GOTO 430
670 END IF
680 INPUT "NUMBER OF X TICS", Xtics
690 !
700 !
710 !
720 READ Comment$, Source$, Lam_ex, Bndwth, Dye$, Power, Rep_rate, Mono$
730 DATA 75MM LENS-EM-0160 IRIS-EX, EXCIMER (XeCl), 308.T, NONE, 1.4, 24, SPEX .85M
740 READ Lam_em, Band, Slits, Pmt$, Hvs, Hvr, Proc_inst$, Gate_time, Ap_dly, Tcs, Tcr, Se
ns_s, Sens_r
750 DATA 390.0, 1, RCA C31034, -1650, -850, DCA-1, 1.0, 1, 3, 30, 10
760 !
770 !
780 !
790 !
800 ! CALC WAIT TIME FOR READ CYCLE
810 !
820 Loop_time=.009!NOTE WAITS ARE ROUNDED TO NEAREST THOUSANDTH.
830 Wt_time=(Tm_cnst/N)-Loop_time
840 !INPUT "ENTER COMMENTS(40CHS)", Comments
850 !INPUT "ENTER EXCITATION SOURCE NAME(18CHS)", Source$
860 !INPUT "ENTER EXCITATION WAVELENGTH(NM), BANDWIDTH(NM), DYE(18CHS)", Lam_ex, B
ndwth, Dye$
870 !INPUT "POWER(WATTS), REP RATE(HZ)", Power, Rep_rate
880 P_power=(Power/Rep_rate)*1000 !PULSE POWER MJ/PULSE
890 !INPUT "ENTER MONOCHROMATOR TYPE(18CHS)", Mono$
900 !INPUT "ENTER EMISSION WAVELENGTH(NM), BANDWIDTH(NM), SLITS(MM)", Lam_em, Band
, Slits
910 !INPUT "ENTER PMT TYPE(10CHS), HIGH VOLTAGE-SAMPLE, REFERENCE", Pmt$, Hvs, Hvr
920 !INPUT "ENTER PROCESSING INSTRUMENT(18CHS)", Proc_inst$
930 !INPUT "ENTER GATE TIME(MSEC), PERATURE DELAY(MSEC), TIME CONSTANTS-SAMPLE
REF(SEC)", Gate_time, Ap_dly, Tcs, Tcr
940 !INPUT "ENTER SENSITIVITY OR GAIN-SAMPLE, REF", Sens_s, Sens_r
950 GOSUB Clear_screen
960 GOSUB Data_print
970 DISP "PAUSE-PRESS CONTINUE TO GO ON"
980 PAUSE
990 GOSUB Clear_screen
1000 PRINTER IS 9
1010 OUTPUT 1:"THERMAL PRINTER ACTIVE"
1020 GOSUB Plot_axes
1030 Tm_test=INT(Test_length/Tm_cnst)
1040 DISP "PAUSE-PRESS CONTINUE TO START SCAN"
1050 PAUSE
1060 DISP "SCANNING"
1070 GOSUB Start_timer
1080 !

```

```

1090 ! MAIN LOOP
1100 ON KEY 2 LABEL "FLOW CHANGE" GOSUB Flow_change
1110 FOR J=1 TO Tm_test
1120 Sum=0.
1130 Sum_sq=0.
1140 GOSUB Read_ad
1150 GOSUB Plot_inten
1160 NEXT J
1170 !
1180 ! END MAIN LOOP
1190 GOSUB Knob_thing
1200 Plot_axes: DEG
1210 GRAPHICS ON
1220 GINIT
1230 LORG 5
1240 READ Label_x$,Label_y$,Vxmin,Vxmax,Vymin,Vymax,Xmin,Ymin,Ymax,Yticno
1250 Xmax=Test_length
1260 DATA TIME-SEC,INTENSITY,20,110,31,90,0.0,10,10
1270 VIEWPORT Vxmin,Vxmax,Vymin,Vymax
1280 WINDOW Xmin,Xmax,Ymin,Ymax
1290 Xtic=(Xmax-Xmin)/Xticno
1300 Ytic=(Ymax-Ymin)/Yticno
1310 AXES Xtic,Ytic,Xmin,Ymin,Xticno,Yticno,5
1320 VIEWPORT 0,131,0,100
1330 LDIR 0
1340 MOVE Xmin+(Xmax-Xmin)/2,Ymin-.10*(Ymax-Ymin)
1350 CSIZE 7*(Vxmax-Vxmin)/131,.6
1360 LABEL USING "K":Label_x$
1370 MOVE Xmin-.10*(Xmax-Xmin),Ymin+(Ymax-Ymin)/2
1380 LDIR 90
1390 CSIZE 7*(Vymax-Vymin)/100,.6
1400 LABEL USING "K":Label_y$
1410 CSIZE 5*(Vymax-Vymin)/100,.6
1420 MOVE Xmin-.05*(Xmax-Xmin),Ymin
1430 LABEL USING "K":Ymin
1440 MOVE Xmin-.05*(Xmax-Xmin),Ymax
1450 LABEL USING "K":Ymax
1460 LDIR 0
1470 CSIZE 5*(Vxmax-Vxmin)/131,.6
1480 MOVE Xmin,Ymin-.05*(Ymax-Ymin)
1490 LABEL USING "K":Xmin
1500 MOVE Xmax,Ymin-.05*(Ymax-Ymin)
1510 LABEL USING "K":Xmax
1520 MOVE Xmin+(Xmax-Xmin)/3.0,Ymin-.3*(Ymax-Ymin)
1530 CSIZE 4.5*(Vxmax-Vxmin)/131,.6
1540 LABEL USING 1550:Samples,Run_num,T_ov,T_dc,T_fc
1550 IMAGE 18A." RUN #".K,1X,K,"C",1X,K,"C",1X,K,"C"
1560 VIEWPORT Vxmin,Vxmax,Vymin,Vymax
1570 CLIP Xmin,Xmax,Ymin,Ymax
1580 PEN 1
1590 MOVE 0,0
1600 RETURN
1610 Start_timer: TS=FTime$(TIMEDATE)
1620 CLIP OFF
1630 CSIZE 4.5*(Vxmax-Vxmin)/131,.6
1640 MOVE Xmax,Ymin-.3*(Ymax-Ymin)
1650 LABEL USING "9A,1X,9A":TS.Date$
1660 MOVE 0,5
1670 CLIP Xmin,Xmax,Ymin,Ymax
1680 Init_time=TIMEDATE

```

NWC TP 6525

```

1690                                     !PRINT "TIMER INITIALIZED."
1700                                     RETURN
1710 Read_ad: Rd_start=TIMEDATE-Init_time
1720 IMAGE #.W
1730 FOR I=1 TO N
1740 OUTPUT 12 USING 1720:-3920.12288
1750 STATUS 12.3:R(I)
1760 R(I)=R(I)+32768
1770 IF R(I)>2047 THEN R(I)=R(I)-4096
1780 R(I)=.005*R(I)
1790 Sum=Sum+R(I)
1800 Sum_sq=Sum_sq+R(I)*R(I)
1810 WAIT Wt_time !NOTE WAITS ROUNDED TO NEAREST THOUSANDTH.
1820 NEXT I
1830 Rav(J)=Sum/N
1840 Sq_sum=Sum*Sum/N
1850 S_sq=(Sum_sq-Sq_sum)/(N-1)
1860 IF S_sq<=0. THEN
1870 Std_dev(J)=0.
1880 ELSE
1890 Std_dev(J)=SOR(S_sq)
1900 END IF
1910 Rd_stop=TIMEDATE-Init_time
1920 Seconds(J)=(Rd_stop+Rd_start)/2.
1930 RETURN
1940 Plot_inten: PLOT Seconds(J),Rav(J)
1950 DISP USING 1960:J,Rav(J),Std_dev(J),Seconds(J)
1960 IMAGE "POINT #".4D.5X,"I=" .2D.3D.,5X,"STD DEV=" .2D.3D.5X,"-
1970 " .4D.1D." SECS." RETURN
1980 Knob_thing: ON KEY 1 LABEL "DATA PRINT" GOSUB Data_print
1990 WAIT 1
2000 DISP "END OF EXPERIMENT"
2010 Tone=81.38
2020 FOR M=1 TO 5
2030 BEEP Tone*.2
2040 Tone=Tone*.2
2050 NEXT M
2060 WAIT 1
2070 BEEP
2080 DISP "USE THE KNOB TO MOVE CURSOR THRU THE C
2090 MOVE 0.0
2100 ON KEY 3 LABEL "CURSOR PRINT" GOTO Cursor_p=
2110 ON KEY 0 LABEL "DISC STORE" GOSUB Disc_store
2120 ON KEY 4 LABEL "QUIT" GOTO Quit
2130 CLIP OFF
2140 ON KEY 5 LABEL "PRINT SPOT" GOSUB Print_spot=
2150 ON KNOB .1 GOSUB Move_bip
2160 Spin: GOTO Spin
2170 RETURN
2180 RETURN
2190 Off_spot: !
2200 IF Old_spot<>0 THEN
2210 DRAW Seconds(Old_spot),Rav(Old_spot)+Space
2220 Old_spot=0
2230 END IF
2240 RETURN
2250 !

```

NWC TP 6525

```

2260 Print_spot:  ! Print point number on graph.
2270               LINE TYPE 1
2280               LDIR 90
2290               LORG 2
2300               PEN 1
2310               IF Old_spot<>0 THEN
2320                 MOVE Seconds(Old_spot),Rav(Old_spot)+4*Space
2330                 LABEL USING 2340:Seconds(Old_spot)
2340                 IMAGE 4D,2D
2350               END IF
2360               Old_spot=0
2370               PEN 0
2380               RETURN
2390               !
2400 Move_blip:
2410               !
2420               Spot=Spot+KNOBK
2430               Spot=INT(Spot)
2440               IF Spot<1 THEN Spot=1
2450               IF Spot>Im_test THEN Spot=Im_test
2460               DISP USING 1960:Spot,Rav(Spot),Std_
dev(Spot),Seconds(Spot)
2470               Space=(Ymax-Ymin)/40
2480               PEN 0
2490               GOSUB Off_spot
2500               MOVE Seconds(Spot),Rav(Spot)+Space
2510               DRAW Seconds(Spot),Rav(Spot)+3*Space
2520               Old_spot=Spot
2530               RETURN
2540 Cursor_print:  PRINTER IS 9
2550               PRINT USING 1960:Spot,Rav(Spot),Std_dev(Spot),Seconds(Spot)
2560               GOTO Spin
2570 Clear_screen:  OUTPUT 2 USING "#.B":255.75
2580               GCLEAR
2590               RETURN
2600 Data_print:  !PRINTER IS 9
2610               PRINT "                GENERAL DATA OUTPUT FROM AD_RLTIME
PROGRAM"
2620               PRINT
2630               PRINT USING 2640:Op$,Date$,Ts
2640               IMAGE "OPERATOR: ".18A.9X." DATE: ".8A.9X." TIME: ".8A
2650               PRINT USING 2660:Samples,Run_num
2660               IMAGE "SAMPLE: ".18A.5X." RUN NUMBER: ".K
2670               PRINT USING 2680:T_ov,T_dc,T_fc
2680               IMAGE "OVEN TEMP: ".K.5X."D CELL TEMP: ".K.5X."F CELL TEMP:
".K
2690               PRINT USING 2700:Gas_fs,Gas_gs
2700               IMAGE "FLOWMETER-F GAS: ".18A.5X."FLOWMETER-G GAS: ".18A
2710               PRINT USING 2720:Flow_f,Flow_g
2720               IMAGE "STARTING FLOWRATE-F: ".K."CM      STARTING FLOWRATE-G
: ".K."CM"
2730               PRINT USING 2740:N,Im_cnst,Test_length
2740               IMAGE 4X.K." SAMPLES AVERAGED OVER (APPROX) ".K." SEC. FOR (AF
PROX) ".K." TOTAL SECONDS."
2750               PRINT USING 2760:Samples,Run_num,T_ov,T_dc,T_fc
2760               IMAGE "GRAPH LABEL: ".18A." RUN #".K.1X.F."C".1X.K."C".1X.K.
"C"
2770               PRINT USING "40A":Comments
2780               PRINT

```

```

2790          PRINT "                                EXCITATION CONDITIONS"
2800          PRINT
2810          PRINT USING 2820:Source$
2820          IMAGE "SOURCE: ".18A
2830          PRINT USING 2840:Lam_ex,Bndwth,Dye$
2840          IMAGE "WAVELENGTH: ".K,"NM ".10X,"BANDWIDTH: ".K,"NM",10X,"E
YE: ".18A
2850          PRINT USING 2860:P_power,Rep_rate,Power
2860          IMAGE K," MJ/PULSE AT ".K,"HZ IS ".K," WATTS."
2870          PRINT
2880          PRINT "                                EMISSION CONDITIONS"
2890          PRINT
2900          PRINT USING 2910:Mono$
2910          IMAGE "MONOCHROMATOR TYPE: ".18A
2920          !WAIT 15
2930          PRINT USING 2940:Lam_em,Band,Slits
2940          IMAGE "WAVELENGTH: ".K,"NM",5X,"BANDWIDTH: ".K,"NM",5X,"SLIT
S: ".K,"MM"
2950          PRINT
2960          PRINT "                                DETECTION ELECTRONICS"
2970          PRINT
2980          PRINT USING 2990:Pmts,Hvs,Hvr
2990          IMAGE "PMT: ".10A,10X,"SAMPLE-HV: ".K,10X,"REFERENCE-HV: ".
3000          PRINT USING 3010:Proc_inst$
3010          IMAGE "PROCESSING INSTRUMENT: ".18A
3020          PRINT USING 3030:Gate_time,Ap_dly,Tcs,Tcr
3030          IMAGE "GATE TIME: ".K,"MSEC,AP.DELAY: ".K,"MSEC,SMPL TIME CH
ST: ".K,"SEC,REF TIME CNST: ".K,"SEC"
3040          PRINT USING 3050:Sens_s,Sens_r
3050          IMAGE "SENSITIVITY OR GAIN - SAMPLE: ".K,5X," REFERENCE: ".
3060          PRINT
3070          RETURN
3080 Flow_change: !PRINTER IS 1
3090          PRINT USING 3100:J
3100          IMAGE "FLOW CHANGE AT POINT # ".4D! CAN'T PRINT SECONDS(J)-
GET 0.000 MOST KEY HITS-J OK THOUGH ?????
3110          !PRINTER IS 9
3120          RETURN
3130 Disc_store: ! STORE DATA ON DISC
3140          INPUT "ENTER DISC VOLUME LABEL".Dsc_lbl$
3150          INPUT "ENTER FILENAME(10CHS).EXAMPLE:.. '001_TM".File_name$ !
RTL NOTE -TM OR -PT FOR TIME OR POINT A/D EXP FILES
3160          CREATE BDAT File_name$.21651.8
3170          ASSIGN @Path TO File_name$:FORMAT OFF
3180          OUTPUT @Path:Seconds(*),Rav(*),Std_dev(*)
3190          OUTPUT @Path:Run_num,N.Test_length,Tm_test,T_ov,T_dc,T_fc,Flc
u_f,Flow_g,Tm_cnst,Lam_ex,Bndwth,Power,Rep_rate,Lam_em,Band,Slits,Hvs,Hcr
3200          OUTPUT @Path:Gate_time,Ap_dly,Tcs,Tcr,Sens_s,Sens_r,Opr$,Date
s,TS,Samples$,Gas_f$,Gas_g$,Comments$,Source$,Dye$,Mono$,Pmt$
3210          ASSIGN @Path TO *
3220          PRINT "DATA STORED ON DISC LABELED ".Dsc_lbl$," IN FILE ".Fil
e_name$
3230          GOTO Move_blip
3240          RETURN
3250 Quit: !
3260          GOSUB Clear_screen
3270          PRINT "                                QUIT"
3280          PRINTER IS 1
3290          GOTO 3310
3300          RETURN

```

NWC TP 6525

```

3310      END ! END FOR PROGRAM!!!!!!
3320      DEF FNTIME$(Now) !GIVEN 'SECONDS' RETURN 'HH:MM:SS'
3330      !
3340      Now=INT(Now) MOD 86400
3350      H=Now DIV 3600
3360      M=Now MOD 3600 DIV 60
3370      S=Now MOD 60
3380      OUTPUT TS USING "#,ZZ,K":H,"":M,"":S
3390      RETURN TS
3400      FNEED
3410      !
3420      DEF FNTIME(TS) !GIVEN 'HH:MM:SS' RETURN 'SECONDS'
3430      !
3440      ON ERROR GOTO Err
3450      ENTER TS:H,M,S
3460      RETURN (3600*H+60*M+S) MOD 86400
3470 Err:      OFF ERROR
3480      RETURN TIMEDATE MOD 86400
3490      FNEED

```

NWC TP 6525

GENERAL DATA OUTPUT FROM AD_RLTIME PROGRAM

OPERATOR: R.LODA DATE: 4/6/83 TIME: 13:53:51
SAMPLE: ANTHRACENE-N2 RUN NUMBER: 1
OVEN TEMP: 159 D CELL TEMP: 155 F CELL TEMP: 164
FLOWMETER-F GAS: NITROGEN FLOWMETER-G GAS: LAB AIR
STARTING FLOWRATE-F: 1CM (40-45) STARTING FLOWRATE-G: 0CM
20 SAMPLES AVERAGED OVER (APPROX) 1 SEC. FOR (APPROX) 1000 TOTAL SECONDS.
GRAPH LABEL: ANTHRACENE-N2 RUN #1 159C 155C 164C
COMMENTS: 75MM LENS-EM-0160 IRIS-EX

EXCITATION CONDITIONS

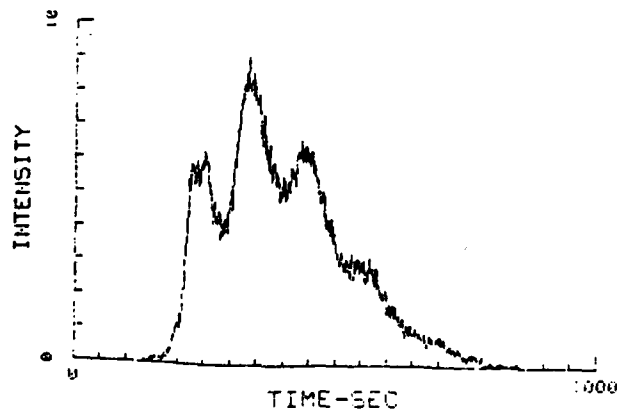
SOURCE: EXCIMER LASER
WAVELENGTH: 308NM BANDWIDTH: 1NM DYE: NONE
10-416655667 MJ/PULSE AT 24HZ IS 1.4 WATTS.
58.35

EMISSION CONDITIONS

MONOCHROMATOR TYPE: SPEX .85M 0.233nm
WAVELENGTH: 390NM BANDWIDTH: 9NM SLITS: 1MM

DETECTION ELECTRONICS

PMT: RCA C31034 SAMPLE-HV: -1650 REFERENCE-HV: -850
PROCESSING INSTRUMENT: DGA-1
GATE TIME: .1MSEC. AP. DELAY: 0MSEC. SMPL TIME CNST: 1SEC. REF TIME CNST: .3SEC
SENSITIVITY OR GAIN - SAMPLE: 30 REFERENCE: 10



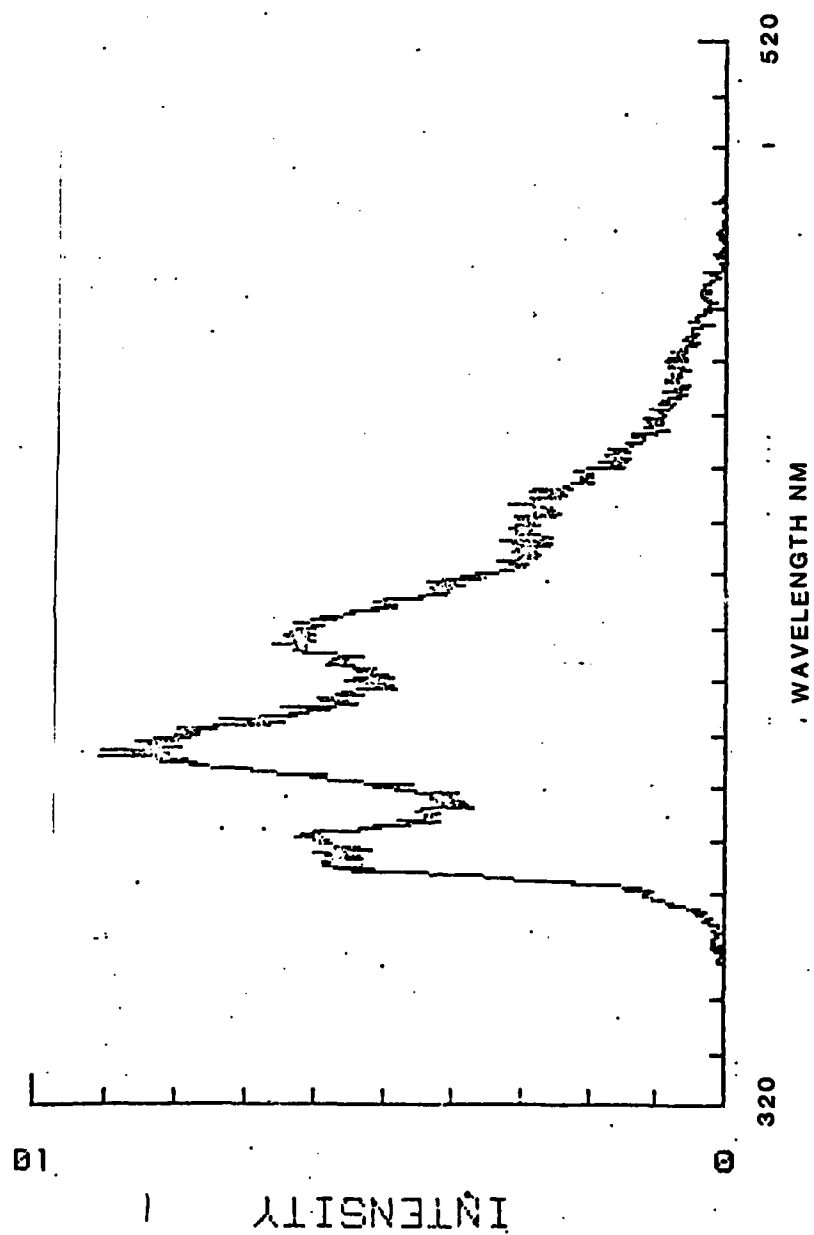
ANTHRACENE-N2 RUN #1 159C 155C 164C (13.5315) 4/5/83

520
 320-520NM AT 2A/SEC
 FLOW CHANGE AT POINT # 100
 FLOW CHANGE AT POINT # 150
 350A
 FLOW CHANGE AT POINT # 200
 3600A
 FLOW CHANGE AT POINT # 250
 3700A
 FLOW CHANGE AT POINT # 300
 3800A
 FLOW CHANGE AT POINT # 350
 3900A
 FLOW CHANGE AT POINT # 400
 4000A
 FLOW CHANGE AT POINT # 450
 4100A
 FLOW CHANGE AT POINT # 500
 4200A
 FLOW CHANGE AT POINT # 550
 4300A
 FLOW CHANGE AT POINT # 600
 4400A
 FLOW CHANGE AT POINT # 651
 4500A
 FLOW CHANGE AT POINT # 701
 4600A
 FLOW CHANGE AT POINT # 751
 4700A
 FLOW CHANGE AT POINT # 801
 480A
 FLOW CHANGE AT POINT # 851
 4900A
 FLOW CHANGE AT POINT # 900
 5000A

4/5/83 Run #1

Here, the points are not flow changes, but points at which the monochromator reading was the listed wavelength value.

POINT # 100	I= -.112	STD DEV= .022	AT 100.9 SECS.
POINT # 150	I= .064	STD DEV= .040	AT 151.1 SECS.
POINT # 200	I= 1.121	STD DEV= .121	AT 201.1 SECS.
POINT # 250	I= 5.902	STD DEV= .148	AT 251.0 SECS.
POINT # 300	I= 4.311	STD DEV= .167	AT 301.0 SECS.
POINT # 350	I= 7.835	STD DEV= .159	AT 350.9 SECS.
POINT # 400	I= 5.560	STD DEV= .124	AT 400.8 SECS.
POINT # 450	I= 5.993	STD DEV= .094	AT 450.3 SECS.
POINT # 500	I= 3.430	STD DEV= .164	AT 500.7 SECS.
POINT # 550	I= 2.754	STD DEV= .120	AT 550.5 SECS.
POINT # 600	I= 1.588	STD DEV= .048	AT 600.5 SECS.
POINT # 651	I= .949	STD DEV= .067	AT 651.5 SECS.
POINT # 701	I= .586	STD DEV= .052	AT 701.4 SECS.
POINT # 751	I= .274	STD DEV= .037	AT 751.4 SECS.
POINT # 800	I= .119	STD DEV= .023	AT 800.3 SECS.
POINT # 801	I= .175	STD DEV= .036	AT 801.3 SECS.
POINT # 851	I= .072	STD DEV= .049	AT 851.4 SECS.
POINT # 900	I= -.099	STD DEV= .023	AT 900.3 SECS.



ANTHRACENE-N2 RUN #1 159C 155C 164C 13:53:51

AD-A146 467

THE DESIGN AND OPERATION OF A REAL-TIME POLYNUCLEAR
AROMATIC HYDROCARBON C. (U) NAVAL WEAPONS CENTER CHINA
LAKE CA R T LODA AUG 84 NWC-TP-6525

2/2

UNCLASSIFIED

F/G 13/2

NL

END

FILMED

DTIC

GENERAL DATA OUTPUT FROM AD_RLTIME PROGRAM

OPERATOR: R.LODA DATE: 4/5/83 TIME: 15:18:43
 SAMPLE: ANTHRACENE-N2 RUN NUMBER: 2
 OVEN TEMP: 159 D CELL TEMP: 155 F CELL TEMP: 164
 FLOWMETER-F GAS: NITROGEN FLOWMETER-G GAS: LAB AIR
 STARTING FLOWRATE-F: 1CM STARTING FLOWRATE-G: 0CM
 20 SAMPLES AVERAGED OVER (APPROX) 1 SEC. FOR (APPROX) 3600 TOTAL SECONDS.
 GRAPH LABEL: ANTHRACENE-N2 RUN #2 159C 155C 164C
 COMMENTS: 75MM LENS-EM-0160 IRIS-EX

EXCITATION CONDITIONS

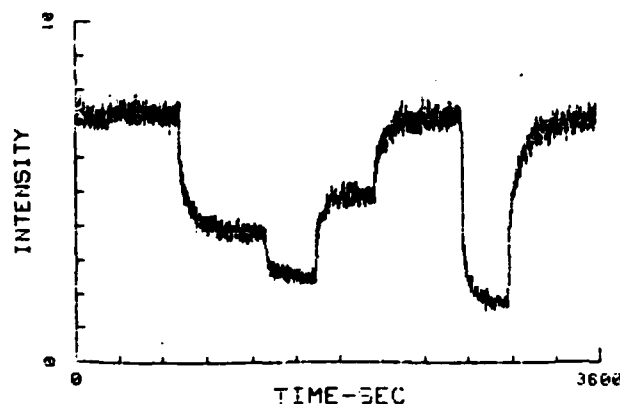
SOURCE: EXCIMER LASER
 WAVELENGTH: 308NM BANDWIDTH: 1NM DYE: NONE
 58.33333333 MJ/PULSE AT 24HZ IS 1.4 WATTS.

EMISSION CONDITIONS

MONOCHROMATOR TYPE: SPEX .85M 0.213 nm
 WAVELENGTH: 390NM BANDWIDTH: 0NM SLITS: 1MM

DETECTION ELECTRONICS

PMT: RCA C31034 SAMPLE-HV: -1650 REFERENCE-HV: -850
 PROCESSING INSTRUMENT: DGA-1
 GAIN TIME: .1MSEC. AP.DELAY: 0MSEC. SMP. TIME CNST: 1SEC. REF TIME CNST: .3SEC
 SENSITIVITY OR GAIN - SAMPLE: 30 REFERENCE: 10



FLOW AT 1CM=40ML/MIN
 FLOW CHANGE AT POINT # 720
 FLOW TO 3.6CM=80ML/MIN
 FLOW CHANGE AT POINT # 1302
 FLOW TO 6.2CM=120ML/MIN
 FLOW CHANGE AT POINT # 1642
 FLOW TO 2.1CM=60ML/MIN
 FLOW CHANGE AT POINT # 2051
 FLOW TO 1.0CM=40ML/MIN
 FLOW CHANGE AT POINT # 2667
 FLOW TO 3.8CM=160ML/MIN
 FLOW CHANGE AT POINT # 2906
 FLOW TO 1.0CM=40ML/MIN

ANTHRACENE-N2 RUN #2 159C 155C 164C 15:18:43 4/5/83

NWC TP 6525

POINT # 588	I= 7.258	STD DEV= .147	AT 585.1 SECS.
POINT # 590	I= 7.701	STD DEV= .048	AT 587.0 SECS.
POINT # 593	I= 7.472	STD DEV= .193	AT 590.0 SECS.
POINT # 603	I= 7.448	STD DEV= .076	AT 600.0 SECS.
POINT # 612	I= 7.146	STD DEV= .057	AT 608.9 SECS.
POINT # 618	I= 6.980	STD DEV= .074	AT 614.9 SECS.
POINT # 622	I= 7.047	STD DEV= .126	AT 618.9 SECS.
POINT # 660	I= 7.300	STD DEV= .081	AT 656.7 SECS.
POINT # 687	I= 7.571	STD DEV= .175	AT 683.5 SECS.
POINT # 708	I= 7.661	STD DEV= .130	AT 704.4 SECS.
POINT # 718	I= 7.195	STD DEV= .082	AT 714.4 SECS.
POINT # 1063	I= 3.786	STD DEV= .095	AT 1062.6 SECS.
POINT # 1080	I= 3.854	STD DEV= .055	AT 1074.5 SECS.
POINT # 1092	I= 3.941	STD DEV= .032	AT 1086.5 SECS.
POINT # 1105	I= 3.736	STD DEV= .058	AT 1099.4 SECS.
POINT # 1122	I= 3.892	STD DEV= .047	AT 1116.3 SECS.
POINT # 1152	I= 3.796	STD DEV= .085	AT 1146.1 SECS.
POINT # 1194	I= 3.927	STD DEV= .167	AT 1188.1 SECS.
POINT # 1226	I= 3.899	STD DEV= .062	AT 1219.9 SECS.
POINT # 1257	I= 3.919	STD DEV= .085	AT 1250.7 SECS.
POINT # 1301	I= 3.517	STD DEV= .086	AT 1294.5 SECS.
POINT # 1618	I= 2.353	STD DEV= .031	AT 1610.2 SECS.
POINT # 1639	I= 2.635	STD DEV= .062	AT 1631.1 SECS.
POINT # 1640	I= 2.461	STD DEV= .033	AT 1632.1 SECS.
POINT # 1641	I= 2.405	STD DEV= .061	AT 1633.0 SECS.
POINT # 1642	I= 2.493	STD DEV= .099	AT 1634.1 SECS.
POINT # 2005	I= 5.013	STD DEV= .075	AT 1995.2 SECS.
POINT # 2017	I= 5.027	STD DEV= .051	AT 2007.2 SECS.
POINT # 2033	I= 4.843	STD DEV= .079	AT 2023.1 SECS.
POINT # 2046	I= 4.949	STD DEV= .039	AT 2026.2 SECS.
POINT # 2057	I= 4.852	STD DEV= .159	AT 2047.3 SECS.
POINT # 2065	I= 5.315	STD DEV= .045	AT 2055.2 SECS.
POINT # 2048	I= 5.098	STD DEV= .065	AT 2038.2 SECS.
POINT # 2518	I= 7.006	STD DEV= .056	AT 2505.7 SECS.
POINT # 2539	I= 7.096	STD DEV= .058	AT 2526.6 SECS.
POINT # 2553	I= 7.191	STD DEV= .185	AT 2545.5 SECS.
POINT # 2578	I= 7.267	STD DEV= .075	AT 2565.4 SECS.
POINT # 2600	I= 7.150	STD DEV= .040	AT 2587.3 SECS.
POINT # 2624	I= 7.409	STD DEV= .119	AT 2611.2 SECS.
POINT # 2635	I= 7.331	STD DEV= .068	AT 2622.1 SECS.
POINT # 2647	I= 7.179	STD DEV= .080	AT 2634.1 SECS.
POINT # 2667	I= 7.290	STD DEV= .165	AT 2654.2 SECS.
POINT # 2913	I= 1.921	STD DEV= .053	AT 2899.0 SECS.
POINT # 2927	I= 1.728	STD DEV= .049	AT 2912.9 SECS.
POINT # 2942	I= 1.752	STD DEV= .086	AT 2927.8 SECS.
POINT # 2953	I= 1.822	STD DEV= .051	AT 2938.8 SECS.
POINT # 2962	I= 1.771	STD DEV= .078	AT 2947.7 SECS.
POINT # 2963	I= 1.856	STD DEV= .054	AT 2954.7 SECS.
POINT # 2974	I= 1.900	STD DEV= .042	AT 2959.7 SECS.
POINT # 2984	I= 1.755	STD DEV= .075	AT 2969.6 SECS.
POINT # 2986	I= 1.810	STD DEV= .047	AT 2971.6 SECS.
POINT # 3583	I= 7.257	STD DEV= .071	AT 3565.5 SECS.
POINT # 3585	I= 7.188	STD DEV= .082	AT 3567.5 SECS.
POINT # 3600	I= 7.261	STD DEV= .127	AT 3582.4 SECS.
POINT # 3596	I= 7.626	STD DEV= .093	AT 3578.4 SECS.
POINT # 3592	I= 6.802	STD DEV= .067	AT 3574.4 SECS.

4/5/83
Run #2

NWC TP 6525

GENERAL DATA OUTPUT FROM AD_RLTIME PROGRAM

OPERATOR: R.LODA DATE: 4/5/83 TIME: 16:30:22
SAMPLE: ANTHRACENE-N2-AIR RUN NUMBER: 3
OVL TEMP: 159 D CELL TEMP: 155 F CELL TEMP: 164
FLOWMETER-F GAS: NITROGEN FLOWMETER-G GAS: LAB AIR
STARTING FLOWRATE-F: 1CM STARTING FLOWRATE-G: 0CM
20 SAMPLES AVERAGED OVER (APPROX) 1 SEC. FOR (APPROX) 3600 TOTAL SECONDS.
GRAPH LABEL: ANTHRACENE-N2-AIR RUN #3 159C 155C 164C
COMMENTS: 75MM LENS-EM-0160 IRIS-EX

EXCITATION CONDITIONS

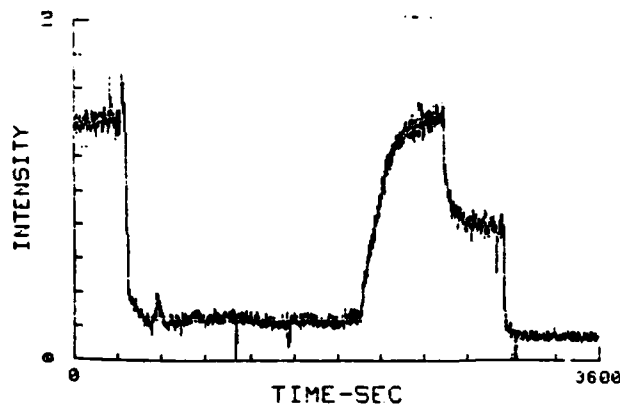
SOURCE: EXCIMER LASER
WAVELENGTH: 308NM BANDWIDTH: 1NM DYE: NONE
58.333333333 MJ/PULSE AT 24HZ IS 1.4 WATTS.

EMISSION CONDITIONS

MONOCHROMATOR TYPE: SPEX .85M ~~0.233nm~~
WAVELENGTH: 390NM BANDWIDTH: ~~0nm~~ SLITS: 1MM

DETECTION ELECTRONICS

PMT: RCA C31034 SAMPLE-HV: -1650 REFERENCE-HV: -850
PROCESSING INSTRUMENT: DSA-1
GATE TIME: .1MSEC. AP.DELAY: 0MSEC. SMPL TIME CNST: 1SEC. REF TIME CNST: .3SEC
SENSITIVITY OR GAIN - SAMPLE: 30 REFERENCE: 10



ANTHRACENE-N2-AIR RUN #3 159C 155C 164C 16:30:22 4/5/83

NWC TP 6525

FLOW TO 1.6CM-40ML/MIN

FLOW CHANGE AT POINT # 238

FLOW N2=0,AIR=1.3CM-40ML/MIN

NOTE TIME DELAY TO PT 420 OR SO FOR AIR QUENCH-TUBING VOLUME&FLOW RATE?

FLOW CHANGE AT POINT # 592

PROBLEMS WITH SETTING FLOW RATE-PRESSURE FLUCTUATIONS

FLOW CHANGE AT POINT # 713

PROBLEMS WITH SETTING FLOW RATE-PRESSURE FLUCTUATIONS

FLOW CHANGE AT POINT # 811

PROBLEMS WITH SETTING FLOW RATE-PRESSURE FLUCTUATIONS

FLOW CHANGE AT POINT # 1100

RTL BLOCKING BEAM TO SAMPLE

FLOW CHANGE AT POINT # 1479

PROBLEMS WITH SETTING FLOW RATE-PRESSURE FLUCTUATIONS

FLOW CHANGE AT POINT # 1842

FLOW N2=1CM-40ML/MIN,AIR=0

NOTE TIME DELAY TO PT 1980 OR SO FOR AIR QUENCH-TUBING VOLUME&FLOW RATE?

FLOW CHANGE AT POINT # 2543

FLOW N2=3.6CM-80ML/MIN,AIR=0

FLOW CHANGE AT POINT # 2903

FLOW N2=0,AIR=4.4CM-80ML/MIN

NOTE TIME DELAY TO PT 2966 OR SO FOR AIR QUENCH-TUBING VOLUME&FLOW RATE?

FLOW CHANGE AT POINT # 3033

RTL BLOCKING BEAM TO SAMPLE

LASER POWER AT IN AT END OF EXPERIMENT

POINT # 38	I= 6.974	STD DEV= .174	AT 37.6 SECS.
POINT # 45	I= 6.669	STD DEV= .163	AT 44.5 SECS.
POINT # 63	I= 6.939	STD DEV= .069	AT 62.6 SECS.
POINT # 106	I= 6.901	STD DEV= .098	AT 105.5 SECS.
POINT # 170	I= 6.920	STD DEV= .122	AT 169.3 SECS.
POINT # 234	I= 7.074	STD DEV= .095	AT 233.0 SECS.
POINT # 238	I= 6.856	STD DEV= .122	AT 237.0 SECS.
POINT # 268	I= 6.995	STD DEV= .104	AT 267.0 SECS.
POINT # 278	I= 7.152	STD DEV= .106	AT 276.9 SECS.
POINT # 296	I= 6.647	STD DEV= .054	AT 284.9 SECS.
POINT # 293	I= 6.827	STD DEV= .055	AT 291.8 SECS.
POINT # 302	I= 6.914	STD DEV= .049	AT 300.8 SECS.
POINT # 308	I= 7.074	STD DEV= .056	AT 306.7 SECS.
POINT # 322	I= 6.918	STD DEV= .161	AT 320.7 SECS.
POINT # 332	I= 7.855	STD DEV= .072	AT 330.6 SECS.
POINT # 337	I= 8.235	STD DEV= .086	AT 335.6 SECS.
POINT # 344	I= 7.365	STD DEV= .091	AT 342.5 SECS.
POINT # 353	I= 7.506	STD DEV= .134	AT 351.5 SECS.
POINT # 362	I= 6.216	STD DEV= .146	AT 360.4 SECS.
POINT # 369	I= 3.520	STD DEV= .071	AT 367.4 SECS.
POINT # 372	I= 2.859	STD DEV= .071	AT 370.4 SECS.
POINT # 377	I= 2.013	STD DEV= .058	AT 375.4 SECS.
POINT # 383	I= 1.828	STD DEV= .078	AT 381.3 SECS.
POINT # 390	I= 1.718	STD DEV= .036	AT 388.3 SECS.
POINT # 403	I= 1.701	STD DEV= .081	AT 401.2 SECS.
POINT # 410	I= 1.708	STD DEV= .123	AT 408.2 SECS.
POINT # 419	I= 1.627	STD DEV= .038	AT 417.1 SECS.
POINT # 422	I= 1.554	STD DEV= .123	AT 430.1 SECS.

4/5/83
Run #3

Note
N₂ → air,
get delayed
response might
equivalent to
volume of system
equivalent.

NWC TP 6525

POINT # 608	I- 1.301	STD DEV- .040	AT 607.0 SECS.
POINT # 659	I- 1.227	STD DEV- .080	AT 658.5 SECS.
POINT # 691	I- .994	STD DEV- .040	AT 690.4 SECS.
POINT # 732	I- .963	STD DEV- .031	AT 731.4 SECS.
POINT # 785	I- 1.241	STD DEV- .030	AT 784.1 SECS.
POINT # 842	I- 1.306	STD DEV- .077	AT 841.0 SECS.
POINT # 867	I- 1.367	STD DEV- .054	AT 865.9 SECS.
POINT # 1045	I- 1.435	STD DEV- .037	AT 1043.2 SECS.
POINT # 1195	I- 1.344	STD DEV- .093	AT 1193.1 SECS.
POINT # 1287	I- 1.156	STD DEV- .054	AT 1284.6 SECS.
POINT # 1364	I- 1.140	STD DEV- .083	AT 1361.2 SECS.
POINT # 1440	I- 1.105	STD DEV- .035	AT 1436.8 SECS.
POINT # 1512	I- 1.137	STD DEV- .058	AT 1508.7 SECS.
POINT # 1582	I- 1.234	STD DEV- .046	AT 1578.3 SECS.
POINT # 1675	I- 1.099	STD DEV- .052	AT 1670.8 SECS.
POINT # 1835	I- 1.300	STD DEV- .043	AT 1830.4 SECS.
POINT # 1840	I- 1.176	STD DEV- .024	AT 1835.4 SECS.
POINT # 1842	I- 1.222	STD DEV- .090	AT 1837.4 SECS.
POINT # 1886	I- 1.436	STD DEV- .037	AT 1881.7 SECS.
POINT # 1895	I- 1.319	STD DEV- .058	AT 1890.6 SECS.
POINT # 1905	I- 1.443	STD DEV- .088	AT 1900.6 SECS.
POINT # 1921	I- 1.260	STD DEV- .046	AT 1916.6 SECS.
POINT # 1936	I- 1.421	STD DEV- .056	AT 1931.6 SECS.
POINT # 1951	I- 1.352	STD DEV- .028	AT 1946.5 SECS.
POINT # 1965	I- 1.300	STD DEV- .046	AT 1960.4 SECS.
POINT # 1985	I- 2.341	STD DEV- .045	AT 1980.3 SECS.
POINT # 1996	I- 2.580	STD DEV- .095	AT 1991.5 SECS.
POINT # 2011	I- 2.583	STD DEV- .041	AT 2006.4 SECS.
POINT # 2026	I- 3.309	STD DEV- .133	AT 2021.3 SECS.
POINT # 2058	I- 3.684	STD DEV- .070	AT 2053.2 SECS.
POINT # 2143	I- 5.604	STD DEV- .091	AT 2137.7 SECS.
POINT # 2281	I- 6.845	STD DEV- .151	AT 2274.9 SECS.
POINT # 2388	I- 7.120	STD DEV- .077	AT 2381.3 SECS.
POINT # 2470	I- 7.103	STD DEV- .091	AT 2462.9 SECS.
POINT # 2527	I- 7.221	STD DEV- .063	AT 2519.7 SECS.
POINT # 2568	I- 5.146	STD DEV- .068	AT 2560.8 SECS.
POINT # 2624	I- 4.324	STD DEV- .084	AT 2616.5 SECS.
POINT # 2704	I- 3.948	STD DEV- .092	AT 2636.3 SECS.
POINT # 2783	I- 4.041	STD DEV- .044	AT 2774.8 SECS.
POINT # 2846	I- 3.639	STD DEV- .039	AT 2837.5 SECS.
POINT # 2885	I- 3.773	STD DEV- .064	AT 2876.3 SECS.
POINT # 2902	I- 4.017	STD DEV- .111	AT 2893.2 SECS.
POINT # 2903	I- 3.766	STD DEV- .113	AT 2894.3 SECS.
POINT # 2948	I- 4.176	STD DEV- .123	AT 2939.1 SECS.
POINT # 2974	I- 1.093	STD DEV- .035	AT 2965.5 SECS.
POINT # 2988	I- .961	STD DEV- .032	AT 2979.5 SECS.
POINT # 3017	I- .773	STD DEV- .038	AT 3008.3 SECS.
POINT # 3043	I- .625	STD DEV- .051	AT 3034.5 SECS.
POINT # 3070	I- .768	STD DEV- .049	AT 3061.4 SECS.
POINT # 3107	I- .739	STD DEV- .023	AT 3098.2 SECS.
POINT # 3140	I- .656	STD DEV- .034	AT 3131.0 SECS.
POINT # 3171	I- .613	STD DEV- .045	AT 3161.8 SECS.
POINT # 3385	I- .924	STD DEV- .022	AT 3374.7 SECS.
POINT # 3600	I- .768	STD DEV- .016	AT 3588.5 SECS.
POINT # 3579	I- .769	STD DEV- .067	AT 3567.6 SECS.
POINT # 3600	I- .768	STD DEV- .018	AT 3588.5 SECS.

*N₂ flow change
near immediate
response, but
that is flow rate
change*

*N₂ - air change
flow rate
constant so
delay is volume
of tubing that
gas needs to go
thru before
it gets to
fluorescence
cell.*

*4/5/83
Run #3*

NWC TP 6525

Appendix B

SPEX DATAMATE SPECIFICATIONS

FLUOROLOG[®] 2

SPECIFICATIONS

DATA PROCESSING AND STORAGE — SPEX DATAMATE

The FLUOROLOG comes standard with the DATAMATE (DM1) scan controller/data processor equipped with options: DM105-data storage/graphics/processing/radiometric correction; DM102-PC acquisition module; DM103-DC acquisition module; 4 DM101-input channels; DM104-second High voltage supply; and 1457B-coupled y-t recorder or DM112 plotter. For complete details and specifications refer to the DATAMATE brochure.

SELF-DIAGNOSTICS AND OPERATIONAL ERROR CHECK

- A Power on initiates primary hardware check. Error codes are displayed on keyboard LED for indication even in event of CRT failure.
- B Internal logic test and software test with errors displayed on CRT.
- C Continuous monitor of all keyboard operations for compatibility with hardware and software demands previously made. Errors displayed in STATUS field.

SPECTROMETER CONTROL

Scans excitation and/or emission spectrometers with 0.02 nm step resolution. Manual control through forward/reverse toggle switches.

A Scan Modes

- 1 Continuous
- 2 Burst 1 — dependent on integration time and increment.
- 3 Burst 2 — requires trigger for move to next increment.
- 4 Burst 3 — requires trigger to initiate integration.
- 5 Burst 4 — requires triggers to initiate integration and movement.
- 6 Set — slews to chosen position and halts.

B Multiple Group Scanning

- 1 1-4 groups with independent start, stop, integration and increment (or speed).
- 2 1-999 scans.

DATA ACQUISITION

Four inputs are available: Two chopped photon counting (S1, S2); two chopped direct current (R1, R2).

A Mainframe Data Input

Integration times	0.1 to 600 sec.
Integration time accuracy	0.01%
Data word length	24 bit mantissa, 8 bits for exponent and sign
Data word max. significant digits	8
Max. counts data point	$\pm 10^{10}$ (bipolar)
Max Count Rate (DM101)	25 MHz

B Data Acquisition Modes

Signals can be acquired and combined in real time according to the modes listed below.

S1	K(S1 - S2)
R1	S1/R1
S1/S2	K(S1/R1) - (S2/R2)
S2	(S1/R1)/(R2/S2)
R2	S1 and S2
S2/R2	S1/R1 and S2/R2

Where K is a selectable constant

DATA STORAGE, GRAPHICS, RADIOMETRIC CORRECTION PROCESSING

A Data Memory

4000 words RAM, 32 bits
Floating-point formatted
Word length: 24-bit mantissa, 8-bit exponent and sign
Precision: 1 part in 16,000,000
8 significant digits, maximum
Maximum value $10 \exp. 18$
Variable-length files, 8 maximum

B Processing

Normalizations
Arithmetic Combinations of Spectra: +, -, x, /
Radiometric Correction Program
Weighted Smoothing (Savitsky-Golay—5, 9, 13, 17, 21 points)
Derivatives (first and second; weighted)
Indefinite Integrals
Definite Integrals and Peak Areas
Log/Antilogs
Shifts of Spectral Axes
Point-by-point insertion or Modification of Spectra

C Graphic Display

Annotated display of any 2 files simultaneously, one file intensified
Real-time display of data acquisition
Labeled axes with scales
File labels maximum 40 characters each file
Files displayed need not coincide (X-axis)
Spectra can be shifted during display
Two independent cursors with coordinates displayed
Vertical/horizontal expand or contract between cursors
Output to recorder of data between cursors

D Multitasking

Simultaneous Data Input
Data Processing
Data Output

E Radiometric Correction

Two spectral curves can be stored and retained on power off for baseline flattening or radiometric correction. Optional calibrated lamps are available from SPEX for generation of correction factors.
Calibration curve can be entered point by point, by scan, or by processing.
250 calibration points maximum.
Automatic interpolation between points
Correction can be in real time or on stored data

ACCESSORIES

A full line of accessories are available for data storage, processing and output

DM110/11	Single/dual disk for data storage
DM106	Data memory expansion to 16000 points
DM107	RS232 interface

DM109	CRT video copier
DM112/113	Alphanumeric digital plotter 8 1/2 x 11 or 17
1457B	Coupled y-t recorder

NWC TP 6525

Appendix C
DIFFUSION RATE PROGRAM

```

10  ! PROGRAM "DIFF_RATE". R LODA 4/7/83
20  !MODIFIED FOR ADDITIONAL OUTPUT 2/2/84
30  !MODIFIED 1/31/84 FOR NEW PPM CALC AND MG/CU-M OUTPUT
40  !SEE HANDBK ENVIR. DATA ON ORG. CHEM. ED. BY KAPEL VERSCHUEREN
50  !VAN NOSTRAND REINHOLD CO. 1983 PG 41 FOR FORMULAE PPM BY VOLUME
60  !AND MASS IN MG/CU-M (CONC.)
70  INPUT "ENTER MOLECULAR WEIGHT OF GAS,SOLID(G/MOLE)".M1,M2
80  INPUT "ENTER HARD SPHERE COLLISION DIAMETER(ANGSTROMS)".D12
90  D12=D12*1.E-8
100 INPUT "ENTER SOLID TEMPERATURE IN DEGREES C".Tc
110 Tk=Tc+273.1
120 P=9.33E+5 !700TORR ATMOSPHERIC PRESSURE AT NWC IN DYNES*CM-2
130 Pressure=700
140 A=3/(8*SQR(2*PI))*6.023E+23)
150 PRINT
160 PRINT "      OUTPUT FROM DIFF_RATE PROGRAM WITH P =","Pressure," TORR"
170 PRINT
180 PRINT "A= ",A
190 B=((8.3144761E+7*Tk)-1.5)/P
200 PRINT "B= ",B
210 C=SQR((M1+M2)/(M1*M2))/(D12 2)
220 PRINT "C= ",C
230 D=A*B*C
240 PRINT "DIFFUSION COEFFICIENT= ".D,"CM+2/SEC-MOLECULE"
250 PRINT "FOR T= ".Tc,"C. COLLISION DIAMETER= ".D12*1.E+8,"ANGSTROMS"
260 PRINT "AND M1= ".M1,"G/MOLE, M2= ".M2,"G/MOLE"
270 L=11.5 !DIFF LENGTH FOR OUR SYSTEM IN CM
280 Tim_ss=(L 2)/(D*D)
290 PRINT "TIME FOR STEADY STATE= ".Tim_ss,"SECONDS"
300 !Area=.196 !CM+2 FOR 5MM TUBING
310 !Area=.126 !CM+2 FOR 4MM TUBING
320 !Area=.159 !CM+2 FOR 4.5MM TUBING AVE OF 4&5 LENGTHS
330 PRINT "DIFF. LENGTH = ".L,"CM. CROSS SEC. AREA =".Area," CM2"
340 R=(D*Area*M2*700)/(760*.0820575*Tk*L)
350 INPUT "ENTER VAPOR PRESSURE OF SOLID IN TORR".Vap_pres
360 R1=LOG(700/(700-Vap_pres))
370 Dif_rate=R*R1*1.E-3
380 PRINT "DIFFUSION RATE= ".Dif_rate,"G/SEC AT ".Vap_pres,"TORR OF SOLID"
390 INPUT "ENTER FLUORESCENCE CELL TEMPERATURE (DEGREES C)".Tfcc
400 PRINT "FLUORESCENCE CELL TEMPERATURE IS ".Tfcc," DEGREES C"
410 PRINT
420 Tfck=Tfcc+273.1
430 INPUT "ENTER FLOWRATE OF GAS IN ML/MIN".Gas_flowm
440 Gas_flows=Gas_flowm/60
450 Conc=(Dif_rate/Gas_flows)*1.E+9
460 PRINT "CONCENTRATION= ".Conc,"MG/CU-M AT ".Gas_flowm," ML/MIN"
470 !
480 !PPM=(W*1E+3/V*1E-3)*(R*T/P*M*1E+06)FROM REF. W/V IN MG/CU-M!
490 !
500 Ppm=(760*.0820575*Tfck*Conc)/(700*M2)
510 Con_fact=Conc/Ppm
520 PRINT "THIS IS ".Con_fact," MG/CU-M = 1 PPM AT THIS T.P. AND M2"
530 PRINT "THE CONCENTRATION IS ".Conc," MG/CU-M. OR ".Ppm," PPM"
540 PRINT "FOR THE ABOVE SET OF CONDITIONS"
550 PRINT
560 GOTO 430
570 END

```

NWC TP 6525

OUTPUT FROM DIFF_LASL PROGRAM WITH P - 585 TORR

A= 2.48386775943E-25
 B= 6.05649789236E+9
 C= 1.35212433269E+14
 DIFFUSION COEFFICIENT= .203407362808 CM+2/SEC-MOLECULE
 FOR T= 65.5 C. COLLISION DIAMETER= 3.9 ANGSTROMS
 AND M1= 29 G/MOLE, M2= 128 G/MOLE
 TIME FOR STEADY STATE= 325.086560719 SECONDS
 DIFF. LENGTH = 11.5 CM. CROSS SEC. AREA = .126 CM2
 DIFFUSION RATE= 3.69665135774E-8 G/SEC AT 2.73 TORR OF SOLID
 FLUORESCENCE CELL TEMPERATURE IS 65.5 DEGREES C

CONCENTRATION= 55.449770366 MG/CU-M AT 40 ML/MIN
 THIS IS 3.54606758196 MG/CU-M = 1 PPM AT THIS T.P. AND M2
 THE CONCENTRATION IS 55.449770366 MG/CU-M, OR
 15.6369750673 PPM
 FOR THE ABOVE SET OF CONDITIONS

CONCENTRATION= 18.4832567887 MG/CU-M AT 120 ML/MIN
 THIS IS 3.54606758196 MG/CU-M = 1 PPM AT THIS T.P. AND M2
 THE CONCENTRATION IS 18.4832567887 MG/CU-M, OR
 5.21232502243 PPM
 FOR THE ABOVE SET OF CONDITIONS

CONCENTRATION= 13.8624425915 MG/CU-M AT 160 ML/MIN
 THIS IS 3.54606758196 MG/CU-M = 1 PPM AT THIS T.P. AND M2
 THE CONCENTRATION IS 13.8624425915 MG/CU-M, OR
 3.90924376632 PPM
 FOR THE ABOVE SET OF CONDITIONS

CONCENTRATION= 8.21478079497 MG/CU-M AT 270 ML/MIN
 THIS IS 3.54606758196 MG/CU-M = 1 PPM AT THIS T.P. AND M2
 THE CONCENTRATION IS 8.21478079497 MG/CU-M, OR
 2.31658889886 PPM
 FOR THE ABOVE SET OF CONDITIONS

CONCENTRATION= 6.93122129575 MG/CU-M AT 320 ML/MIN
 THIS IS 3.54606758196 MG/CU-M = 1 PPM AT THIS T.P. AND M2
 THE CONCENTRATION IS 6.93122129575 MG/CU-M, OR
 1.95462188341 PPM
 FOR THE ABOVE SET OF CONDITIONS

OUTPUT FROM DIFF_LASL PROGRAM WITH P - 492 TORR

A= 2.48386775943E-25
 B= 7.20131864649E+9
 C= 1.35212433269E+14
 DIFFUSION COEFFICIENT= .241856145359 CM+2/SEC-MOLECULE
 FOR T= 65.5 C. COLLISION DIAMETER= 3.9 ANGSTROMS
 AND M1= 29 G/MOLE, M2= 128 G/MOLE
 TIME FOR STEADY STATE= 273.406325491 SECONDS
 DIFF. LENGTH = 11.5 CM. CROSS SEC. AREA = .126 CM2
 DIFFUSION RATE= 4.39735287896E-8 G/SEC AT 2.73 TORR OF SOLID
 FLUORESCENCE CELL TEMPERATURE IS 65.5 DEGREES C

CONCENTRATION= 32.9801465922 MG/CU-M AT 80 ML/MIN
 THIS IS 2.98233376124 MG/CU-M = 1 PPM AT THIS T.P. AND M2
 THE CONCENTRATION IS 32.9801465922 MG/CU-M, OR
 11.058502915 PPM
 FOR THE ABOVE SET OF CONDITIONS

NWC TP 6525

OUTPUT FROM DIFF_RATE PROGRAM WITH P = 700 TORR

A= 2.48386775943E-25
 B= 7.29872649457E+9
 C= 7.69517242317E+13
 DIFFUSION COEFFICIENT= .139506330485 CM²/SEC-MOLECULE
 FOR T= 159 C, COLLISION DIAMETER= 5.14 ANGSTROMS
 AND M1= 28 G/MOLE. M2= 178 G/MOLE
 TIME FOR STEADY STATE= 473.992827207 SECONDS
 DIFF. LENGTH = 11.5 CM, CROSS SEC. AREA = .126 CM²
 DIFFUSION RATE= 2.27536938515E-8 G/SEC AT 2.25 TORR OF SOLID
 FLUORESCENCE CELL TEMPERATURE IS 164 DEGREES C

CONCENTRATION= 34.1305407772 MG/CU-M AT 40 ML/MIN
 THIS IS 4.57093833206 MG/CU-M = 1 PPM AT THIS T.P. AND M2
 THE CONCENTRATION IS 34.1305407772 MG/CU-M, OR
 7.46685653952 PPM
 FOR THE ABOVE SET OF CONDITIONS

CONCENTRATION= 17.0652703886 MG/CU-M AT 80 ML/MIN
 THIS IS 4.57093833206 MG/CU-M = 1 PPM AT THIS T.P. AND M2
 THE CONCENTRATION IS 17.0652703886 MG/CU-M, OR
 3.73342826984 PPM
 FOR THE ABOVE SET OF CONDITIONS

CONCENTRATION= 11.3768469257 MG/CU-M AT 120 ML/MIN
 THIS IS 4.57093833206 MG/CU-M = 1 PPM AT THIS T.P. AND M2
 THE CONCENTRATION IS 11.3768469257 MG/CU-M, OR
 2.4889527989 PPM
 FOR THE ABOVE SET OF CONDITIONS

CONCENTRATION= 8.5326351943 MG/CU-M AT 160 ML/MIN
 THIS IS 4.57093833206 MG/CU-M = 1 PPM AT THIS T.P. AND M2
 THE CONCENTRATION IS 8.5326351943 MG/CU-M, OR
 1.86671413492 PPM
 FOR THE ABOVE SET OF CONDITIONS

CONCENTRATION= 6.82610815544 MG/CU-M AT 200 ML/MIN
 THIS IS 4.57093833206 MG/CU-M = 1 PPM AT THIS T.P. AND M2
 THE CONCENTRATION IS 6.82610815544 MG/CU-M, OR
 1.49337130794 PPM
 FOR THE ABOVE SET OF CONDITIONS

CONCENTRATION= 4.55073877029 MG/CU-M AT 300 ML/MIN
 THIS IS 4.57093833206 MG/CU-M = 1 PPM AT THIS T.P. AND M2
 THE CONCENTRATION IS 4.55073877029 MG/CU-M, OR
 .995580871958 PPM
 FOR THE ABOVE SET OF CONDITIONS

Air

OUTPUT FROM DIFF_RATE PROGRAM WITH P =

700

TORR

A= 2.48386775943E-25
 B= 7.29872649457E+9
 C= 7.57966365927E+13
 DIFFUSION COEFFICIENT= .137412263854 CM+2/SEC-MOLECULE
 FOR T= 159 C. COLLISION DIAMETER= 5.14 ANGSTROMS
 AND M1= 29 G/MOLE, M2= 178 G/MOLE
 TIME FOR STEADY STATE= 481.216145817 SECONDS
 DIFF. LENGTH = 11.5 CM. CROSS SEC. AREA = .126 CM2
 DIFFUSION RATE= 2.24121484115E-3 G/SEC AT 2.25 TORR OF SOLID
 FLUORESCENCE CELL TEMPERATURE IS 164 DEGREES C

CONCENTRATION= 33.6182226172 MG/CU-M AT 40 ML/MIN
 THIS IS 4.57093833206 MG/CU-M = 1 PPM AT THIS T.P. AND M2
 THE CONCENTRATION IS 33.6182226172 MG/CU-M, OR
 7.35477492257 PPM
 FOR THE ABOVE SET OF CONDITIONS

CONCENTRATION= 16.8091113086 MG/CU-M AT 30 ML/MIN
 THIS IS 4.57093833206 MG/CU-M = 1 PPM AT THIS T.P. AND M2
 THE CONCENTRATION IS 16.8091113086 MG/CU-M, OR
 3.67738746129 PPM
 FOR THE ABOVE SET OF CONDITIONS

NWC TP 6525

OUTPUT FROM DIFF_RATE PROGRAM WITH P = 700 TORR

A= 2.48386775943E-25
 B= 5.06292064969E+9
 C= 1.35212433269E+14

DIFFUSION COEFFICIENT= .17003809062 CM²/SEC-MOLECULE
 FOR T= 65.5 C. COLLISION DIAMETER= 3.9 ANGSTROMS
 AND M1= 29 G/MOLE, M2= 128 G/MOLE
 TIME FOR STEADY STATE= 388.883454049 SECONDS
 DIFF. LENGTH = 11.5 CM, CROSS SEC. AREA = .126 CM²
 DIFFUSION RATE= 3.08902175695E-8 G/SEC AT 2.73 TORR OF SOLID
 FLUORESCENCE CELL TEMPERATURE IS 65.5 DEGREES C

CONCENTRATION= 23.1676631771 MG/CU-M AT 80 ML/MIN
 THIS IS 4.24315779038 MG/CU-M = 1 PPM AT THIS T.P. AND M2
 THE CONCENTRATION IS 23.1676631771 MG/CU-M, OR
 5.46000510037 PPM
 FOR THE ABOVE SET OF CONDITIONS

OUTPUT FROM DIFF_SEA PROGRAM WITH P = 760 TORR

A= 2.48386775943E-25
 B= 4.66193433621E+9
 C= 1.35212433269E+14

DIFFUSION COEFFICIENT= .156570973154 CM²/SEC-MOLECULE
 FOR T= 65.5 C. COLLISION DIAMETER= 3.9 ANGSTROMS
 AND M1= 29 G/MOLE, M2= 128 G/MOLE
 TIME FOR STEADY STATE= 422.332432813 SECONDS
 DIFF. LENGTH = 11.5 CM, CROSS SEC. AREA = .126 CM²
 DIFFUSION RATE= 2.84392018378E-8 G/SEC AT 2.73 TORR OF SOLID
 FLUORESCENCE CELL TEMPERATURE IS 65.5 DEGREES C

CONCENTRATION= 21.3294763784 MG/CU-M AT 80 ML/MIN
 THIS IS 4.60685702956 MG/CU-M = 1 PPM AT THIS T.P. AND M2
 THE CONCENTRATION IS 21.3294763784 MG/CU-M, OR
 4.62994102954 PPM
 FOR THE ABOVE SET OF CONDITIONS

OUTPUT FROM DIFF_LASL PROGRAM WITH P = 585 TORR

A= 2.48386775943E-25
 B= 6.05649789236E+9
 C= 1.35212433269E+14

DIFFUSION COEFFICIENT= .203407362808 CM²/SEC-MOLECULE
 FOR T= 65.5 C. COLLISION DIAMETER= 3.9 ANGSTROMS
 AND M1= 29 G/MOLE, M2= 128 G/MOLE
 TIME FOR STEADY STATE= 325.086560719 SECONDS
 DIFF. LENGTH = 11.5 CM, CROSS SEC. AREA = .126 CM²
 DIFFUSION RATE= 3.69665135774E-8 G/SEC AT 2.73 TORR OF SOLID
 FLUORESCENCE CELL TEMPERATURE IS 65.5 DEGREES C

CONCENTRATION= 27.724885183 MG/CU-M AT 80 ML/MIN
 THIS IS 3.54606758196 MG/CU-M = 1 PPM AT THIS T.P. AND M2
 THE CONCENTRATION IS 27.724885183 MG/CU-M, OR
 7.81848753364 PPM
 FOR THE ABOVE SET OF CONDITIONS

NWC TP 6525

Appendix D

SPEX DIFFUSION RATE PROGRAM

NWC TP 6525

1) 29 TO R0	M1 GAS G/MOLE
2) 128 TO R1	M2 SOLID G/MOLE
3) 3.9 TO R2	HARD SPHERE DIA-A
4) 7.7994E+05 TO R3 LASL(585 TORR)	ATM PRESSURE-DYNES/CM ²
5) 338.6 TO R4	TEMPERATURE-K
6) .126 TO R5	DIFF CELL AREA-CM ²
7) 11.5 TO R6	DIFF TUBE LENGTH-CM
8) 2.73 TO R7	VAP PRESSURE-TORR
9) 80 TO R8	FLOW RATE-ML MIN
10) 2 * 3.14159 TO R9	
11) SQT R9 TO R9	
12) 8 * R9 TO R9	
13) 6.023 * R9 TO R9	
14) 3 / R9 TO R9	
15) 8.715E07 * R4 TO RA	R IN (DYNE-CM)/(MOLE-K)
16) SQT RA TO RB	
17) RA * RB TO RB	
18) RB / RC TO RA	
19) R0 * R1 TO RB	
20) R0 + R1 TO RC	
21) RC / RB TO RB	
22) SQT RB TO RB	
23) R2 * R2 TO RC	
24) RB / RC TO RB	
25) R9 * RA TO RC	
26) RC * RB TO RC	
27) 1E-07 * RC TO RC	DIFF COEF-CM ² /(SEC-MOLECULE)
28) R6 * R6 TO RD	
29) RD / 2 TO RD	
30) RD / RC TO RD	STEADY STATE TIME-SEC
31) RC * R5 TO RE	
32) RE * R1 TO RE	
33) 585 * RE TO RE	
34) RE / 760 TO RE	
35) RE / .08205 TO RE	
36) RE / R4 TO RE	
37) RE / R6 TO RE	
38) 585 - R7 TO RF	
39) 1 / RF TO RF	
40) 585 * RF TO RF	
41) LOG RF TO RF	
42) 2.303 * RF TO RF	

NWC TP 6525

```

43) RE * RF TO RE          DIFF RATE-MG/SEC
44) RS / 60 TO RF
45) RE / RF TO RF
46) 1E+06 * RF TO RF      CONC-MG/M3
    
```

Execution of this program, which is set up for naphthalene, in air, at LASL altitude, at 338.6°K (vapor pressure of 2.73 torr), 46.47, and using a collision diameter of 3.9 Angstroms, gives 27.7 mg/m³ (register RF) with a flow rate of 80 ml/min.

To convert the mg/m³ values to ppm by volume, in air, one can take the value of register RF and substitute it into the following equation, which is derived from the ideal gas law:

$$\text{ppm} = \frac{W(g) \cdot 10^3 (\text{mg/g})}{V(l) \cdot 10^{-3} (\text{m}^3/l)} \cdot \frac{RT}{P M_2 \cdot 10^6} \quad (D.1)$$

where:

W/V = Register RF value in mg/m³
R = 0.08205 (l-atm)/(mole-°K)
T = Temperature in °K
P = Pressure in atmospheres (0.647 at LASL)
M₂ = Molecular Weight of PAH in g/mole

Substitution of the 27.7 mg/m³ value into equation D.1 gives a concentration of 7.82 ppm by volume.

To convert the above program for use at other altitudes (i.e. sea level, or NWC level), statements number 4, 33, 38, and 40 must be adjusted to reflect the proper atmospheric pressure. Also, four conversion factor tables, generated using equation D.1, are given below. They list the number of mg/m³ equal to 1 ppm as a function of temperature, for the range of PAH molecular weights listed in Table I (INTRODUCTION). Values are calculated for atmospheric pressures of 760, 700, 585 and 492 torr, which would correspond to the values at sea level, the NWC, China Lake, CA, and the LASL. These tables can be used with the Spec Diffusion Rate Program output when ppm values are required. It should be noted that at a given temperature and pressure, the values span approximately a factor of two, as do the molecular weights (128-252 g/mole). At a given temperature and molecular weight, the conversion factors differ by the ratio of the pressures. Because of these dependencies, it is probably best to quote the concentrations in mg/m³ rather than ppm.

CONVERSION FACTORS FOR F= 492
 1PPM = X MG/CU-M FROM TABLE

TORR

T (C)	C10H8	C11H10	C14H10	C16H10	C18H12	C20H12
20.000	3.447	3.824	4.793	5.439	6.140	6.786
25.000	3.389	3.760	4.713	5.348	6.037	6.672
30.000	3.333	3.698	4.635	5.260	5.937	6.562
35.000	3.279	3.638	4.560	5.175	5.841	6.455
40.000	3.227	3.579	4.487	5.092	5.747	6.352
45.000	3.176	3.523	4.416	5.012	5.657	6.252
50.000	3.127	3.469	4.348	4.934	5.569	6.156
55.000	3.079	3.416	4.282	4.859	5.484	6.062
60.000	3.033	3.364	4.217	4.786	5.402	5.971
65.000	2.988	3.315	4.155	4.715	5.322	5.882
70.000	2.944	3.266	4.094	4.647	5.245	5.797
75.000	2.902	3.219	4.036	4.580	5.169	5.713
80.000	2.861	3.174	3.978	4.515	5.096	5.632
85.000	2.821	3.130	3.923	4.452	5.025	5.554
90.000	2.782	3.086	3.869	4.391	4.956	5.477
95.000	2.744	3.044	3.816	4.331	4.888	5.403
100.000	2.708	3.004	3.765	4.273	4.823	5.330
105.000	2.672	2.964	3.715	4.216	4.759	5.260
110.000	2.637	2.925	3.667	4.161	4.697	5.191
115.000	2.603	2.888	3.620	4.108	4.636	5.124
120.000	2.570	2.851	3.574	4.055	4.577	5.059
125.000	2.537	2.815	3.529	4.004	4.520	4.996
130.000	2.506	2.780	3.485	3.955	4.464	4.934
135.000	2.475	2.746	3.442	3.906	4.409	4.873
140.000	2.445	2.713	3.401	3.859	4.356	4.814
145.000	2.416	2.680	3.360	3.813	4.304	4.757
150.000	2.387	2.649	3.320	3.768	4.253	4.700
155.000	2.360	2.618	3.281	3.724	4.203	4.645
160.000	2.332	2.587	3.243	3.681	4.155	4.592
165.000	2.306	2.558	3.206	3.639	4.107	4.539
170.000	2.280	2.529	3.170	3.598	4.061	4.488
175.000	2.254	2.501	3.135	3.558	4.015	4.438
180.000	2.229	2.473	3.100	3.518	3.971	4.389
185.000	2.205	2.446	3.066	3.480	3.928	4.341
190.000	2.181	2.420	3.033	3.442	3.885	4.294
195.000	2.158	2.394	3.001	3.405	3.844	4.248
200.000	2.135	2.369	2.969	3.369	3.803	4.204
205.000	2.113	2.344	2.938	3.334	3.763	4.160
210.000	2.091	2.320	2.908	3.300	3.724	4.116
215.000	2.069	2.296	2.878	3.266	3.686	4.074
220.000	2.048	2.273	2.849	3.233	3.649	4.033

NWC TP 6525

CONVERSION FACTORS FOR P= 585
1PPM = X MG/CU-M FROM TABLE

TORR

T (C)	C10H8	C11H10	C14H10	C16H10	C18H12	C20H12
20.000	4.098	4.547	5.699	6.468	7.300	8.069
25.000	4.030	4.470	5.604	6.359	7.178	7.933
30.000	3.963	4.397	5.511	6.254	7.059	7.802
35.000	3.899	4.325	5.422	6.153	6.945	7.676
40.000	3.836	4.256	5.335	6.054	6.834	7.553
45.000	3.776	4.189	5.251	5.959	6.726	7.434
50.000	3.718	4.124	5.170	5.867	6.622	7.319
55.000	3.661	4.061	5.091	5.778	6.521	7.208
60.000	3.606	4.000	5.015	5.691	6.423	7.099
65.000	3.553	3.941	4.940	5.607	6.328	6.994
70.000	3.501	3.884	4.868	5.525	6.236	6.892
75.000	3.451	3.828	4.798	5.445	6.146	6.793
80.000	3.402	3.774	4.731	5.368	6.059	6.697
85.000	3.354	3.721	4.664	5.293	5.975	6.604
90.000	3.308	3.670	4.600	5.220	5.892	6.513
95.000	3.263	3.620	4.538	5.150	5.812	6.424
100.000	3.219	3.571	4.477	5.080	5.734	6.338
105.000	3.177	3.524	4.418	5.013	5.659	6.254
110.000	3.135	3.478	4.360	4.948	5.585	6.173
115.000	3.095	3.433	4.304	4.884	5.513	6.093
120.000	3.055	3.390	4.249	4.822	5.443	6.015
125.000	3.017	3.347	4.196	4.761	5.374	5.940
130.000	2.980	3.306	4.144	4.702	5.308	5.866
135.000	2.943	3.265	4.093	4.645	5.242	5.794
140.000	2.908	3.226	4.043	4.588	5.179	5.724
145.000	2.873	3.187	3.995	4.534	5.117	5.656
150.000	2.839	3.149	3.948	4.480	5.057	5.589
155.000	2.806	3.112	3.902	4.428	4.998	5.524
160.000	2.773	3.077	3.857	4.377	4.940	5.460
165.000	2.742	3.041	3.812	4.327	4.883	5.397
170.000	2.711	3.007	3.769	4.278	4.828	5.337
175.000	2.680	2.974	3.727	4.230	4.774	5.277
180.000	2.651	2.941	3.686	4.183	4.722	5.219
185.000	2.622	2.909	3.646	4.138	4.670	5.162
190.000	2.594	2.877	3.607	4.093	4.620	5.106
195.000	2.566	2.846	3.568	4.049	4.570	5.051
200.000	2.539	2.816	3.530	4.006	4.522	4.998
205.000	2.512	2.787	3.493	3.964	4.475	4.946
210.000	2.486	2.758	3.457	3.923	4.428	4.895
215.000	2.461	2.730	3.422	3.883	4.383	4.844
220.000	2.436	2.702	3.387	3.844	4.339	4.795

NWC TP 6525

CONVERSION FACTORS FOR P= 700
1PPM = X MG/CU-M FROM TABLE

TORR

T (C)	C10H8	C11H10	C14H10	C16H10	C18H12	C20H12
20.000	4.904	5.440	6.820	7.739	8.735	9.655
25.000	4.822	5.349	6.705	7.609	8.589	9.493
30.000	4.742	5.261	6.595	7.484	8.447	9.336
35.000	4.665	5.175	6.487	7.362	8.310	9.185
40.000	4.591	5.093	6.384	7.245	8.177	9.038
45.000	4.518	5.013	6.283	7.131	8.048	8.896
50.000	4.448	4.935	6.186	7.020	7.924	8.758
55.000	4.381	4.860	6.092	6.913	7.803	8.624
60.000	4.315	4.787	6.000	6.809	7.686	8.495
65.000	4.251	4.716	5.912	6.709	7.572	8.369
70.000	4.189	4.647	5.825	6.611	7.462	8.247
75.000	4.129	4.581	5.742	6.516	7.355	8.129
80.000	4.070	4.516	5.660	6.424	7.250	8.014
85.000	4.014	4.453	5.581	6.334	7.149	7.902
90.000	3.958	4.391	5.505	6.247	7.051	7.793
95.000	3.905	4.332	5.430	6.162	6.955	7.687
100.000	3.852	4.274	5.357	6.079	6.862	7.584
105.000	3.801	4.217	5.286	5.999	6.771	7.484
110.000	3.752	4.162	5.217	5.921	6.683	7.386
115.000	3.703	4.108	5.150	5.844	6.596	7.291
120.000	3.656	4.056	5.084	5.770	6.513	7.198
125.000	3.610	4.005	5.020	5.697	6.431	7.108
130.000	3.565	3.955	4.958	5.627	6.351	7.019
135.000	3.522	3.907	4.897	5.558	6.273	6.933
140.000	3.479	3.860	4.838	5.490	6.197	6.849
145.000	3.437	3.813	4.780	5.425	6.123	6.768
150.000	3.397	3.768	4.724	5.361	6.051	6.688
155.000	3.357	3.724	4.669	5.298	5.980	6.609
160.000	3.318	3.681	4.615	5.237	5.911	6.533
165.000	3.281	3.639	4.562	5.177	5.843	6.459
170.000	3.243	3.598	4.510	5.119	5.777	6.386
175.000	3.207	3.558	4.460	5.061	5.713	6.314
180.000	3.172	3.519	4.411	5.006	5.650	6.245
185.000	3.137	3.480	4.363	4.951	5.588	6.176
190.000	3.103	3.443	4.316	4.898	5.528	6.110
195.000	3.070	3.406	4.270	4.845	5.469	6.045
200.000	3.038	3.370	4.224	4.794	5.411	5.981
205.000	3.006	3.335	4.180	4.744	5.354	5.918
210.000	2.975	3.300	4.137	4.695	5.299	5.857
215.000	2.944	3.266	4.095	4.647	5.245	5.797
220.000	2.915	3.233	4.053	4.599	5.192	5.738

NWC TP 6525

CONVERSION FACTORS FOR F= 760
1PPM = X MG/CU-M FROM TABLE

TORR

T (C)	C10H8	C11H10	C14H10	C16H10	C18H12	C20H12
20.000	5.324	5.907	7.404	8.402	9.484	10.482
25.000	5.235	5.808	7.280	8.261	9.325	10.306
30.000	5.149	5.712	7.160	8.125	9.171	10.136
35.000	5.065	5.619	7.044	7.993	9.022	9.972
40.000	4.984	5.529	6.931	7.866	8.878	9.812
45.000	4.906	5.442	6.822	7.742	8.738	9.658
50.000	4.830	5.358	6.716	7.622	8.603	9.509
55.000	4.756	5.276	6.614	7.506	8.472	9.364
60.000	4.685	5.197	6.515	7.393	8.345	9.223
65.000	4.615	5.120	6.418	7.284	8.221	9.087
70.000	4.548	5.046	6.325	7.178	8.101	8.954
75.000	4.483	4.973	6.234	7.074	7.985	8.826
80.000	4.419	4.903	6.146	6.974	7.872	8.701
85.000	4.358	4.834	6.060	6.877	7.762	8.579
90.000	4.298	4.768	5.976	6.782	7.655	8.461
95.000	4.239	4.703	5.895	6.690	7.551	8.346
100.000	4.182	4.640	5.816	6.600	7.450	8.234
105.000	4.127	4.578	5.739	6.513	7.351	8.125
110.000	4.073	4.519	5.664	6.428	7.255	8.019
115.000	4.021	4.460	5.591	6.345	7.162	7.916
120.000	3.970	4.404	5.520	6.264	7.071	7.815
125.000	3.920	4.348	5.451	6.186	6.982	7.717
130.000	3.871	4.294	5.383	6.109	6.895	7.621
135.000	3.824	4.242	5.317	6.034	6.811	7.528
140.000	3.777	4.190	5.253	5.961	6.728	7.437
145.000	3.732	4.140	5.190	5.890	6.648	7.348
150.000	3.688	4.091	5.129	5.820	6.569	7.261
155.000	3.645	4.044	5.069	5.752	6.493	7.176
160.000	3.603	3.997	5.010	5.686	6.418	7.093
165.000	3.562	3.951	4.953	5.621	6.344	7.012
170.000	3.521	3.907	4.897	5.557	6.273	6.933
175.000	3.482	3.863	4.842	5.495	6.203	6.856
180.000	3.444	3.820	4.789	5.435	6.134	6.780
185.000	3.406	3.779	4.737	5.375	6.067	6.706
190.000	3.369	3.738	4.686	5.317	6.002	6.633
195.000	3.333	3.698	4.635	5.260	5.938	6.563
200.000	3.298	3.659	4.586	5.205	5.875	6.493
205.000	3.264	3.621	4.539	5.150	5.813	6.425
210.000	3.230	3.583	4.492	5.097	5.753	6.359
215.000	3.197	3.546	4.446	5.045	5.694	6.294
220.000	3.164	3.510	4.400	4.994	5.636	6.230

NWC TP 6525

Appendix E

SPEX FLUORIMETER CORRESPONDENCE



April 19, 1983

Dr. James Short
Rural Route #1
Box 197
Switz City, Indiana 47465

Dr. Richard Loda
Naval Weapons Center
Mail Code 3851
China Lake, CA 93555

Dear Drs. Short and Loda:

I am sending each of you a copy of this letter and duplicate information packet concerning our FLUOROLOG 2 spectrofluorometers as the same instrument applies to each of you.

When looking at PAH gasses from burning flares, extreme sensitivity will be required due to the low molecular densities involved. You will note that with fluorescein 0.1 ppt is detectable even with our least expensive model 111C instrument with single monochromators, room temperature PMT and 150 watt Xe lamp. Even better minimum levels of detectability are possible with our model 112 instrument which might include a cooled PMT and 450 watt lamp. Single photon counting detection, efficient classically ruled gratings in our monochromators, and very good 1:1 imaging optics account for much of the sensitivity of the FLUOROLOG 2 instruments. By taking these values and backtracking to the vapor pressures included in the burning flares, your 1 ppm levels should be easy to achieve.

The Datamate scan controller, photometer, and data system included with the FLUOROLOG 2 instruments is quite easy to use despite its initial apparent complexity. Being microprocessed, default values are loaded into the Datamate on start up making the taking of data easy. As required, additional steps can be added to the data acquisition such as repetitive scanning, peak location, excitation and emission correction, etc. Once the appropriate steps are determined, a simple program can be developed by simply telling the Datamate to perform the various steps in sequence. This is called keystroke programming. You will note in some of the attached Tech Notes on the Datamate how it is not only easy to use but can be quite powerful.

NWC TP 6525

Drs. Short and Loda
April 19, 1983

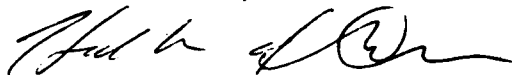
Delivery and installation of an instrument will probably not be a limiting problem in your possible purchase of an instrument. This is assuming that Spex will be informed as the purchase of an instrument progresses. The mentioned mid-June delivery and installation at Los Alamos is well within our capabilities.

I hope this information helps in your determination of the suitability of our FLUOROLOG 2 instruments in your work. I will contact Richard and make arrangements for samples to be run either in Los Angeles, Santa Barbara, the San Francisco Bay Area, or in our New Jersey factory.

In the meantime, if either of you have any questions concerning the FLUOROLOG 2, feel free to give me a call.

Sincerely,

SPEX INDUSTRIES, INC.



Hollis F. Davis
Western Regional Manager

ps
Attachments



29 April 1983

Dr. Richard Loda
Naval Weapons Center
Code 3851
China Lake, CA 93555

Dear Dr. Loda:

Enclosed are the fluorescence spectra of gas phase phenanthrene and pyrene which you requested. The spectra were obtained on a FLUOROLOG F112 system with a 450W Xenon lamp, and a cooled R928 detector. The price of this system with a dual disk drive is approximately \$36000. Hollis Davis can discuss prices with you in greater detail.

The operating parameters are as follows: for pyrene excitation spectrum, emission wavelength = 400 nm, 5 and 10 nm bandpass for excitation and emission monochromators respectively, a 1 nm step size and 1 second integration time. For pyrene emission spectrum 321 nm excitation wavelength, 10 and 5 nm bandpass, 1 nm step size and 1 second integration time. For phenanthrene excitation spectrum, 366 nm emission wavelength, 5 and 10 nm bandpass, 1 nm step size and 1 second integration time. For phenanthrene emission spectrum, 241 nm excitation wavelength 10 and 5 nm bandpass, 1 nm step size, and 1 second integration time.

Plot A shows uncorrected (dashed trace) and corrected excitation spectra of pyrene at 60°C. The correction was done by a rhodamine B quantum counter. Plot B is uncorrected (solid line) and corrected emission spectra of pyrene at 60°C. The instrument response function for corrected emission spectra was determined with a standard lamp. Plots C and D are excitation and emission spectra at 60°C of phenanthrene.

Because of the signal levels, I did not think that synchronous scanning would be very informative. Therefore, I obtained emission spectra of a mixture of phenanthrene and pyrene exciting at two different excitation wavelengths (241 and 321 nm). I performed the above experiment at 60, 50 and 30°C. The results are given in Plots E-J.

NWC TP 6525

Dr. Richard Loda
29 April 1983
Page 2

I think you will agree that these results clearly show that our instrument is capable of detecting PAH's in the gaseous state at the part per million level. If you have any questions about the data, please contact me.

Sincerely yours,

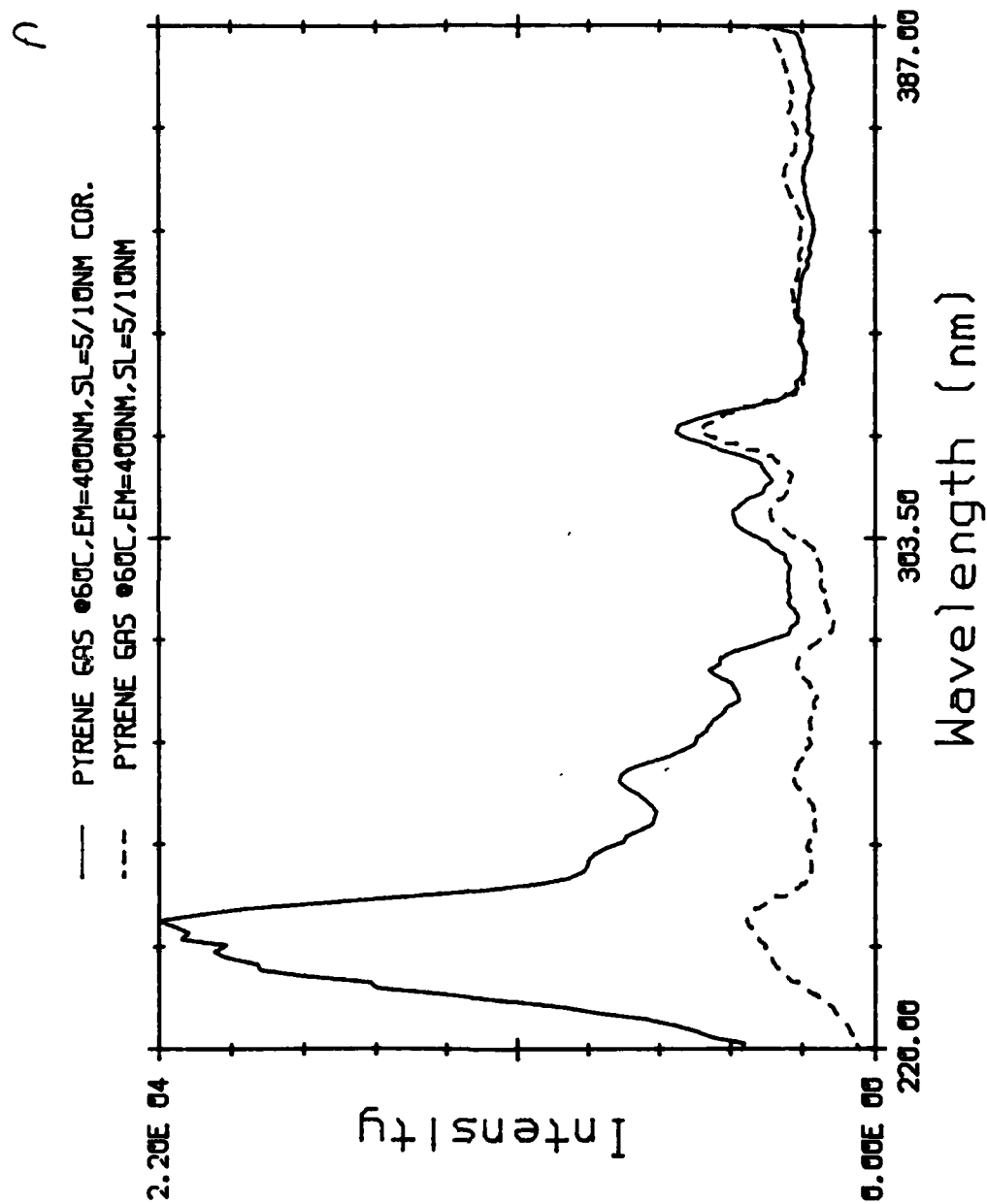
SPEX INDUSTRIES, INC.

A handwritten signature in cursive script that reads "Frank Purcell".

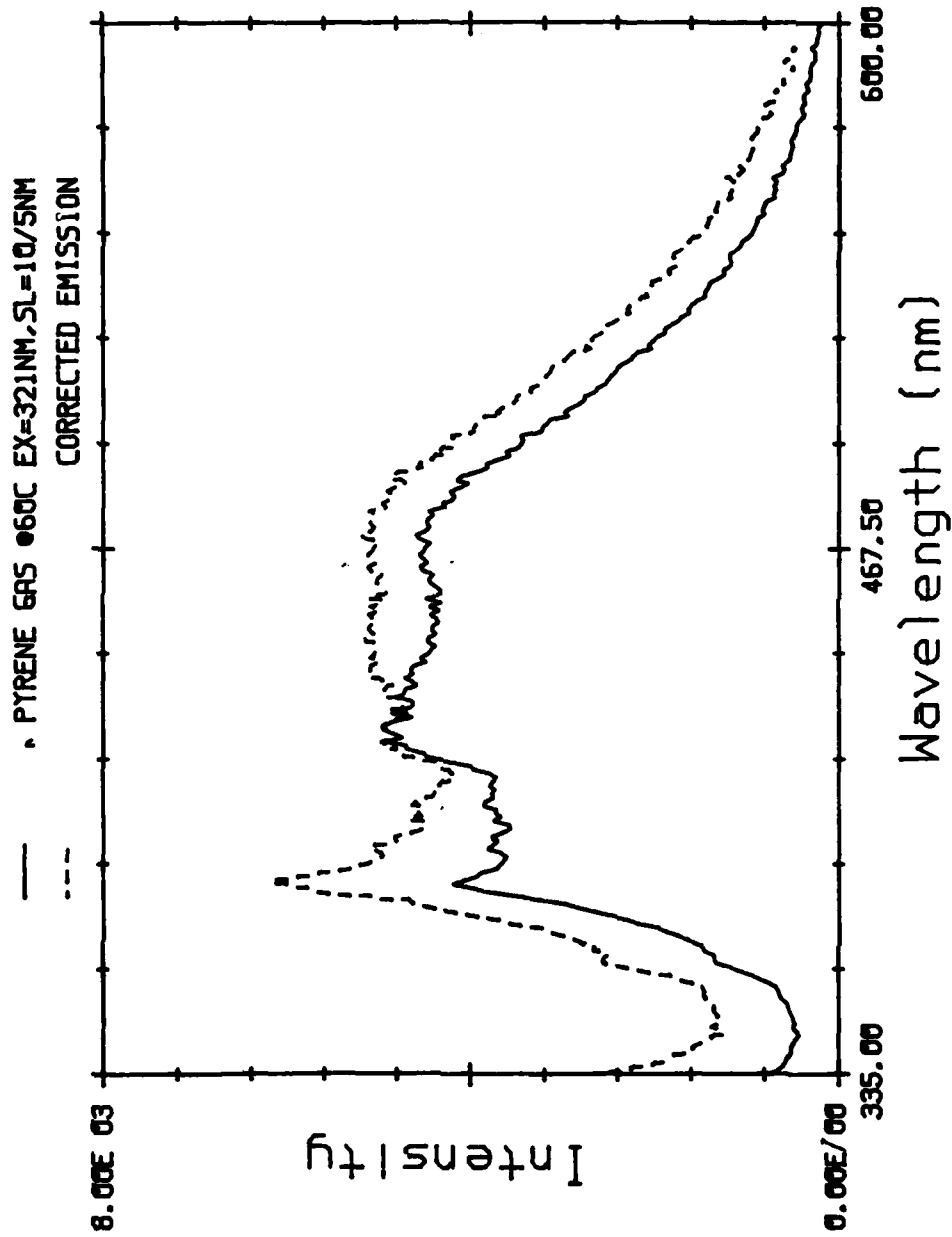
Frank Purcell, Ph.D.
Applications Manager

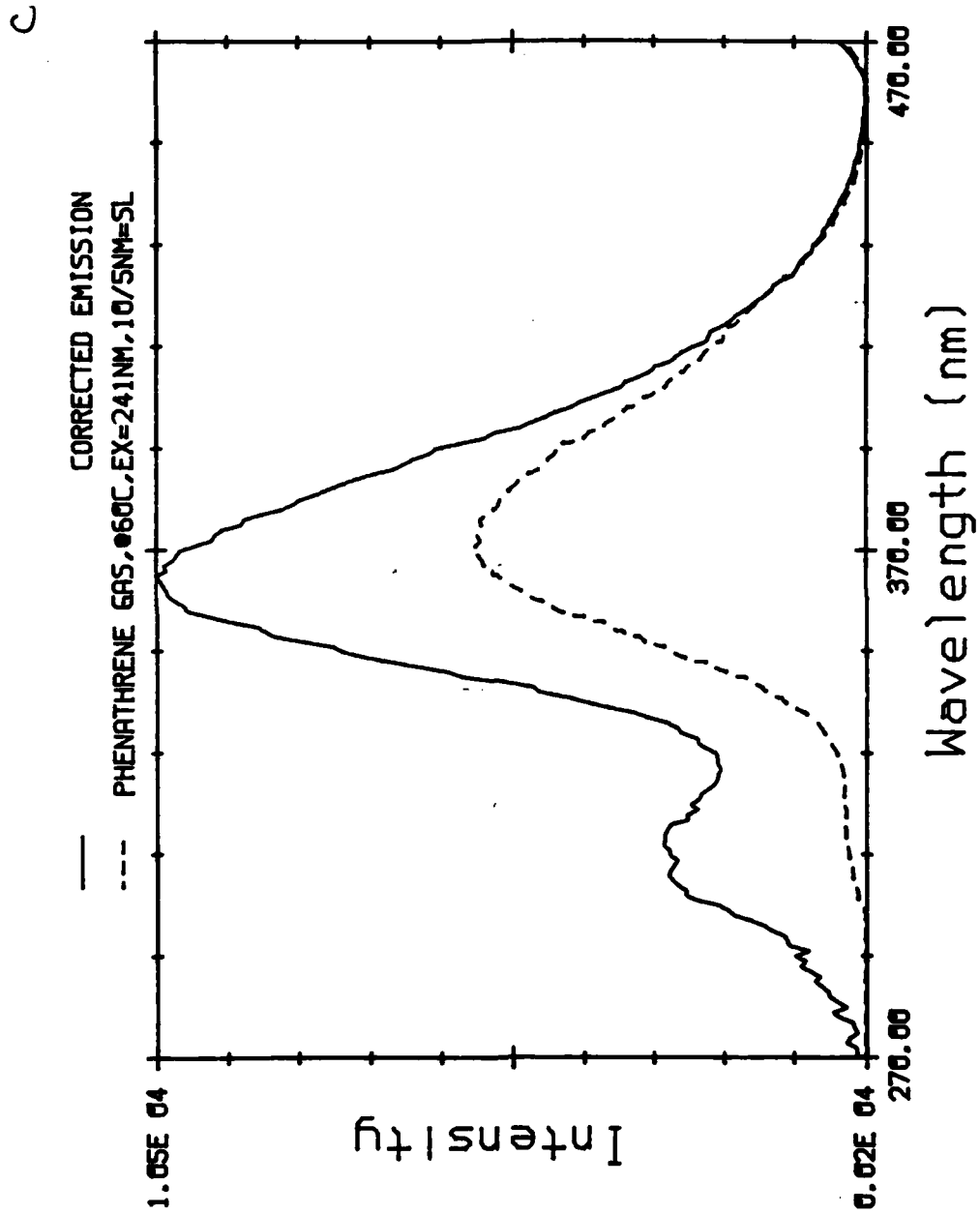
FP/mt
Enc.

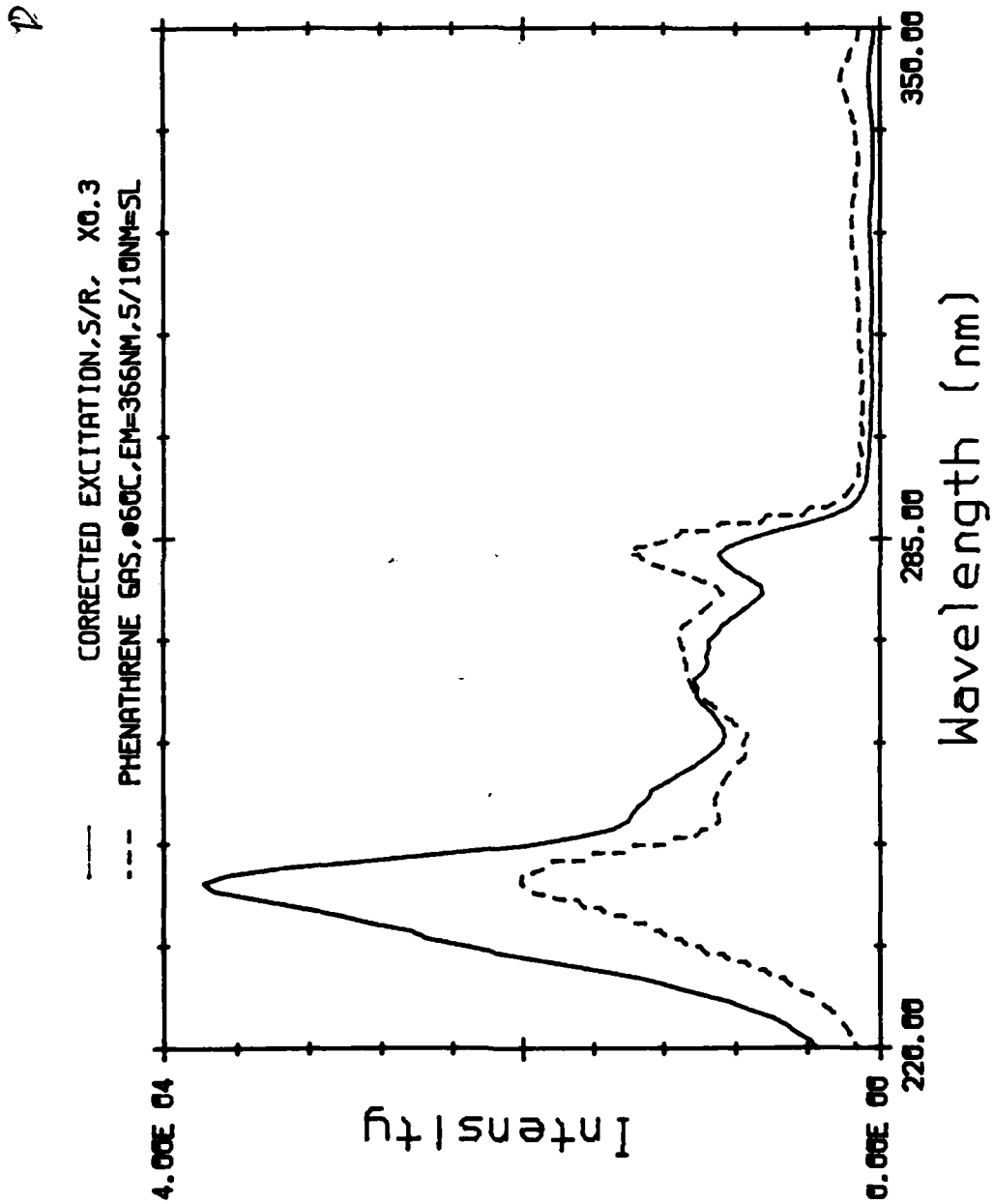
cc: Hollis Davis

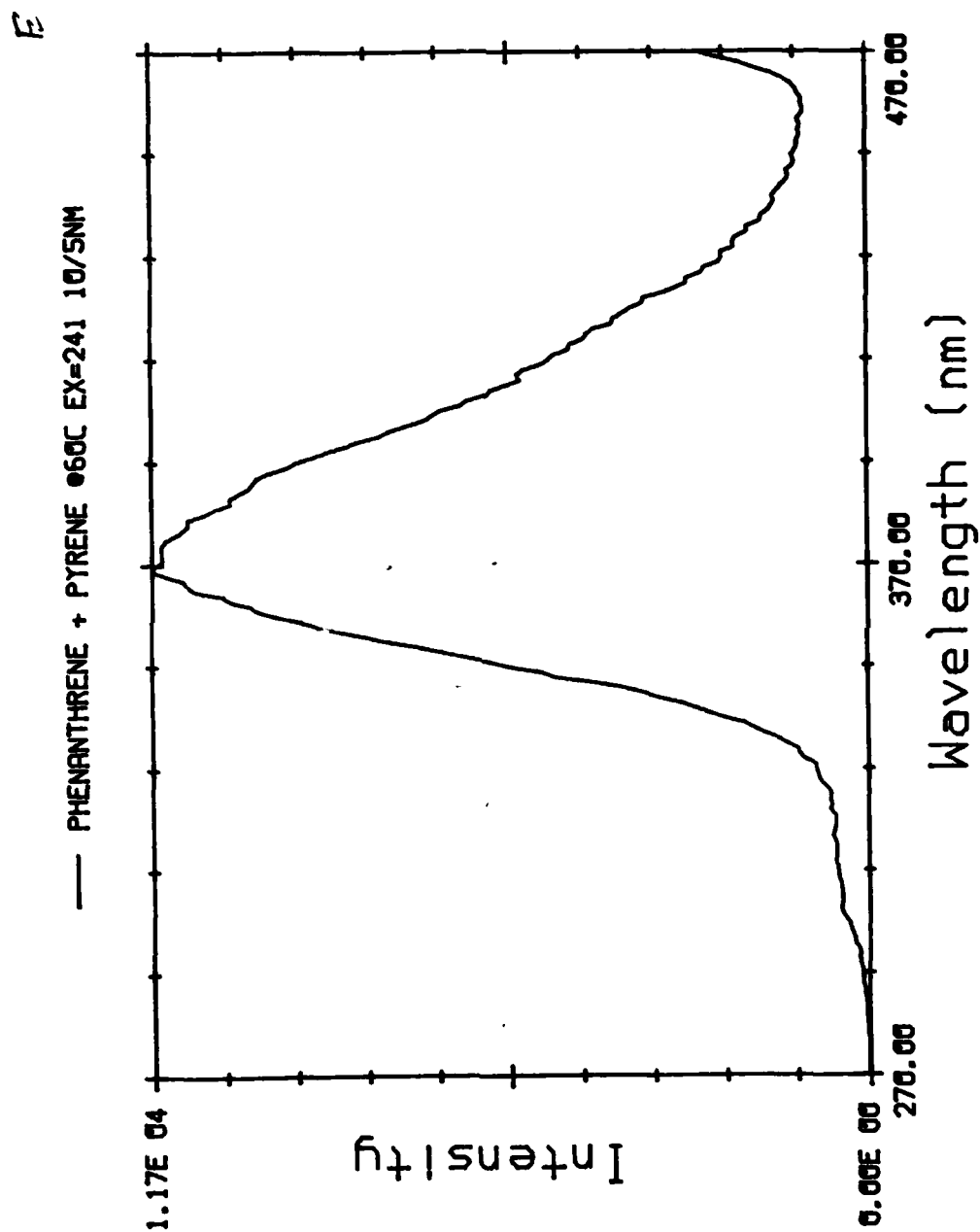


B



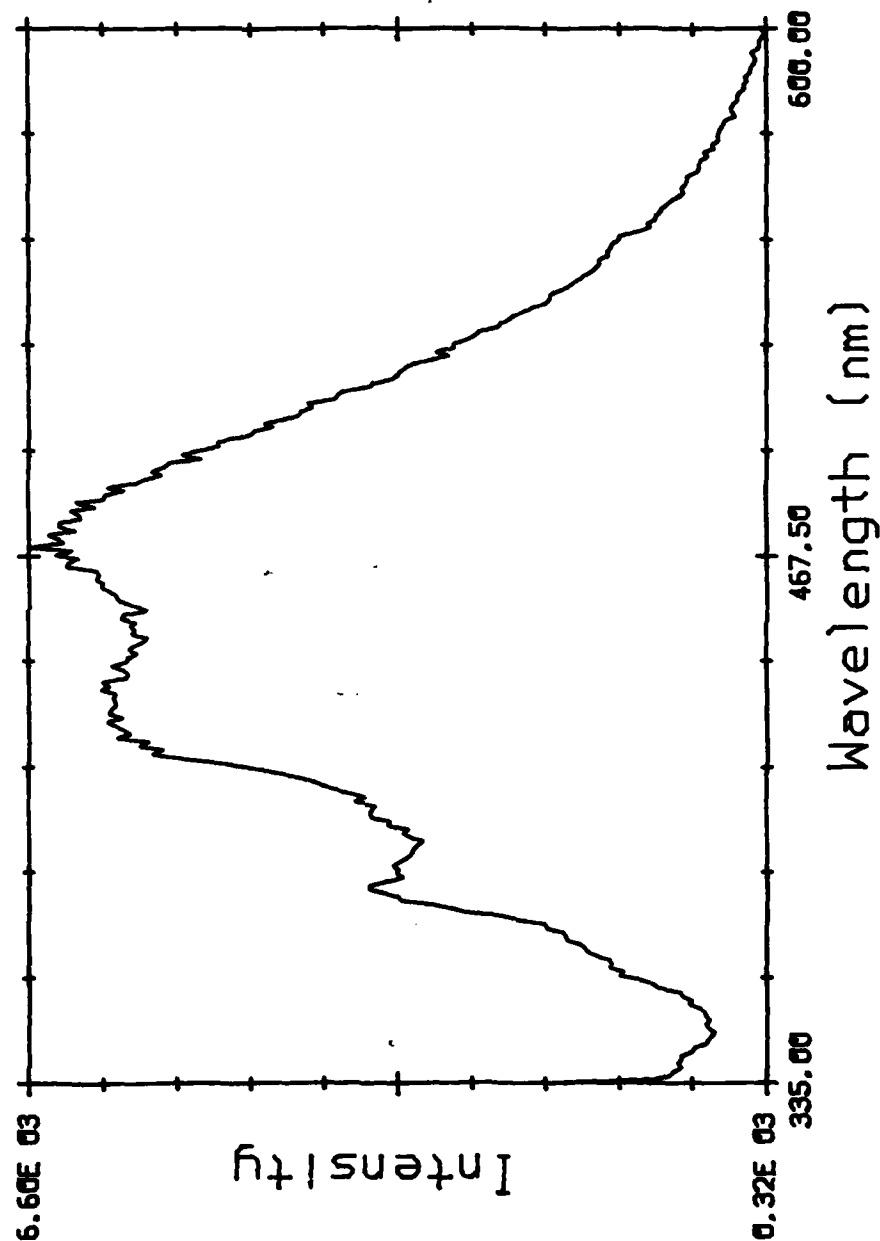






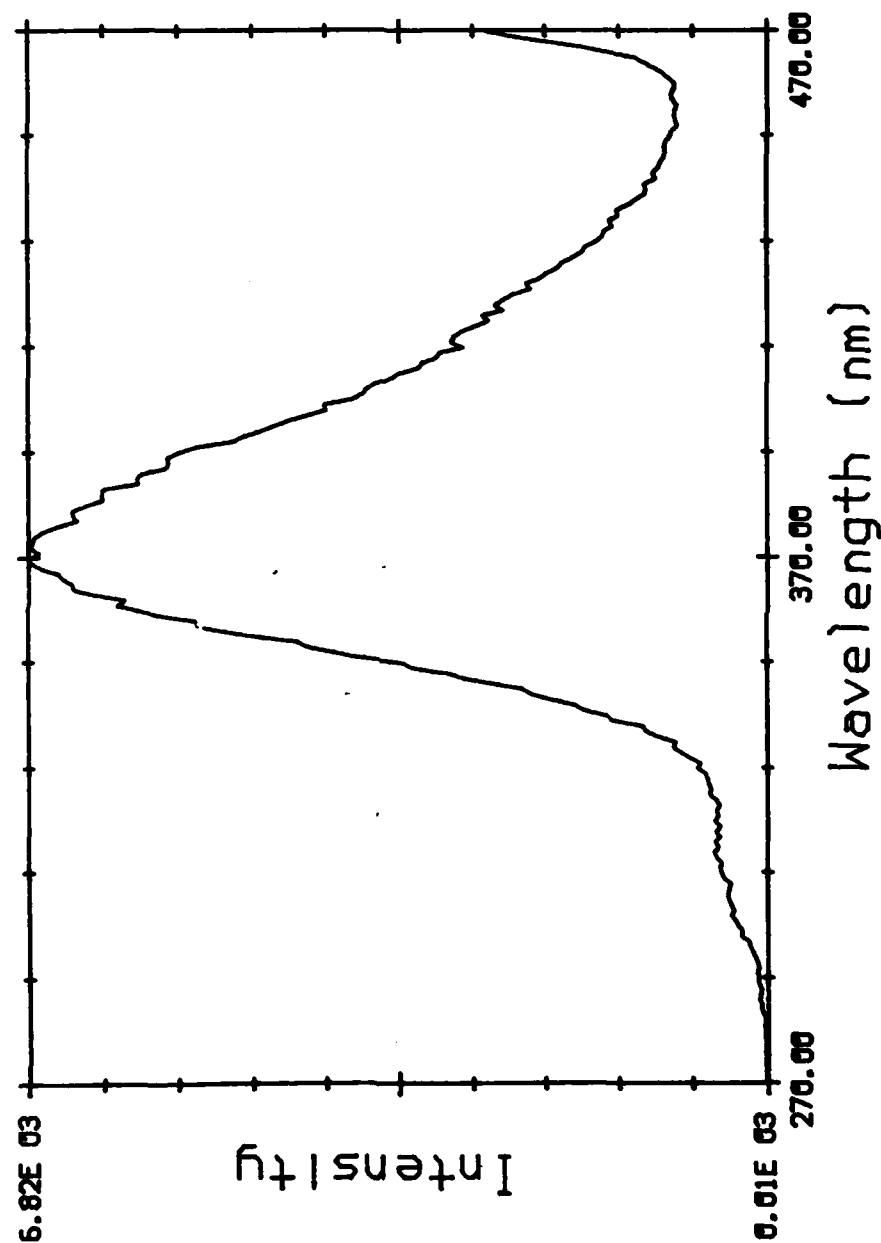
P

— PHENANTHRENE + PYRENE 050C EX=321 10/5NM



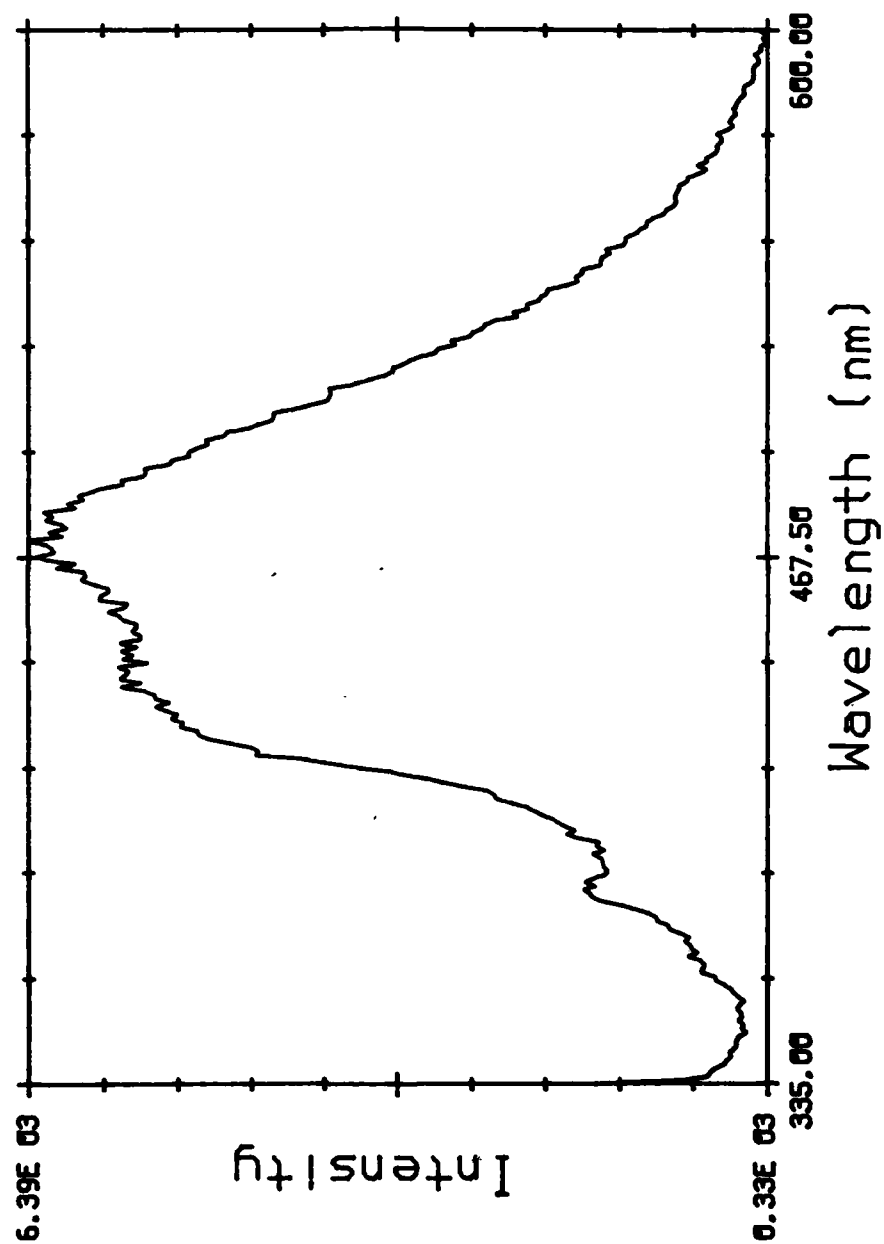
6

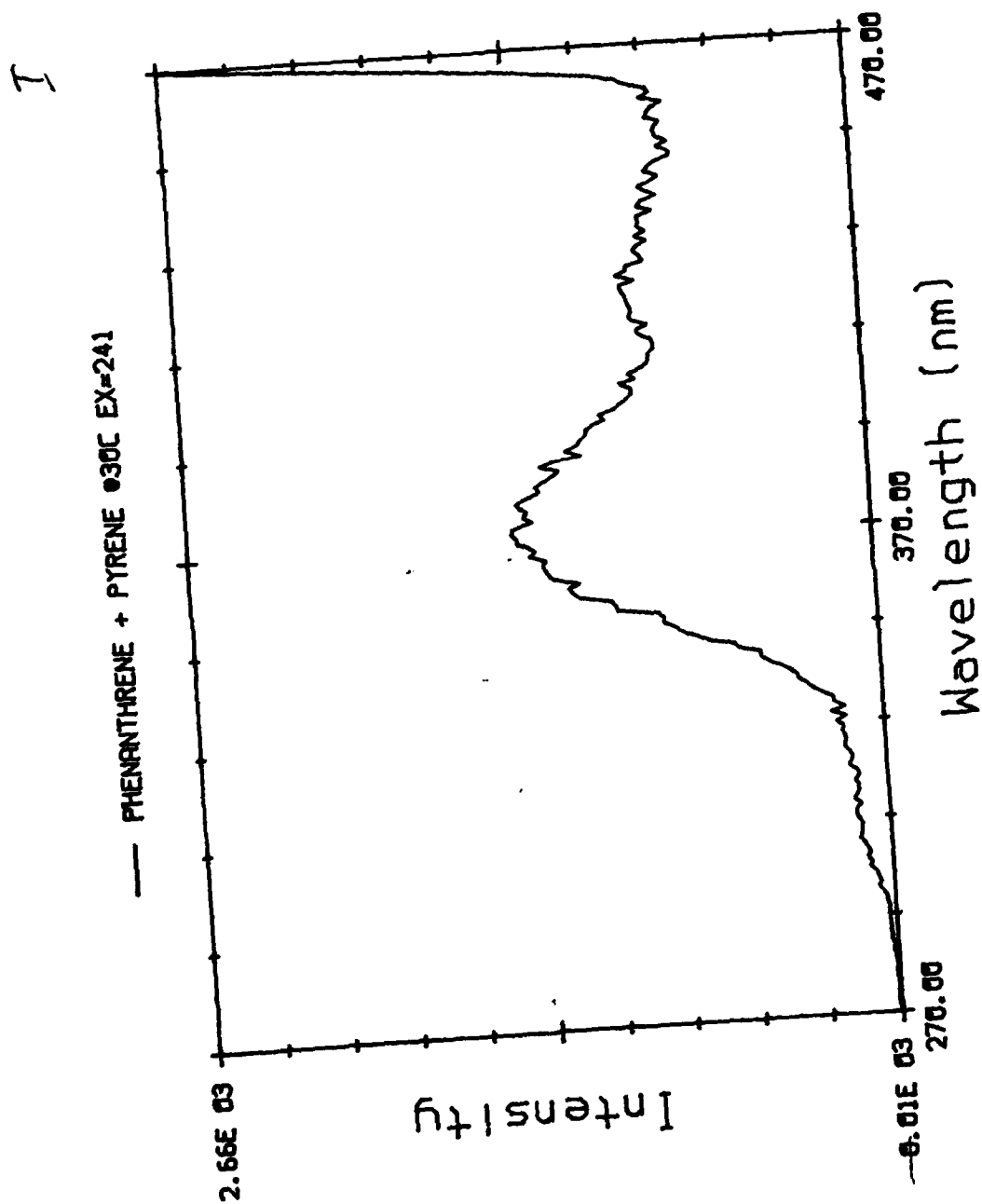
— PHENANTHRENE + PYRENE 050C EX=241 10/5NM



H

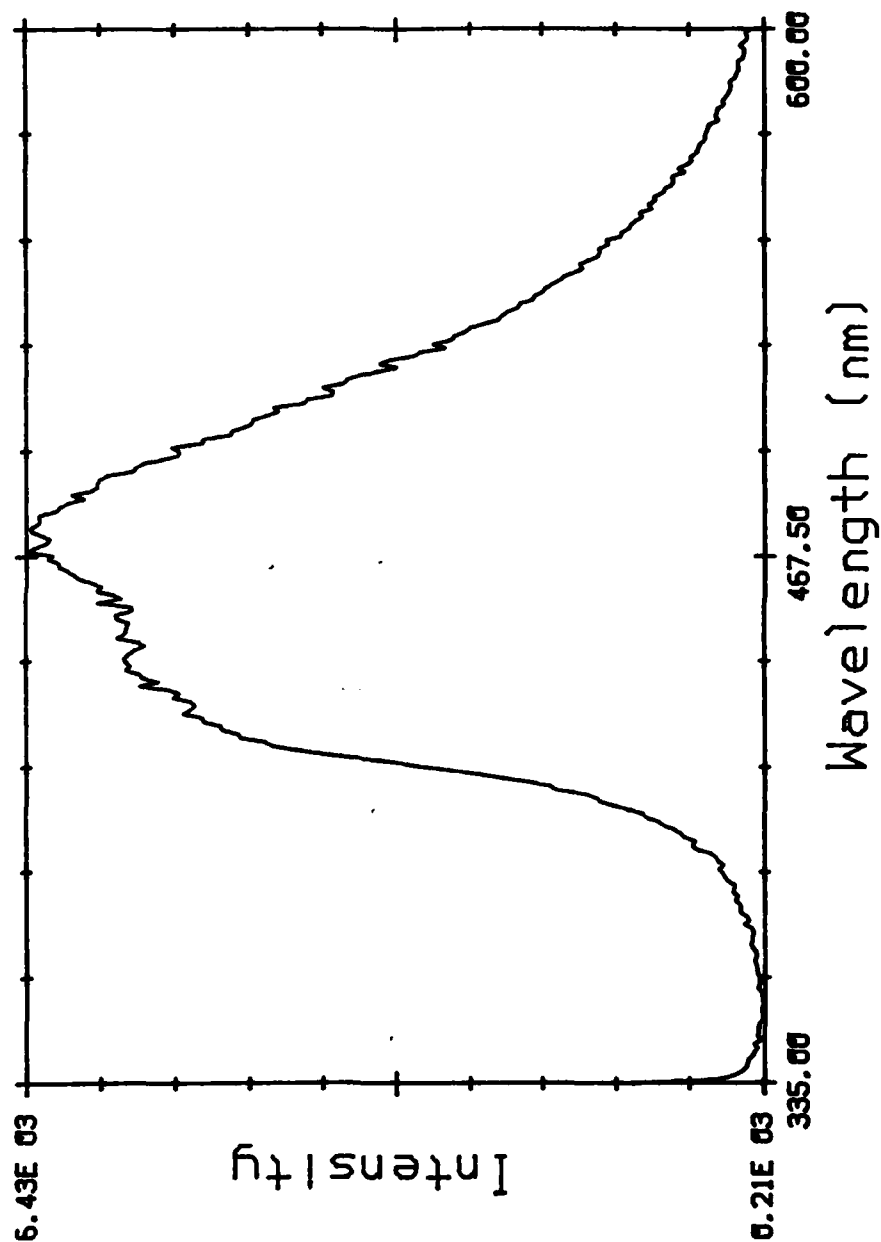
— PHENANTHRENE + PYRENE @50C EX=321 10/5NM





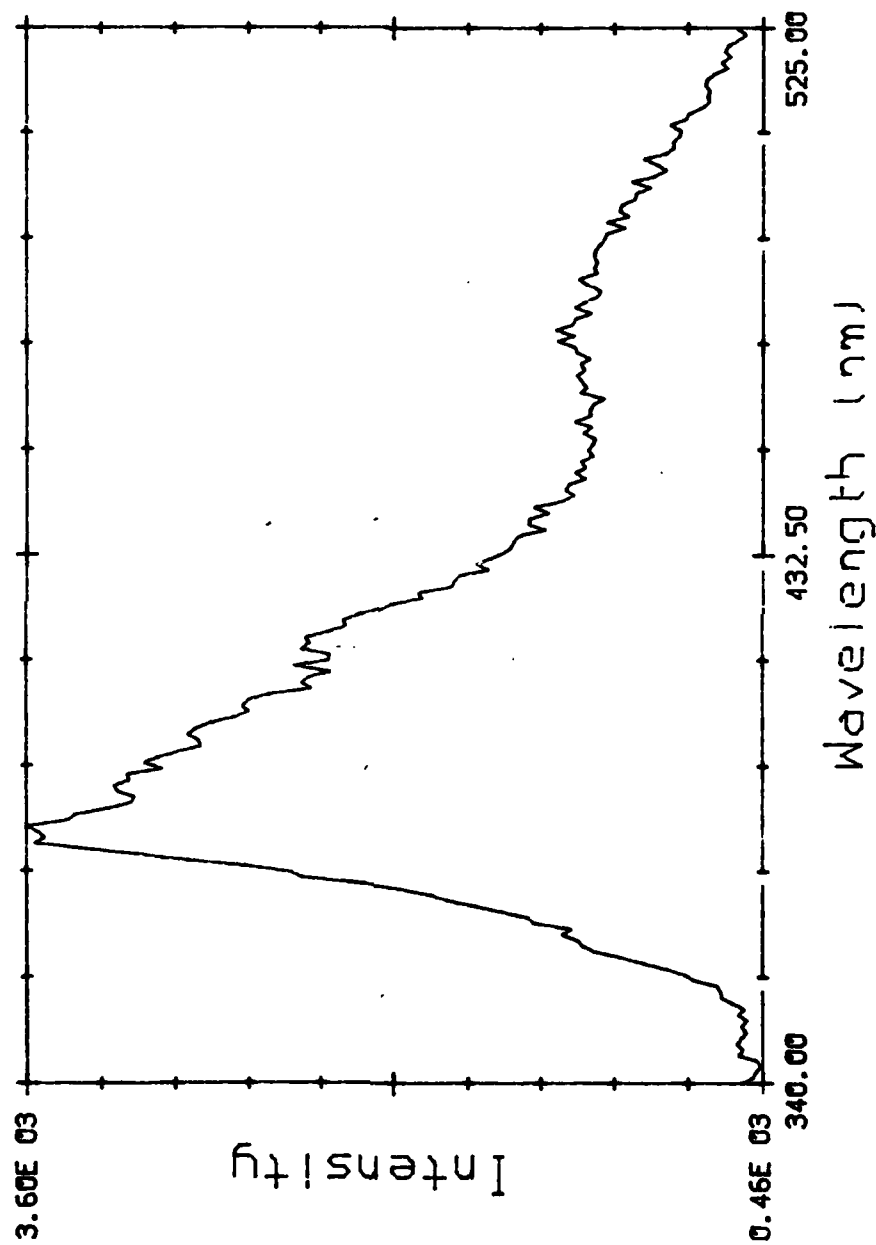
J

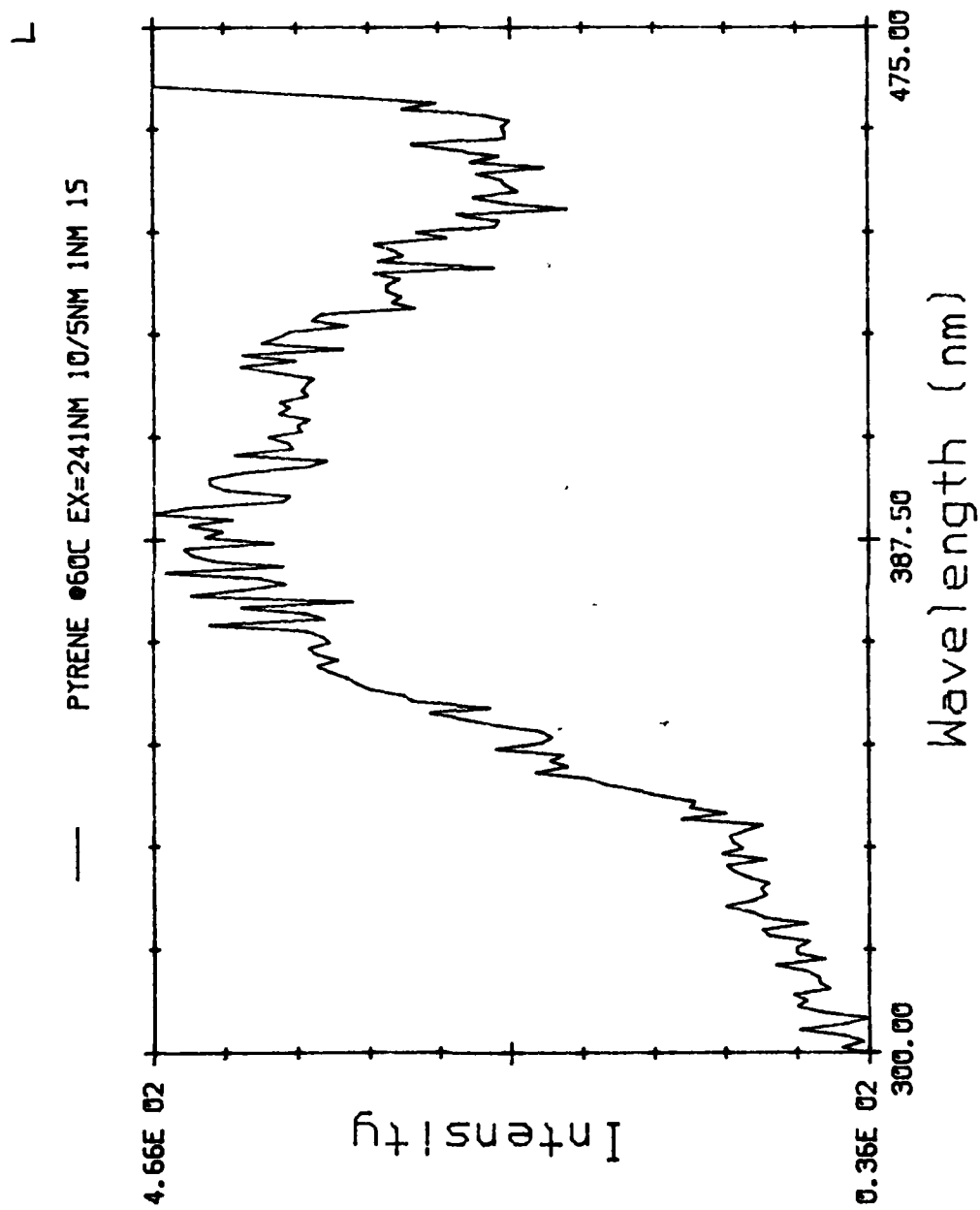
— PHENANTHRENE + PYRENE 030C EX-321



K

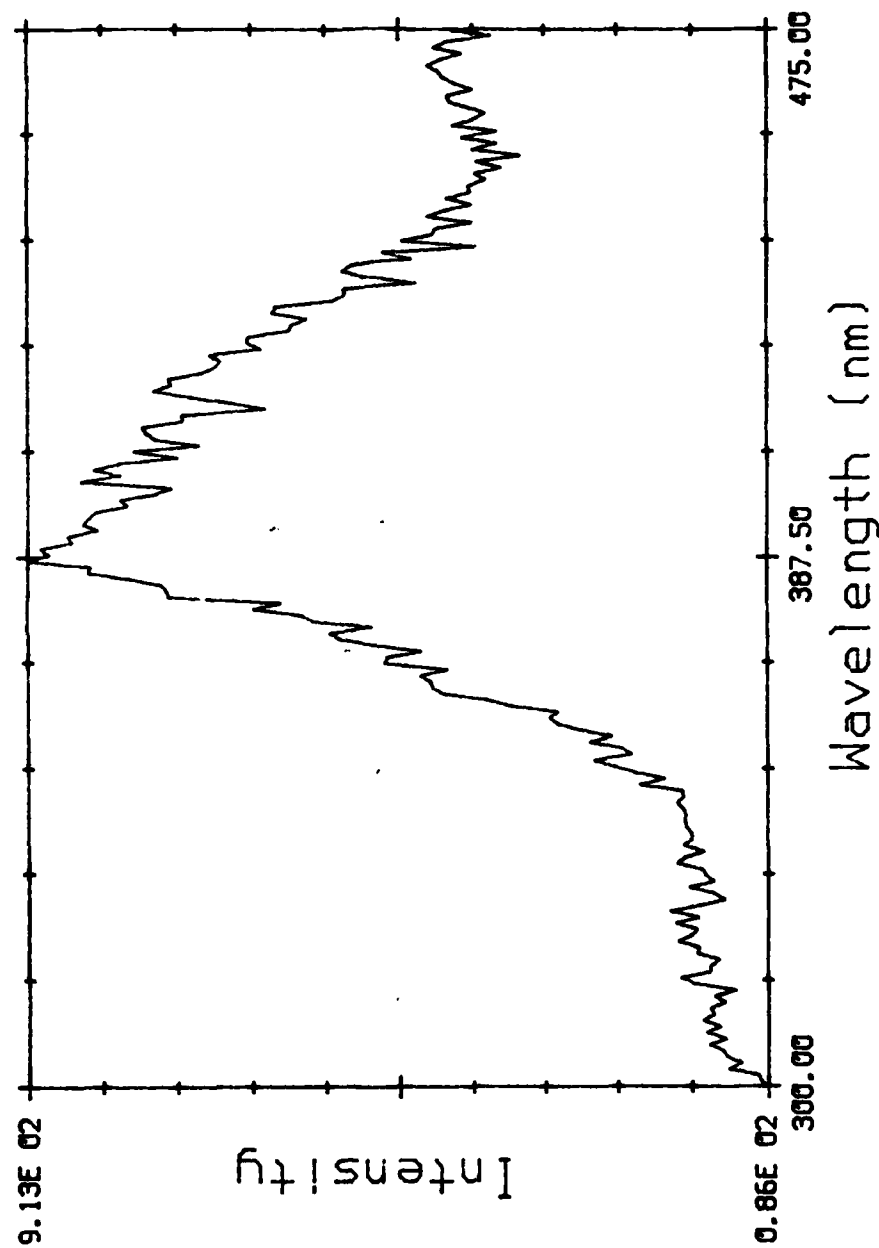
— PYRENE 660C EX=321NM 10/5NM 1NM 15





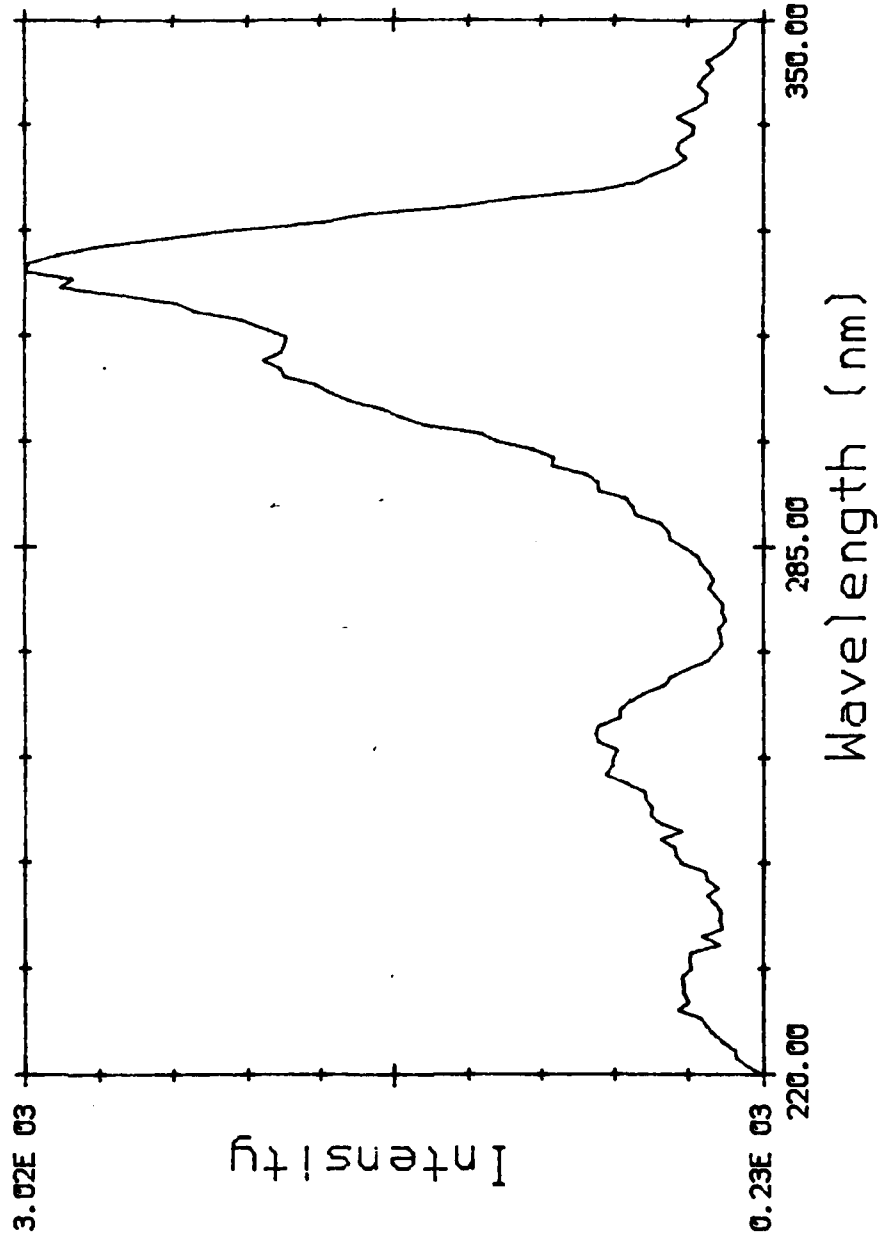
M

— PYRENE 60C EX=260NM 10/5NM 1NM 15



2

EM=390 10/5NM



INITIAL DISTRIBUTION

- 9 Naval Air Systems Command
 - AIR-03B, H. Andrews (1)
 - AIR-03D, G. Heiche (1)
 - AIR-310G, R. Shumaker (1)
 - AIR-320R, H. Rosenwasser (1)
 - AIR-330 (1)
 - AIR-35 (1)
 - AIR-536A1 (1)
 - AIR-7226 (2)
- 5 Chief of Naval Operations
 - OP-225 (1)
 - OP-354 (1)
 - OP-506 (1)
 - OP-982E (1)
 - OP-982F (1)
- 1 Chief of Naval Material (MAT-08)
- 5 Chief of Naval Research, Arlington
 - ONR-440 (1)
 - ONR-443 (1)
 - ONR-460 (1)
 - ONR-470 (1)
 - ONR-472 (1)
- 3 Naval Facilities Engineering Command, Alexandria
 - Code 032, S. Hurley (1)
 - Code 112 (1)
 - Code 54 (1)
- 7 Naval Sea Systems Command
 - SEA-04E (1)
 - SEA-05R1 (1)
 - SEA-05R14 (1)
 - SEA-05R16 (1)
 - SEA-09B312 (2)
 - SEA-62R32 (1)
- 1 Commander in Chief, U.S. Pacific Fleet (Code 325)
- 1 Commander, Third Fleet, Pearl Harbor
- 1 Commander, Seventh Fleet, San Francisco
- 2 Naval Academy, Annapolis (Director of Research)
- 2 Naval Air Development Center, Warminster
 - Library (1)
- 1 Naval Air Propulsion Center, Trenton (PE-71, A. F. Klarman)
- 1 Naval Energy and Environmental Support Activity, Port Hueneme
- 3 Naval Ocean Systems Center, San Diego
 - Code 513
 - S. Yamamoto (1)
 - A. Zirino (1)
 - Code 5131, J. H. Salazar (1)
- 2 Naval Ordnance Station, Indian Head
 - Code E, Pollution Abatement Program Manager (1)
 - Technical Library (1)
- 3 Naval Research Laboratory
 - Code 4300 (1)
 - Code 6100 (1)
 - Library (1)

- 3 Naval Ship Weapon Systems Engineering Station, Port Hueneme
 - Code 5711, Repository (2)
 - Code 5712 (1)
- 2 Naval Surface Weapons Center, Dahlgren
 - G51 (1)
 - Technical Library (1)
- 5 Naval Surface Weapons Center, White Oak Laboratory, Silver Spring
 - Code R11 (2)
 - Code R16, J. Hoffsommer (1)
 - Code R17 (1)
 - Code R141, G. Young (1)
- 1 Naval Underwater Systems Center, Newport (Code 364, R. Kronk)
- 1 Naval War College, Newport
- 6 Naval Weapons Support Center, Crane
 - Code 3025, D. Burch (1)
 - Code 50C, B. E. Douda (1)
 - Code 505, J. E. Short (1)
 - NAPEC (1)
 - R&E Library (2)
- 4 Office of Naval Technology, Arlington
 - MAT-0716 (1)
 - MAT-072 (1)
 - MAT-0723 (1)
 - MAT-0724 (1)
- 1 Army Armament Materiel Readiness Command, Rock Island (DRSMC-DSM-D(R), G. T. Zajicek)
- 1 Army Environmental Hygiene Agency, Aberdeen Proving Ground (HSHB-EA-A)
- 1 Army Medical Bioengineering Research and Development Laboratory, Fort Dietrick
 - (J. Barkeley)
- 1 Army Toxic and Hazardous Materials Agency, Aberdeen Proving Ground (DRXTH-TE-D)
- 3 Air Force Systems Command, Andrews Air Force Base
 - DLFP (1)
 - DLWA (1)
 - SDZ (1)
- 1 Air Force Armament Division, Eglin Air Force Base (D. Harrison)
- 1 Air Force Intelligence Service, Bolling Air Force Base (AFIS/INTAW, Maj. R. Lecklider)
- 12 Defense Technical Information Center
- 1 Los Alamos National Laboratory, Los Alamos, NM (R. Koenig, MS E517)
- 3 The Johns Hopkins University, Applied Physics Laboratory, Chemical Propulsion
 - Information Agency, Laurel, MD
 - T. W. Christian (2)
 - J. Hannum (1)